NUCLEATION AND GROWTH KINETICS

IN A COOLING CRYSTALLIZER

by

Carroll Wilson Chambliss

A Dissertation Submitted to the

Graduate Faculty in Partial Fulfillment of

The Requirements for the Degree of

DOCTOR OF PHILOSOPHY

Major Subject: Chemical Engineering

Approved:

In Charge of Major Work

Head of Major Department

Dean Of Graduate College

Iowa State University
Of Science and Technology
Ames, Iowa

1966

TABLE OF CONTENTS

ABSTRACT

A laboratory continuous, mixed suspension, mixed product removal, cooling crystallizer was designed and operated to obtain crystal growth and nucleation rates. An analysis proposed by previous investigators based on a crystal population balance for both steady state and transient crystallizer conditions was used to determine the kinetic rates from product size distribution for ammonium alum and ammonium sulfate. While the classic theories express nucleation rate as a complex function of supersaturation, a simple power model appears to be sufficient to correlate nucleation and growth rates in such a way as to make possible the prediction of size distribution.

Nucleation rate varied linearly with suspension density suggesting that crystals already in suspension were a heterogeneous source of nuclei and that for the systems studied this mode of nucleation was predominant. As a result of this linear dependence, increasing the amount of solids in suspension did not change the size distribution. If there had been no dependence on the solids in suspension, the size distribution would have been enhanced. Enhancement of the size distribution was achieved, however, by increasing the residence time.

INTRODUCTION

Crystallization from solution is an important separation process in the chemical industry. It is a low cost way of obtaining pure materials from impure mixtures while at the same time improving the handling characteristics of the material. The production of heavy chemicals such as potash, phosphates and other fertilizer constituents depends heavily on elaborate crystallization processes. The same can be said for the production of fine chemicals and drugs. Crystallization process objectives require that pure, well formed crystals with a well controlled size distribution be produced.

When the concentration of a solution exceeds the equilibrium concentration, a driving force for a phase change exists. The concentration of solute in excess of the equilibrium concentration is called the supersaturation. Supersaturation is produced in a continuous process in a number of ways, but primarily by a) cooling a nearly saturated solution, b) evaporation of the solvent, c) the addition of a third component to reduce the solubility of the solute, or d) chemical reaction in a solvent in which the resulting product has a low solubility.

There are two phase change phenomena, nucleation and crystal growth, which arise from a supersaturation driving force. These two phenomena compete for solute in terms of their respective dependence on supersaturation. The relative

kinetic rates of these competing phenomena are the primary factors determining the size distribution of the crystal product. Attainment of a suitable size distribution is one of the most perplexing problems in industrial crystallization. Usually the size distribution is too wide and too heavily weighted toward small crystals or fines. This happens because, qualitatively, nucleation is related to supersaturation in a non-linear manner, while the growth dependence is more nearly linear. The non-linearities in the nucleation kinetics are such that as supersaturation increases, the growth rate increases, but nucleation rate increases to a greater degree.

In order to determine an optimum or at least suitable supersaturation level in a crystallizer to produce crystals of the proper size, it is essential that the relative kinetic rates of nucleation and growth be known. The classic theories of nucleation, while fundamentally satisfying, do not predict observed nucleation rates in continuous crystallization from solution. The results from classic experiments available in the literature are not applicable because these experiments were conducted from clear solutions. In these experiments homogeneous nucleation was usually assumed and the experimental results were frequently not reproducible. The adequate design of continuous, mixed suspension crystallizers requires the development of proper experiments to determine the rates

of nucleation and growth. The nature of these experiments must be such that heterogeneous nucleation effects and non-linear growth effects can be quantitatively discerned.

The purpose of this work was to use an analysis technique developed by Randolph and Larson (17) to study the nucleation and growth kinetics in a continuous cooling crystallizer. The intent was to determine the applicability of the technique to a cooling crystallizer and to see if the required constraints could be maintained. Another objective was to see if heterogeneous effects could be measured and correlated. In conjunction with these determinations it was necessary also to test the applicability of McCabe's ΔL law for the system indicated. Finally it was intended that kinetic data be obtained for ammonium alum and ammonium sulfate so that correlations leading to a kinetic model for each system could be made.

LITERATURE REVIEW

Nucleation

The classical theory of nucleation treats phase changes which Gibbs described as large in degree, but small in extent. These discontinuous changes can be analyzed by considering their energy requirements. When a solid particle is formed within a homogeneous fluid, the total work required is equal to the sum of the work to form the particle surface and the work to form the bulk of the particle. The overall work or excess free energy reaches a maximum when the particle achieves a critical size. At this point if the particle has sufficient energy to continue growing, it is called a nucleus (6). Although the mean energy of a fluid system at constant temperature and pressure is constant, there are fluctuations about this constant mean value in isolated regions of the fluid. These fluctuations supply the necessary energy to form stable nuclei (11).

A fundamental expression for the rate of nucleation was first given by Volmer and Weber (13). They proposed that the rate of spontaneous nucleation followed an Arrhenius type relationship:

$$\frac{dN^\circ}{dt} = c \exp\left(-\frac{\Delta G*}{kT}\right) \tag{1}$$

where $\Delta G*$ is the free energy of formation of a nucleus.

The free energy change in forming a nucleus from homogeneous solution consists of both a bulk and a surface contribution (11). The surface free energy is usually expressed as the product of the surface tension and the surface area of the nucleus, although the use of these quantities for particles of nuclei size is questionable (13). From a practical standpoint the surface tension of crystals in suspension cannot be calculated anyway (13). The pre-exponential factor, c, in Equation 1 has been estimated in a number of ways depending on the proposed mechanism of nucleation. Becker and Doring (27) postulated a mechanism which explains satisfactorily the nucleation of water droplets from super-cooled water vapor. For nucleation in condensed phases Turnbull and Fisher (25) stated that the free energy of activation for short range diffusion across the phase inter-face should be included in the rate expression.

Nielsen (13) has estimated the pre-exponential factor in Equation 1 and expressed the free energy of nuclei forma-tion as a function of supersaturation in the following equation:

$$\frac{dN^o}{dt} \cong 10^{30} \exp\left(-\frac{\beta \sigma^3 v^2}{k^3 T^3 (\ln S)^2}\right) \qquad (2)$$

where β is a geometric factor, σ is the crystal surface tension, v is the molecular volume, k is Boltzmann's constant, T is absolute temperature, and S is the ratio

of the supersaturated solution concentration to the equilibrium concentration. Barium sulfate nucleation data were correlated with this expression above a certain supersaturation. Nielsen pointed out that though basic theoretical calculations show nucleation rate to be a complex function of supersaturation, a simple concentration power model gives a good approximation of nucleation rate.

There have been numerous experiments where a clear solution was cooled and the supersaturation level was noted when the first crystals appeared. Ostwald (27) called this region of spontaneous nucleation the labile region. Miers and Issac (10) determined a supersolubility curve dividing the labile region from a metastable region where nucleation could be induced by seeding. In solutions seeded at their saturation point, Ting and McCabe (24) observed concentration levels where nuclei first appeared and then where a large shower of nuclei were produced. Since the rate of cooling influenced these levels, there appears to be a time probability of nucleation for any supersaturated solution.

In a continuous, mixed crystal suspension it is not possible to decide whether nucleation occurs only because of supersaturation or whether in addition the crystals already present contribute to the nucleation process. Powers (14) suggested the possibility of a "buffer reservoir layer" of fluidized material around crystals in suspension

as a source of nuclei. With stirring this loosely bonded
material supposedly separates from the parent crystal to
form nuclei. Strickland-Constable and Mason (21) observed
showers of small particles around the point of fracture of
irregular growth on crystals in suspension. According to
Uhlmann and Chalmers (26), nucleation on heterogeneities
occurs at a lower potential than that required for homo-
geneous nucleation. These observations suggest that
nucleation in a crystal suspension probably depends on the
solid phase already present in addition to supersaturation.
This dependence on the solids in suspension can be expressed
in terms of the suspension density or the crystal surface
area.

Crystal Growth

For a crystal to grow in solution, solute must be
transported through the solution to the crystal surface and
oriented into the crystal lattice. Early theories of
crystal growth (3) considered only the diffusional part of
the process probably because of observations made on systems
where diffusion was rate controlling. By assuming that
solute molecules diffuse through a thin laminar film of
liquid adjacent to the crystal face, the following equation
was proposed (11):

$$\frac{dm}{dt} = \frac{D}{X} A (c - c*) \tag{3}$$

where m = crystal mass

A = crystal surface area

c = solute concentration in the supersaturated
solution

c*= equilibrium saturation concentration

D = diffusivity of the solute

X = film thickness

One obvious weakness in this theory is that no limiting
value of growth rate is achieved as the diffusional resis-
tance is lowered by agitation. Also a substance generally
dissolves at a faster rate than it grows, which contradicts
a mechanism of pure diffusion.

The diffusion theory was modified by Berthoud (20) to
include a first order surface reaction, giving the following
equation:

$$\frac{dm}{dt} = \frac{DA}{X + D/k_R} (c-c*) \tag{4}$$

where k_R is the reaction rate constant. For a rapid surface
reaction k_R is large and Equation 4 reduces to Equation 3.
If the diffusional resistance is low due to vigorous agita-
tion, X is small and the surface reaction is controlling.
Although Equation 4 provides a lucid qualitative description
of the two step growth process, the assumption of a first
order surface reaction for all materials is questionable (11).

Frank (4) in a classic work showed that if a crystal
contained a dislocation which was self-perpetuating, the

large discrepancy between theoretically estimated and exper-
imentally observed growth rates of a number of materials
could be explained. Nielsen (13) pointed out that the dis-
location growth spiral may be rate determining for very
small crystals at measurable supersaturations, but not for
large crystals except at extremely low supersaturations.

In a recent book Nielsen (13) treats the previously
mentioned cases of diffusion, surface reaction, and dis-
location controlled growth in detail. Since the exact
growth mechanism of a substance is frequently in doubt,
growth rate is often expressed simply as a linear function
of supersaturation. Jenkins (5) found experimentally that
growth rate was a linear function of supersaturation for a
variety of crystals in both aqueous and organic solutions.
In this case Equation 4 may be written as:

$$\frac{dm}{dt} = k_G \, A \, s \tag{5}$$

where s is the supersaturation and k_G is a constant which
depends on the temperature and the agitation. Both crystal
mass and crystal area may be expressed in terms of a char-
acteristic crystal dimension L to give the following
expression for linear growth rate:

$$r = \frac{dL}{dt} = k_g \, s \tag{6}$$

McCabe (8) observed that each crystal in a suspension
grows at the same rate irrespective of its size if subjected

to the same conditions. Exceptions to this principle, which
is known as McCabe's ΔL law, have been found in industrial
crystallizers where large crystals with high settling
velocities tend to move through the solution faster than
smaller crystals. This reduces their resistance to
diffusion and consequently they grow faster. However, if
agit.tion is vigorous and the velocities of crystals of
different size relative to the solution are the same, the
law generally holds (9).

Crystal Size Distribution

Size distributions have usually been expressed in terms
of cumulative weight per cent. A more meaningful distri-
bution function in terms of rate of production of nuclei
and particle growth is the population density. Population
density is the slope of a cumulative numbers versus size
curve or in terms of a limit:

$$n = \lim_{\Delta L \to o} \frac{\Delta N}{\Delta L} \qquad (7)$$

where n is population density (number of particles/length),
and ΔN is the number of particles in size increment ΔL.
With population density thus defined, Randolph and Larson
(17) used it in an overall population balance for an
arbitrary suspension of particles under unsteady state
conditions subject to the following conditions and
assumptions:

1. The suspension occupies a variable volume V enclosed by fixed boundaries, except for a free gravity surface.

2. This volume has inputs and outputs which can be considered mixed across their respective pipe diameters, but the suspension contained in the volume under consideration is not necessarily mixed.

3. The particles in the suspension are small enough and numerous enough to be considered a continuous distribution over a given size range of particles and over a given volume element of the suspension.

4. No particle breakage occurs, except possibly the chipping of a particle into unequal pieces such that one piece is essentially unchanged in size while the other is small enough to be considered a nucleus.

A balance on the total number of particles in the suspension within an arbitrary size range can be written in terms of the local population density, $\bar{n}$:

$$\frac{d}{dt} \int_V \int_{L_1}^{L_2} \bar{n}\,dL\,dV = \int_{L_1}^{L_2} (Q_i\bar{n}_i - Q_o\bar{n}_o)\,dL \qquad (8)$$

where $\bar{n}$ is the point population density per unit volume, number/ft.^{4} and Q is the input or output suspension volumetric flow rate ft.^{3}/hr. If the left hand side of Equation 8 is differentiated using Leibnitz's rule and the order of integration is interchanged, the following equation is obtained:

$$\int_{L_1}^{L_2} \left(\int_V \left[\frac{\partial \bar{n}}{\partial t} + \frac{\partial}{\partial L} \left(\bar{n} \frac{\partial L}{\partial t} \right) \right] dV + \bar{n}_s \frac{dV}{dt} - Q_i \bar{n}_i + Q_o \bar{n}_o \right) dL = 0 \qquad (9)$$

Since the size range L_1 to L_2 is completely arbitrary, it is necessary that the integrand of Equation 9 vanish identically to give:

$$\int_V \left[\frac{\partial \bar{n}}{\partial t} + \frac{\partial}{\partial L} \left(\bar{n} \frac{\partial L}{\partial t} \right) \right] dV + \frac{dV}{dt} \bar{n}_s - Q_i \bar{n}_i + Q_o \bar{n}_o = 0 \qquad (10)$$

The volume integration would be necessary to describe a classified suspension. Removal of a classified product does not necessarily imply a classified suspension, for this can be accomplished by wet screening, elutriation, etc. The first term in Equation 10 represents the transients in population density of crystals of a given size. The second term represents the bulk transport of crystals into and out of this size range by virtue of their rate of growth in suspension. The third term represents changes in population due to changes in total suspension volume where $\bar{n}_s$ is the local population density of crystals at the suspension surface. The fourth and fifth terms represent inputs and outputs of crystals to the suspension. An independent derivation for the distribution of particle sizes in a mixed suspension of constant volume was made by Behnken et al., (1)

For continuous, mixed suspension, mixed product removal (MSMPR) crystallization, Randolph (16) made the following assumptions in an analysis of the size distribution behavior:

a) Constant suspension volume.

b) Constant suspension density can be maintained by controlling energy inputs.

If assumption a) is applied to Equation 10, then $n = \bar{n}V$, $\frac{dV}{dt} = 0$, $Q_o = Q_i$, and $\bar{n}_o = \bar{n}$ for mixed product removal giving:

$$\frac{\partial n}{\partial t} + \frac{\partial}{\partial L}\left(n \frac{\partial L}{\partial t}\right) = \frac{Q_i}{V}(n_i - n) \qquad . \ (11)$$

This equation is useful when growth rate, $\frac{dL}{dt}$, depends on size and when there are seed crystals in the feed. However, by assuming that McCabe's ΔL law holds for the growth rate r, $\left(r = \frac{dL}{dt} \neq f(L)\right)$ and considering the non-seeded case, $n_i = 0$, Equation 11 reduces to:

$$\frac{\partial n}{\partial t} + r \frac{\partial n}{\partial L} = \frac{-n}{T} \qquad (12)$$

where residence time, $T = V/Q_i$.

For steady state operation integration of equation 12 from 0 to L gives the following exponential size distribution equation in which the subscript zero denotes steady state operation:

$$n = n_o^o \exp\left(- \frac{L}{r_o T_o}\right) \qquad (13)$$

where n is population density, n_o^o is population density of nuclei, L is particle diameter, r_o is growth rate and T_o is the residence time. Equivalent steady state equations have been derived by Saeman (19) and Bransom et al., (2). They considered the number rate of loss of crystals from any size increment to be proportional to the population density in that increment and the fraction of the mixed suspension withdrawn per unit time. However, this approach cannot be used if McCabe's ΔL law is not applicable (15). When growth rate depends on size, the size increment changes as the particles grow and a population balance such as Bransom's over a constant size increment is invalid.

A method of determining growth and nucleation rates from steady state data using Equation 13 has been developed by Bransom et al., (2) and Randolph (16). If $\log_e$ (n) vs. L is plotted, a straight line of slope $(-1/r_o T_o)$ and intercept $\log_e (n_o^o)$ results. Growth rate r_o is simply calculated from the slope for known residence time T_o. Growth rate in a mixed crystal suspension has been shown to be a linear function of supersaturation as expressed in Equation 6 (5). Nucleation rate as discussed previously is a more complicated function of supersaturation. However, a power model gives a fairly good approximation of nucleation rate for limited ranges of supersaturation (13). Robinson and Roberts (18) proposed the following power model:

$$\frac{dN^\circ}{dt} = k_1 s^i \qquad (14)$$

where $\frac{dN^\circ}{dt}$ is the total nucleation rate (no. of nuclei/sec.).
A model of this type suggests that homogeneous nucleation
is the predominant source of nuclei. When this model is
used, nucleation rate can be related through a common
dependency on supersaturation to growth rate.

$$\frac{dN^\circ}{dt} = k_2 \, r^i \qquad (15)$$

In order to get the nucleation rate in terms of experimen-
tally measurable quantities, $\frac{dN^\circ}{dt}$ was related to the nuclei
population density and the growth rate by use of the chain
rule.

$$\frac{dN^\circ}{dt} = r \, n^\circ \qquad (16)$$

Equations 15 and 16 may be combined at steady state to
give the following expression for the population density of
nuclei.

$$n_o^\circ = k_2 (r_o)^{i-1} \qquad (17)$$

A set of values of n_o° and r_o can be obtained at different
residence times for a constant suspension density as pro-
posed in assumption b). The exponent (i-1) can then be
calculated from the slope of a log-log plot of n_o° vs. r_o.
This is the steady state method of finding the kinetic
order of the nucleation rate. Equation 17 is the key
relationship in determining the crystal size distribution.

Randolph (16) plotted the log of the nucleation rate $\frac{dN^o}{dt}$ vs. the log of the growth rate to obtain a straight line of slope equal to 3 with data collected by Bransom et al., (2) for the cyclonite-nitric acid-water system. Murray (12) and Timm (22) found the exponent i to be equal to 2 and 1.25 respectively for the crystallization of ammonium alum from water by the addition of ethanol. However, a small particle counter was available to Timm which allowed him to calculate n_o^o values more accurately.

Randolph (15) divides continuous crystallization processes into two classes -- those in which per-pass yield is a variable and those in which a quantitative yield is observed. Apparently in the first case the degree of supersaturation varies and the yield depends on the residence time. When there is only an infinitesimal level of supersaturation, the yield is quantitative. Even with yield a variable, the substitution of growth rate for supersaturation in Equation 14 is permissible as long as crystal size distribution and not yield is of interest, since crystal size distribution is a function only of the relative growth and nucleation rates.

The transient size distribution Equation 12 has been solved for step changes in residence time and feed concentration (16, 12, 22). Knowledge of the relative order of the nucleation rate to the growth rate is needed to solve this equation. The equation is more conveniently handled

if the following dimensionless substitutions are made.

Let $x = L/r_0 T_0$

 $y = n/n_0^0$

 $\theta = t/T_0$ (18)

 $\emptyset = r/r_0$

Substitution of Equations 18 into Equation 12 gives:

$$\frac{\partial y}{\partial \theta} = -\emptyset \frac{\partial y}{\partial x} - y \left(\frac{T_0}{T}\right) \qquad (19)$$

An initial condition is the steady state solution Equation 13, which satisfied Equation 19 at a residence time equal to T_0. In dimensionless form, the initial condition is:

$$y(o,x) = e^{-x} \qquad (20)$$

The following boundary condition relating growth and nucleation rates is obtained by making Equation 17 dimensionless:

$$y(\theta,o) = n^0/n_0^0 = \left(^r/r_0\right)^{i-1} = \emptyset^{i-1} \qquad (21)$$

For a step change in residence time for a cooling or evaporative crystallizer there would have to be a simultaneous change in the energy inputs to maintain the constraints a) and b) of constant suspension volume and density. When a constant suspension density is maintained, the mass in the crystallizer is constant, and the growth rate is constrained for a step change in residence time according to the following expression:

$$\phi = \frac{2\ T_o/T}{\int_0^\infty x^2 y\, dx} \tag{22}$$

For a step change in feed concentration, the assumption of constant suspension density is no longer valid. Murray (12) derived the following constraint on growth rate for feed concentration disturbances.

$$\phi = \frac{2\ \dfrac{\Delta C}{\Delta C_o}}{\int_0^\infty y x^2\, dx} \tag{23}$$

The transient response to disturbances in feed concentration and in production rate (residence time) can be obtained by solving Equation 19 with the above conditions -- Equations 20, 21, and 22 or 23.

Randolph (16) solved the transient equation for a step change in production rate and a fourth order kinetic nucleation rate using standard finite difference techniques on a digital computer.

Using a modified version of Randolph's program, Timm (22) found that a solution using a 1.25 order kinetic nucleation rate in the Randolph and Larson (17) model (Equation 21) represented the experimental transient data for the alum-ethanol-water system. Fitting experimental transient data with solutions of the transient equation is therefore another method of determining the kinetic

nucleation order. Murray (12) transformed and simulated
the transient equation on an analog computer for a step
change in feed concentration and in production rate. Agree-
ment was found between experimental and theoretical pro-
duction rate transients, but the experimental concentration
data did not agree too well with theory, perhaps because of
the concentration range used. Wolff (28) solved Equation 19
for a step change in inlet concentration using a nucleation
model which included a dependence on suspension density or
total crystal surface area. This model agreed qualitatively
with experimental results for the alum-ethanol-water system.
Use of either suspension density or total crystal surface
area in the nucleation model gave almost identical results.

THEORETICAL DEVELOPMENT

Effect of Solids in Suspension on Size Distribution

Several investigators have suggested that crystals already in suspension are a source of nuclei (15, 7, 28, 23). Powers (14) speaks of a "buffer reservoir layer" of stagnant fluid surrounding crystals in suspension in which nucleation occurs. Strickland-Constable and Mason (21) found that large numbers of new crystals are produced in the neighborhood of fractured dendritic growth. They also suggested attrition as a source of new crystal generation. The population balance, Equation 8, is not restricted to a particular manner of new particle generation, therefore, it is applicable for any particle formation mechanism as long as the new particles formed are near nuclei size and the proper kinetic model for particle generation is used.

In previous studies (12, 23) the fact that solids contribute to nucleation was recognized, but no quantitative analyses were performed because suspension density was usually kept constant. To recognize the effect of the amount of solids in suspension on nucleation rate, the following mass and area dependent models were proposed in an unpublished paper by Larson et al. (7):

$$\frac{dN^o}{dt} = k_M M^j s^i \qquad (24)$$

$$\frac{dN^o}{dt} = k_A \ A^h \ s^i \tag{25}$$

where the suspension density M is the mass of crystals per unit volume of slurry and the area A is the surface area of crystals per unit volume of slurry. The suspension density model is compatible with the boundary condition, Equation 21, for step changes in residence time since M remains constant. Each model incorporates a parameter directly related to the amount of solids in suspension, hence as will be seen they produce similar results. Area dependence is regarded as the more fundamental quantity in the understanding of heterogeneous nucleation. However, for practical reasons it is desirable to relate the heterogeneous effects to the suspension density, since it can be more easily and accurately determined.

In order to get these models in terms of experimentally measurable quantities, they may be combined with Equations 6 and 16 to give:

$$n^o = K_M \ M^j \ r^{i-1} \tag{26}$$

$$n^o = K_A \ A^h \ r^{i-1} \tag{27}$$

For constant M or A these reduce to a relationship where nucleation order i can be calculated for a set of three runs at different residence times just as the earlier model based on supersaturation alone. However, the objective here is to obtain data at different suspension densities and

suspension areas so that the exponents j and h can be calculated from steady state data.

In order to analyze the data it is necessary to derive an expression relating growth rate to suspension density or area. An unsteady state mass balance around the crystal-lizer involving suspension density and a constant environment gives:

$$\frac{d\ (C + M)V}{dt} = C_i\ Q_i - (C + M)Q_o \tag{28}$$

For small changes in supersaturation compared to the change in suspended solids, Equation 28 reduces to:

$$\frac{dM}{dt} = \frac{1}{T}\ (\Delta C - M) \tag{29}$$

where $\Delta C = C_i - C$, $T = V/Q$, and $Q_i = Q_o = Q$. At steady state $\Delta C = M$. The suspension density M may be related to the size distribution by:

$$M = \frac{k_V\ \rho \int_o^\infty n\ L^3\ dL}{V} \tag{30}$$

Equation 30 may be differentiated by the use of Leibnitz' rule. Combination with Equations 12 and 29 gives the following expression for growth rate in terms of ΔC and size distribution:

$$r = \frac{V\Delta C}{3k_V\ T\ \rho \int_o^\infty n\ L^2 dL} \tag{31}$$

where the integral in the denominator is proportional to the surface area of the crystal suspension. At steady state Equation 13 may be substituted into the integral in Equation

31 and ΔC may be replaced by M. Then integration of

Equation 31 gives:

$$r_o^4 = \frac{V\ M}{6\ k_V \rho n_o^o\ T_o^4} \tag{32}$$

Now for two steady state runs at different suspension

densities where all other conditions are held constant,

Equation 32 gives:

$$\left(\frac{r_{o_1}}{r_{o_2}}\right)^4 = \frac{M_1}{M_2}\left(\frac{n_{o_2}^o}{n_{o_1}^o}\right) \tag{33}$$

Substitution for n_o^o from Equation 26 into Equation 33 gives:

$$\frac{r_{o_1}}{r_{o_2}} = \left(\frac{M_2}{M_1}\right)^{\frac{j-1}{i+3}} \tag{34}$$

Special cases of this general equation will be used later to

show the effect of suspension density M on size distribution.

A similar relationship can be derived in terms of the

area of the crystal suspension A. At steady state M and A

can be calculated by substitution of Equation 13 into the

following expressions and integrating.

$$M = \frac{k_V \rho}{V}\int_o^\infty n\ L^3\ dL = \frac{6\ k_V \rho n_o^o\ (r_o\ T_o)^4}{V} \tag{35}$$

$$A = k_a \int_o^\infty nL^2\ dL = 2\ k_a\ n_o^o\ (r_o\ T_o)^3 \tag{36}$$

By combining Equations 33, 27, 35, and 36 for two levels

of suspension density, one obtains:

$$\frac{r_{o_1}}{r_{o_2}} = \left(\frac{A_2}{A_1}\right)^{\frac{h-1}{i+2}} \tag{37}$$

Nuclei population density can be expressed solely in terms of M or A respectively for two levels of M.

$$\frac{n^o_{o_1}}{n^o_{o_2}} = \left(\frac{M_1}{M_2}\right)^{\frac{i+4j-1}{i+3}} \tag{38}$$

$$\frac{n^o_{o_1}}{n^o_{o_2}} = \left(\frac{A_1}{A_2}\right)^{\frac{i+3h-1}{i+2}} \tag{39}$$

Finally it can be shown (17) that the dominant particle size on a weight basis is:

$$L_d = 3rT \tag{40}$$

This parameter which is extremely useful as an indicator of overall size distribution changes can be expressed in terms of M or A alone.

$$\frac{L_{d_1}}{L_{d_2}} = \left(\frac{M_2}{M_1}\right)^{\frac{j-1}{i+3}} \tag{41}$$

$$\frac{L_{d_1}}{L_{d_2}} = \left(\frac{A_2}{A_1}\right)^{\frac{h-1}{i+2}} \tag{42}$$

The consequences of the following values of j and h are of interest:

$$\text{Case I.} \quad j, h = 1 \tag{43}$$

Case II.   j, h, = o   (44)

Case III.   j, h > o ≠ 1   (45)

For Case I, nucleation rate depends linearly on M or A_o.
Growth rate is therefore unaffected by changes in suspension
density or area according to Equations 34 and 37. If data
represented by Equation 13 are plotted on semilog paper for
different levels of suspension density, one should obtain
parallel lines. This is due to the equal growth rates and
constant residence time which combine to give the same slope
for different suspension densities. Size distribution is
neither enhanced nor degraded by a change in the amount of
solids in suspension. This can readily be seen from Equations
41 and 42 where there is no change in L_d. The nuclei popu-
lation density ratio (Equations 38 and 39) varies linearly
with the M or A ratio as expected.

For Case II, when the nucleation rate is dependent on
supersaturation alone (homogeneous nucleation), the size
distribution is enhanced when the amount of solids in sus-
pension is increased. Also from Equations 41 and 42 it can
be seen that the lower the kinetic order i, the greater will
be the enhancement. It is obvious that a semilog plot of
Equation 13 will result in non-parallel lines, since the
growth rate and consequently the slope is proportional to M
or A raised to some power related to the kinetic order
(Equations 34 and 37). The intercept n_o^o will likewise be

dependent on M or A to some power including i. For an increase in solids, the intercept increases while the slope decreases if i is greater than one. Thus non-parallel lines which do not intersect for positive L will be obtained if Case II is an appropriate model.

For Case III there are two situations possible. First if j and h are greater than one, an increase in solids will cause a decrease in growth rate with a corresponding decrease in size distribution. However, nuclei population density will increase. This will produce non-parallel lines on a semilog plot of population density versus size which cross for positive size. This is due to the increase in intercept (n_o^o) accompanying the increase in slope $(-\frac{1}{r_oT_o})$. The second situation is for j and h greater than zero but less than one. Here some enhancement of the size distribution is expected for an increase in solids. However, as j and h approach one, the enhancement decreases.

The above analysis indicates that the operation of the crystallizer at different levels of suspension density will permit one to distinguish between heterogeneous and homogeneous nucleation effects. As discussed earlier, the relationship among the lines of a semilog plot of steady state Equation 13 for constant residence time and different suspension densities should establish the exponents j and h. Another method, for constant growth rate, would be to make

a log-log plot of $\frac{dN^o}{dt}$ versus M or A. The nucleation rate, $\frac{dN^o}{dt}$, could be obtained from Equation 16, M could be obtained directly, and A could be calculated from Equation 36. For constant growth rate, the slope of this log-log plot would be j or h in accordance with:

$$\frac{dN^o}{dt} = K_1 \, M^j \, r^i \qquad (46)$$

$$\frac{dN^o}{dt} = K_2 \, A^h \, r^i \qquad (47)$$

Effect of Residence Time on Size Distribution

The effect of residence time on steady state size distribution can be obtained from Equation 32, which when combined with Equation 26 for constant suspension density gives:

$$r_o = k_r \, (T_o)^{-\frac{4}{i+3}} \qquad (48)$$

Both nuclei population density and dominant particle size are expressible in terms of residence time alone for steady state conditions of constant suspension density.

$$n_o^o = k_n (T_o)^{\frac{4(1-i)}{i+3}} \qquad (49)$$

$$L_d = k_d (T_o)^{\frac{i-1}{i+3}} \qquad (50)$$

From Equation 50, which was originally derived by Randolph (15), it is apparent that size distribution can

increase, decrease, or remain constant with changes in residence time, depending on i. For the majority of crystal systems, i is greater than one and the size distribution increases with residence time. The higher the kinetic order of nucleation, the more pronounced is the increase. Thus one could substantially increase the size distribution of a higher order system by increasing the residence time. As i approaches one, residence time has less and less of an effect on the size distribution. For i = 1 both L_d and n_o^o are independent of residence time and r_o varies inversely with T_o. If a system has kinetics of this order, a very rapid production rate could be used without affecting the size distribution. For known system kinetics, Equation 50 should be of considerable value in the design and operation of industrial crystallizers, since it can be used to select the proper residence time to produce a desired size distribution.

EXPERIMENTAL

Equipment

Crystallizer

A continuous MSMPR cooling crystallizer was fabricated of stainless steel Panelcoil. Figure 1 shows its various features and dimensions. Near perfect mixing of the suspension was obtained after the unit was equipped with three baffles symmetrically spaced around the perimeter of the internal draft tube and extending to the outer wall. The volume of the vessel with draft tube in place was 10.5 liters. Cooling water was circulated through the walls of both the draft tube and the outer cylinder. All surfaces exposed to the suspension were electropolished to prevent surface nucleation and crystal buildup. Agitation was provided by a three inch diameter three-blade propeller located near the bottom of the draft tube. The propeller was driven by a 1725 rpm, one-fourth horsepower motor. Even with this much agitation, the sampled crystals showed no signs of significant attrition before sieving. The propeller circulated the suspension down through the draft tube and up through the annulus. No vortex was produced because of the baffles.

The feed was introduced at the surface of the suspension. Product was removed through a 3/8 inch line which was bent

Figure 1. Crystallization vessel
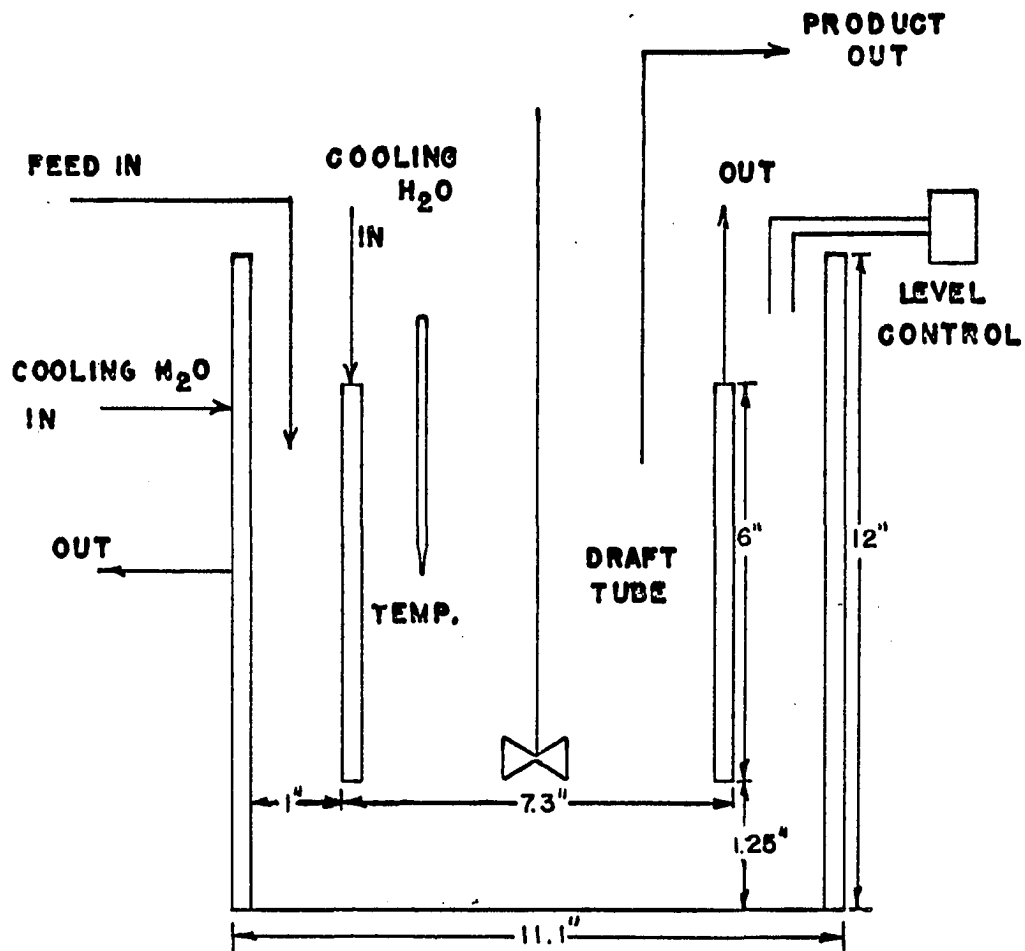
COOLING CRYSTALLIZER

slightly to dip into the suspension. Essentially constant

suspension volume was maintained by an on-off liquid level

controller. Two probes set at slightly different levels

were connected to a relay which started the product removal

pump when liquid contacted both probes. A time-delay relay

was used to lengthen the pumping time for high feed rates

so that the pump motor was not overheated by starting and

stopping. Since a known volume of suspension was pumped

for each time-delay setting, the contact probes were set at

a level so that the product removal line was cleared of

suspension by pumping air for the last two seconds of the

cycle. This prevented classification from particles settling

out in the line while liquid flowed back into the crystal-

lizer. A Jabsco rubber-impeller rotary pump was used for

product removal. It provided sufficient suction to withdraw

a mixed product from the crystallizer.

Auxiliary equipment

Figure 2 shows all the process equipment and the

material flow pattern. A stirred 30 gallon drum inside a

55 gallon drum was the source of unsaturated, heated con-

stant temperature feed. Temperature control was maintained

by heaters immersed in water circulated through the annulus

area between the drums.

Heated feed was continuously pumped through a filter

to a constant head tank with a centrifugal pump. From the

Figure 2. Flow diagram of crystallization system

    1. Constant head tank

    2. Product removal pump

    3. Temperature regulator

    4. Feed rotameter

    5. Feed thermometer

    6. Feed tank

    7. Temperature control relay

    8. Draft tube cooling water rotameter

    9. Crystallizer cooling water rotameter

  10. Crystallizer

  11. Immersion heater

  12. Constant temperature bath circulating pump

  13. Feed pump

  14. Level control relay
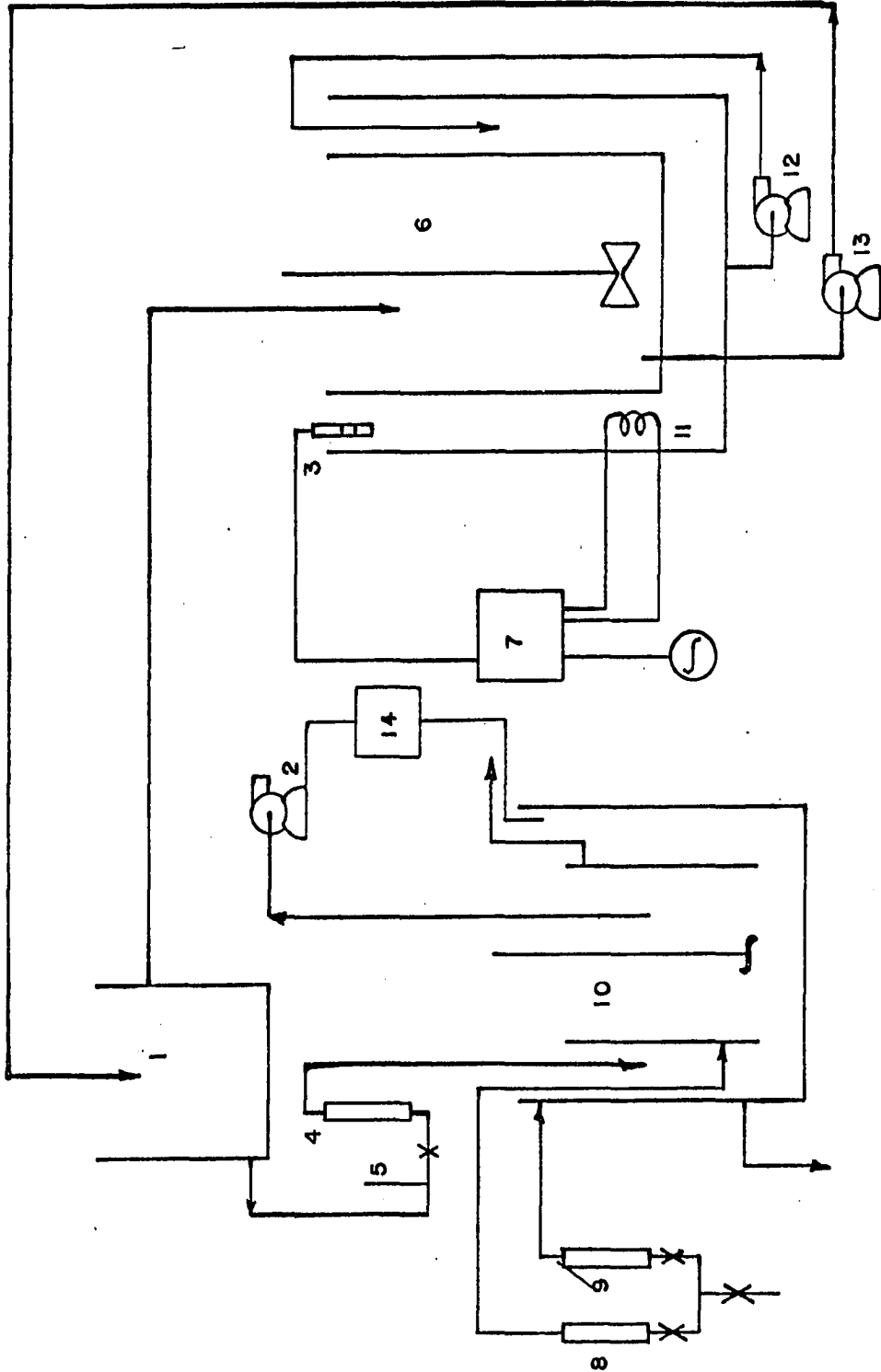
constant head tank, the feed flowed through a rotameter to the crystallizer where it was cooled by circulation of water through the walls of the vessel and through the draft tube. Rotameters and thermometers were installed in the cooling water lines so that the amount of heat removed from the crystallizer by the cooling water could be calculated. An evacuated, calibrated suction flask was used for sampling the suspension directly rather than taking a sample from the effluent because of the probability of particle breakage in the product removal pump.

Crystal sizing equipment

A calibrated set of 3 inch, U.S. Standard sieves was used in conjunction with a Model A Coulter Counter for size distribution analysis   All samples were sieved in the same manner and for the same length of time with a Ro-Tap testing sieve shaker. The Coulter Counter was used for analysis of the crystals which were too small for accurate sieving.

Theory of the Coulter Counter

The Coulter Counter determines the number and size of particles dispersed uniformly in an electrically conductive liquid. This is done as shown in Figure 3 by forcing the suspension to flow through a small aperture having an immersed electrode on either side. As a particle passes through the aperture, it changes the resistance between

Figure 3. Schematic diagram of Coulter Counter

THRESHOLD

MAIN AMPLIFIER

CIRCUIT

PULSE AMPLIFIER

PULSE BRIGHTENING SIGNAL

ABOVE THRESHOLD

HORIZONTAL SWEEP

SCOPE

COUNTER DRIVER

DIGITAL REGISTER

COUNTER "START - STOP"
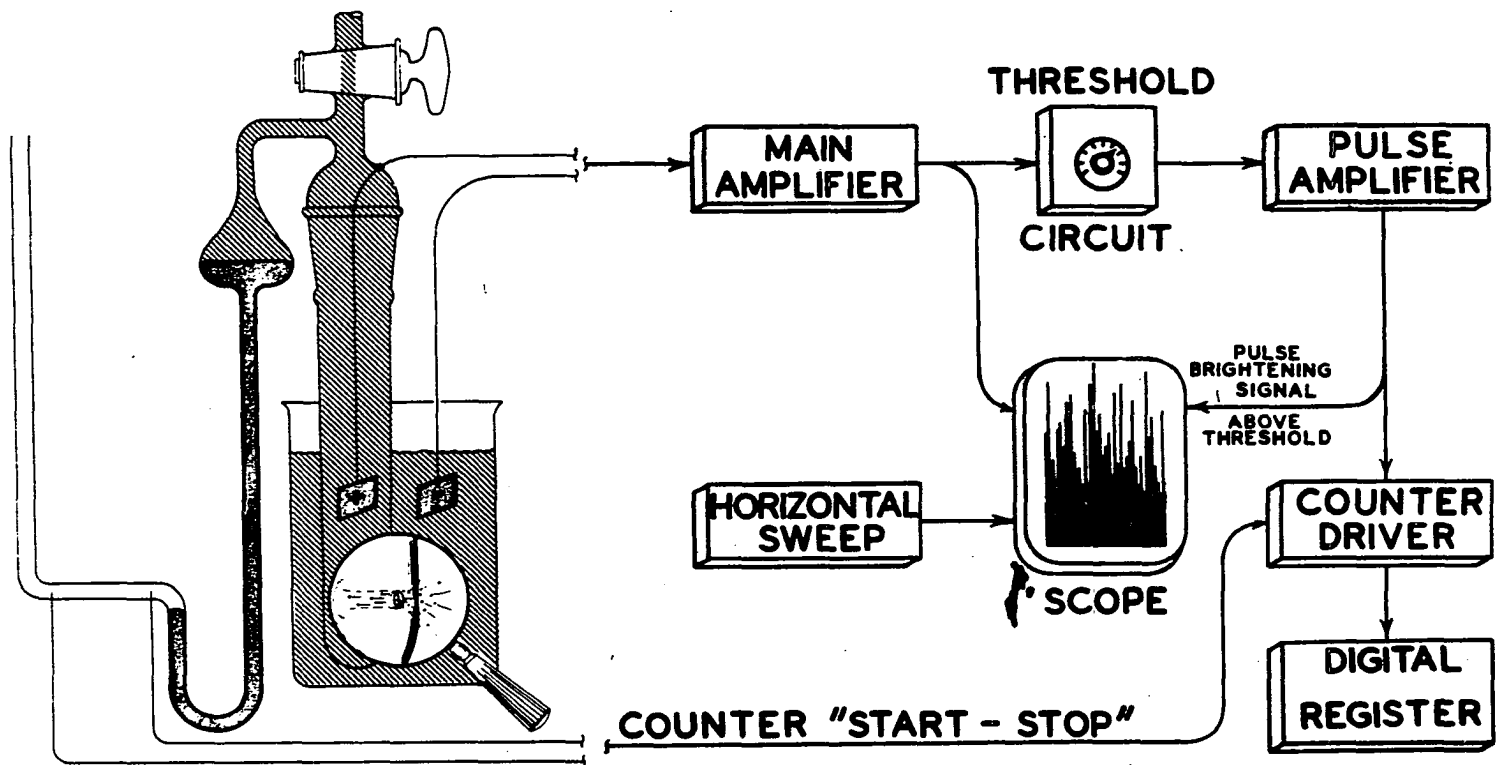
the electrodes producing a voltage pulse of magnitude proportional to particle volume. Voltage pulses are amplified and fed to a threshold circuit having an adjustable threshold level. A pulse is counted and appears on a digital register when the threshold level is reached or exceeded. Calibration with a suspension of mono-sized spheres permits the translation of threshold levels into equivalent spherical diameters.

When making a count, the vacuum stopcock is opened and a controlled external vacuum initiates flow through the aperture. This unbalances the mercury siphon and when the stopcock is closed to the vacuum pump, the siphoning action of the mercury continues the sample flow. Then the advancing mercury column makes contact with start and stop probes to activate the electronic counter. The probes are located precisely 2 ml. apart providing a constant sample volume for all counts.

Interchangeable aperture tubes are available for counting particles in different size ranges. Pulse height and instrument response are proportional to particle volume, and to fluid resistivity for particles up to 30 or 40 percent of the aperture diameter. The particle resistivity has very little or no effect. A particular aperture should not be used to count particles smaller than about 10 percent of the aperture diameter because of coincident particle passages.

The counts can be precisely corrected for the passage of more than one particle at a time through the aperture as long as the correction does not exceed 5 to 10 percent of the count. Results are expressed in spherical equivalents because the counter discerns the particles on the basis of their volume rather than their shape.

Materials

The alum used was aluminum ammonium sulfate, $Al_2(SO_4)_3$ $(NH_4)_2 SO_4 \cdot 24 H_2O$. It was sold as "Ammonium Alum, Code 125, Rice Statuary" by the General Chemical Division, Allied Chemical Corporation in 100 pound bags.

Uncoated, "pure and clean" ammonium sulfate, $(NH_4)_2SO_4$, was donated by Phillips Petrolium Company in 100 pound bags.

Procedure

Feed preparation

Feed of the desired concentration was prepared initially by mixing the material to be crystallized with distilled water. Sixty gallons of feed were required for a steady state run, while twice as much was needed for a transient run. It was necessary to heat the mixture to get all the solids into solution. The feed solutions were filtered prior to the runs to remove any extraneous undissolved material.

Because of the large quantity of feed required, it was prepared in a set of two or three stainless steel drums depending on the nature of the run. To insure that all the drums were of equal concentration, the feed was circulated among them by a series of pumps prior to startup. Since it was necessary to keep the feed at a fairly high temperature (100-130°F) to prevent crystallization, concentration changes due to evaporation were troublesome.

Before each run it was necessary to collect samples from each drum. The samples were evaporated to dryness and weighed to obtain the concentration in the drum. If the concentration was unacceptable, the weight of the solution in the drum was calculated by measuring the volume of solution and converting it to weight by multiplying by the solution density. The amount of water or crystalline material needed to bring the solution to the desired concentration was calculated from a material balance, and was added to the solution. Samples of the newly prepared solution were taken and the process repeated until the desired concentration was obtained. This painstaking feed preparation was necessary because runs of constant suspension density were made in sets of three and slight deviations in the feed concentration from run to run would, on occasion, cause large variations in suspension density.

Operation of the crystallizer for steady state and transient runs

After the desired feed concentration was achieved, the crystallization equipment was prepared for startup. The feed was stirred and heated to a temperature 10°F above its saturation point in a 30 gallon drum submerged in a constant temperature bath. When the last traces of solids disappeared the feed was pumped to a constant head tank from which it flowed through a rotameter into the crystallizer. A filter was installed above the constant head tank to remove any extraneous material which had escaped earlier filtration. The feed flow rate was adjusted to give the proper residence time. After the crystallizer was filled, the agitator was started and the cooling water valves were opened. The level controller and the product removal pump were put into operation. Cooling water rates were adjusted until the temperature in the crystallizer remained constant at 72° F. From this point on for a steady state run the operation was automatic except for periodic checking of the suspension and feed temperatures, rotameter readings, and solution volume in the constant temperature feed drum. Temperature fluctuations of 1 to 2°F occurred during several runs, but these were always of short duration. Feed samples were taken every four to five residence times. Sampling of the crystal suspension was begun after 12-16 residence times

had elapsed. It was found that this amount of time was necessary for the largest size fraction of the crystals to approach steady state. Four or more samples were taken until 20 residence times had elapsed. If the population density of corresponding size fractions of these samples did not vary, the steady state condition was confirmed.

The preparations for a transient run were similar to those for a steady state run except 120 gallons of feed of the same concentration was prepared. Initially a residence time of 45 minutes was maintained for 20 residence times or 15 hours. This gave the steady state size distribution used as an initial condition for the solution of the transient equation. The residence time was then decreased stepwise to 15 minutes by a threefold increase in feed flow rate. The cooling water rates were increased to maintain a constant temperature of 72°F in the suspension. Sampling during the 45 minute portion of the transient run was carried out as for any steady state run. However, after the step change in residence time, samples of the suspension were taken every 15 minutes for twenty residence times until steady state was again attained.

Sampling and filtration

Samples of the crystal suspension were removed by vacuum into a suction flask of calibrated volume. This procedure permitted rapid withdrawal of a portion of the

mixed suspension and eliminated possibilities of classification during sampling. Samples taken from different locations in the crystallizer showed the same size distribution. This indicated that the suspension was perfectly mixed. Samples ranging in volume from 100 to 500 ml. were taken depending on the suspension density.

The samples were rapidly filtered by suction immediately after withdrawal from the crystallizer. A fritted-disc, Buchner type funnel of 40-60 micron pore size was used for filtration. All the crystals were washed from the sampling flask with filtrate. The filtrate was saved for evaporation so that a material balance around the crystallizer could be made. After most of the mother liquor had been drawn off, the suction was stopped and the crystals were washed on the filter with acetone. The suction was then continued until the crystals were dry enough for easy removal from the filter. Then they were removed and scattered out on a paper for further drying before weighing. When the filtration and drying were carried out carefully, neither alum nor ammonium sulfate formed agglomerates.

Sieve and Coulter Counter analyses of the sample

The weighed, dry crystals were sieved in a nest of calibrated, 3 inch, U.S. Standard sieves. Agitation was provided by a RoTap testing sieve shaker. Each sample was shaken for five minutes. No change in the weight of crystals

on each sieve occurred if the crystals were shaken longer than five minutes. Sieves of the following mesh and aperture sizes were used for alum, where the apertures expressed in microns are in parenthesis: 16(1190), 18(1000), 20(840), 25(710), 35(500), 40(420), 50(297), 70(210), 100(149), 140 (105), 200(74), and the pan. The larger size distribution for ammonium sulfate left so few crystals on the last two sieves that these sieves were discarded leaving the 100 mesh sieve directly above the pan. Each size fraction was removed from the sieve, by brushing the back of the wire mesh, and placed in weighed two ounce sample bottles. The bottles were weighed again and the weight of the crystals in each size fraction was obtained by difference.

The Coulter Counter was used to count the number of crystals in the 40-150 micron size range. The theory of its operation was previously explained. As previously mentioned, interchangeable aperature tubes were available for counting crystals in different size ranges. Aperture tubes of 560 and 280 microns diameter were used for counting alum. Only the 560 micron tube was used for ammonium sulfate. Because of the scarcity of small crystals in this system, the two smallest sieves were not used. Therefore the fines contained crystals ranging in size up to 149 microns -- the aperture diameter of the sieve above the pan. The 280 micron aperture tube was unsuitable to count these fines because of their size.

Crystals from both systems were counted in a 4 percent
by weight solution of ammonium thiocyanate in isopropanol.
Both alum and ammonium sulfate were insoluble in this
electrically conductive medium. Insolubility of the crystals
in the medium was very important because of the very small
amount of sample required for counting. The solution resis-
tivity and background counts were checked for each run before
the crystals were added to the solution.

Mono-sized particles were dispersed in the electrolyte
solution for calibration of each aperture tube. This per-
mitted the calculation of a constant, which was characteristic
of the electrolyte solution used. From this constant,
instrument settings corresponding to different particle sizes
were determined.

For alum the 280 micron tube was used first to count
the fines or crystals of diameter less than 74 microns. The
weight of sample dispersed in the electrolyte solution was
calculated by difference. Fifty milligrams in 400 ml. of
solution gave reasonable counts for this aperture. Agitator
speed in the baffled beaker was set to uniformly disperse
the crystals. At least three counts were made for each
threshold setting corresponding to a given particle size and
the counts were averaged. This average number was corrected
for coincident particle passages. Two sets of different
threshold settings for the same particle sizes were used on

each sample to check the counter. The results were essentially the same.

A composite sample of the fines and of the crystals from the last two sieves was mixed for counting with the 560 micron aperture. With this aperture, particles of average sizes from 65 to 140 microns were counted, providing data which overlapped that determined by the 280 micron aperture and the last two sieves. A greater amount of sample (0.1 to 0.15 grams) was required for this aperture because of the smaller number of particles of larger size. The greater volume of suspension withdrawn prior to each count because of the larger aperture permitted only one set of threshold settings per count sample. In order to check the uniformity of the mixture of crystals in the sample bottle, another sample from the same bottle was dispersed and counted using the same settings. The results were equivalent. The same procedure was used to count ammonium sulfate crystals with the 560 micron aperture except only the fines were used due to the elimination of the last two sieves as previously explained.

RESULTS

Analysis of Data

Population densities were obtained from a sieve analysis and in the small size range from a Coulter Counter. Since a sieve analysis gives the size distribution in terms of weight, a conversion to number of particles was necessary to calculate population densities. A volumetric shape factor k_v was used to make this conversion. Because alum has a regular octahedral habit, its volumetric shape factor can be readily determined in terms of the length of one edge. For an octahedron the shape factor $k_v = 0.4714$. The habit of ammonium sulfate as shown in Figure 4 was such that at best only an approximate volumetric shape factor could be found. Actual k_v's for ammonium sulfate were calculated by two different methods as explained in Appendix B. However, since the calculated k_v's based on the second largest dimension of the crystal, ranged in value from 0.95 to 1.35, an assumed value of 1.0 was used. Using an assumed shape factor shifts the population density of all sieve fractions by a constant amount, therfore, the size distribution determined by sieving was not affected.

The following procedure was used to obtain population density as a function of size for the sieves:
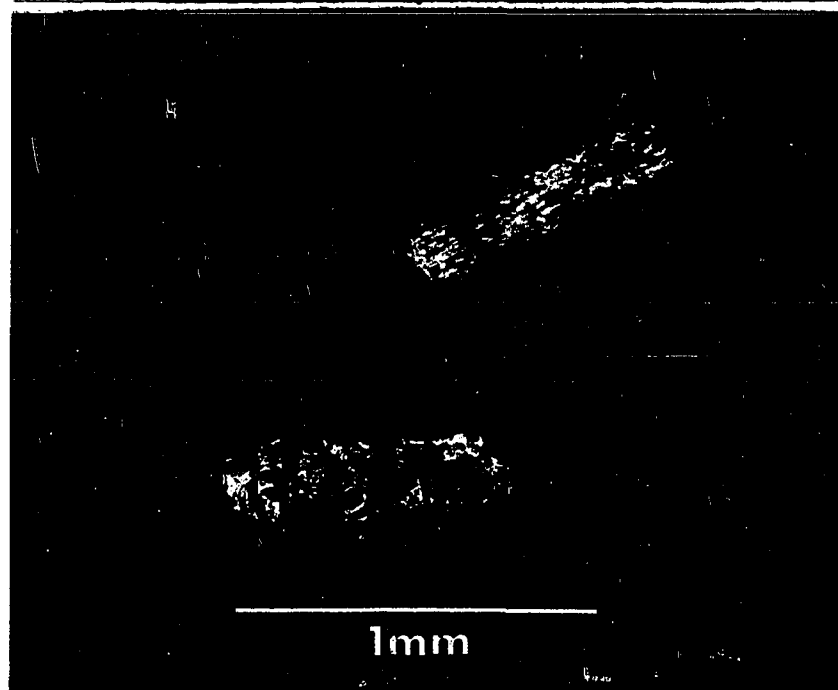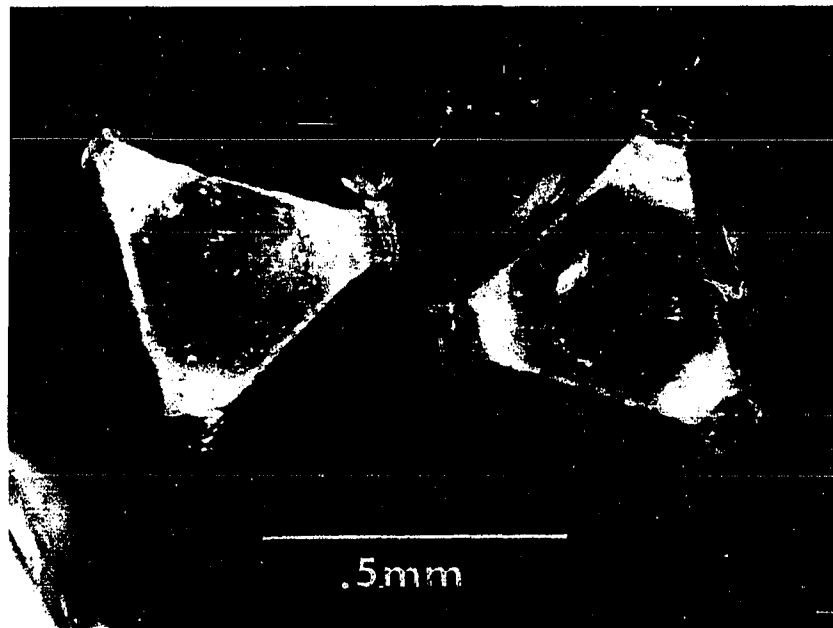
   a) The arithmetic average diameter L of each size

Figure 4. Photomicrograph of ammonium alum and ammonium
           sulfate crystals

           Ammonium alum crystals, + 40 - 35 mesh*

           Ammonium sulfate crystals, + 50 - 40 mesh*

           _____

           * U.S. Standard mesh

.5mm

1mm

fraction was determined.

b) The total weight W of crystals of a given size fraction was divided by the crystal density ρ, the cube of the average diameter L^3, and the volumetric shape factor k_v. This gives the number of crystals in the size fraction.

c) The population density of crystals in each size fraction was obtained by dividing the number of crystals in each fraction by the width ΔL of the fraction. ΔL is the difference in aperture diameter between successive sieves.

d) The population density of crystals in the crystallizer was found by multiplying by the ratio of the crystallizer volume V to the suspension sample volume v. The equation used to calculate the population density is:

$$ n = \frac{W}{\rho k_v L^3 \Delta L} \frac{V}{v} \tag{51} $$

where the variables in the equation are defined above. The values of ΔL for different sieve fractions were not equal because of the way in which the sieves were constructed.

Population density data for small sizes were calculated from the Coulter Counter size analysis by the following equation:

$$ n = \frac{\Delta N}{\Delta L} \frac{v_e}{v_c} \frac{w_t}{w_e} \frac{V}{v} \tag{52} $$

where ΔN is the number of particles counted of average size L in size increment ΔL, v_c is the volume of electrolyte

traversing the aperture while the count is made, w_e is the grams of crystals dispersed in the total volume of electrolyte v_e, w_t is the total weight of crystals selected for counting from the suspension sample volume v, and V is the crystallizer volume.

The Coulter Counter counts the number of particles, of particle volume greater than a given particle volume, that pass through an aperture while dispersed in a precisely known volume of electrolyte. While the correct number of crystals of a given volume is counted, the number is reported in terms of the diameter of a sphere of equivalent volume for non-spherical crystals. This created no question as to the continuity of sieve and Coulter Counter data for alum, since its known shape factor of 0.471 is approximately equal to that of a sphere $(\pi/6)$. However, for ammonium sulfate with a shape factor close to 1.0, it was necessary to calculate the magnitude of the error due to the reporting of Coulter Counter data in terms of the diameter of an equivalent sphere instead of a characteristic dimension of the crystal. The volume of an actual crystal in terms of its characteristic dimension D may be equated to the volume of a sphere of diameter L because the counter cannot distinguish between crystals on a volume basis.

$$V_{crystal} = V_{sphere} \qquad (53)$$

$$k_v D^3 = \frac{\pi}{6} L^3 \tag{54}$$

$$D = \left(\frac{\pi}{6 k_v}\right)^{1/3} L \tag{55}$$

For $k_v = 1.0$:

$$D = 0.806 \, L \tag{56}$$

Now when population density is calculated as a function of L and D respectively, the following equations are obtained:

$$n(L) = K_c \frac{\Delta N}{\Delta L} = K_c \left(\frac{N_{L_2} - N_{L_1}}{L_2 - L_1}\right) \tag{57}$$

$$n(D) = K_c \left(\frac{N_{L_2} - N_{L_1}}{D_2 - D_1}\right) \tag{58}$$

By taking the ratio of population densities and substituting for D in terms of Equation 56, the effect of the differing shape factor is obtained.

$$\frac{n(D)}{n(L)} = \frac{L_2 - L_1}{D_2 - D_1} = \frac{L_2 - L_1}{0.806 \, (L_2 - L_1)} = 1.24 \tag{59}$$

While the computed population density is increased by using Equation 59, the average particle size corresponding to the population density in each size increment is decreased by using Equation 56. The change from the spherical value in each case is 24 percent and 19 percent respectively. When the data are used to make a semilog plot of population density versus size, these two effects tend to compensate for each other and give points which lie on the line of

negative slope determined by the sieve analysis.

Considering the scatter of the Coulter Counter data, the error due to the use of the diameter of an equivalent sphere was not serious enough to affect the steady state plots significantly. The continuity of the sieve and counter data without correction further suggested that the error was not significant. Finally it should be noted that the conversion to the characteristic crystal dimension was made by multiplying the diameter of an equivalent sphere by the cube root of the ratio of the shape factors. The shape factor of a crystal must be more than 1.0 for the cube root of this ratio to deviate greatly from 1.0 and thus seriously affect Coulter Counter data based on the diameter of an equivalent sphere.

<div align="center">

Steady State Determination of Growth

and Nucleation Rates

</div>

For a continuous MSMPR cooling crystallizer operating at steady state, Equation 13 is applicable. Therefore semi-log plots of population density versus crystal size result in a linear relationship with a slope proportional to $(- \frac{1}{r_o T_o})$ and an intercept equal to the nuclei population density (n_o^o). Figures 5 through 22 show that the steady state crystallization of alum and ammonium sulfate proceeds according to Equation 13. Three sets of runs of 15, 30, and

Figure 5.   Size distribution of ammonium alum in terms of
            population density

            Residence time = 15 minutes
            Suspension density = 5.0 grams crystals per
            100 milliliters suspension

            Δ - Coulter Counter
            0 - Sieve

Figure 6. Size distribution of ammonium alum in terms of
population density

Residence time = 30 minutes
Suspension density = 5.5 grams crystals per 100
milliliters suspension

O - Sieve

Figure 7.   Size distribution of ammonium alum in terms
             of population density

             Residence time = 45 minutes
             Suspension density = 5.3 grams crystals per
             100 milliliters suspension

             Δ - Coulter Counter
             0 - Sieve

Figure 8. Size distribution of ammonium alum in terms
          of population density

          Residence time = 15 minutes
          Suspension density = 9.0 grams crystals per
          100 milliliters suspension

          Δ - Coulter Counter
          0 - Sieve

Figure 9. Size distribution of ammonium alum in terms
of population density

Residence time = 30 minutes
Suspension density = 10.5 grams crystals per
100 milliliters suspension

Δ - Coulter Counter
0 - Sieve

Figure 10. Size distribution of ammonium alum in terms
            of population density

            Residence time = 45 minutes
            Suspension density = 14.7 grams crystals per
            100 milliliters suspension
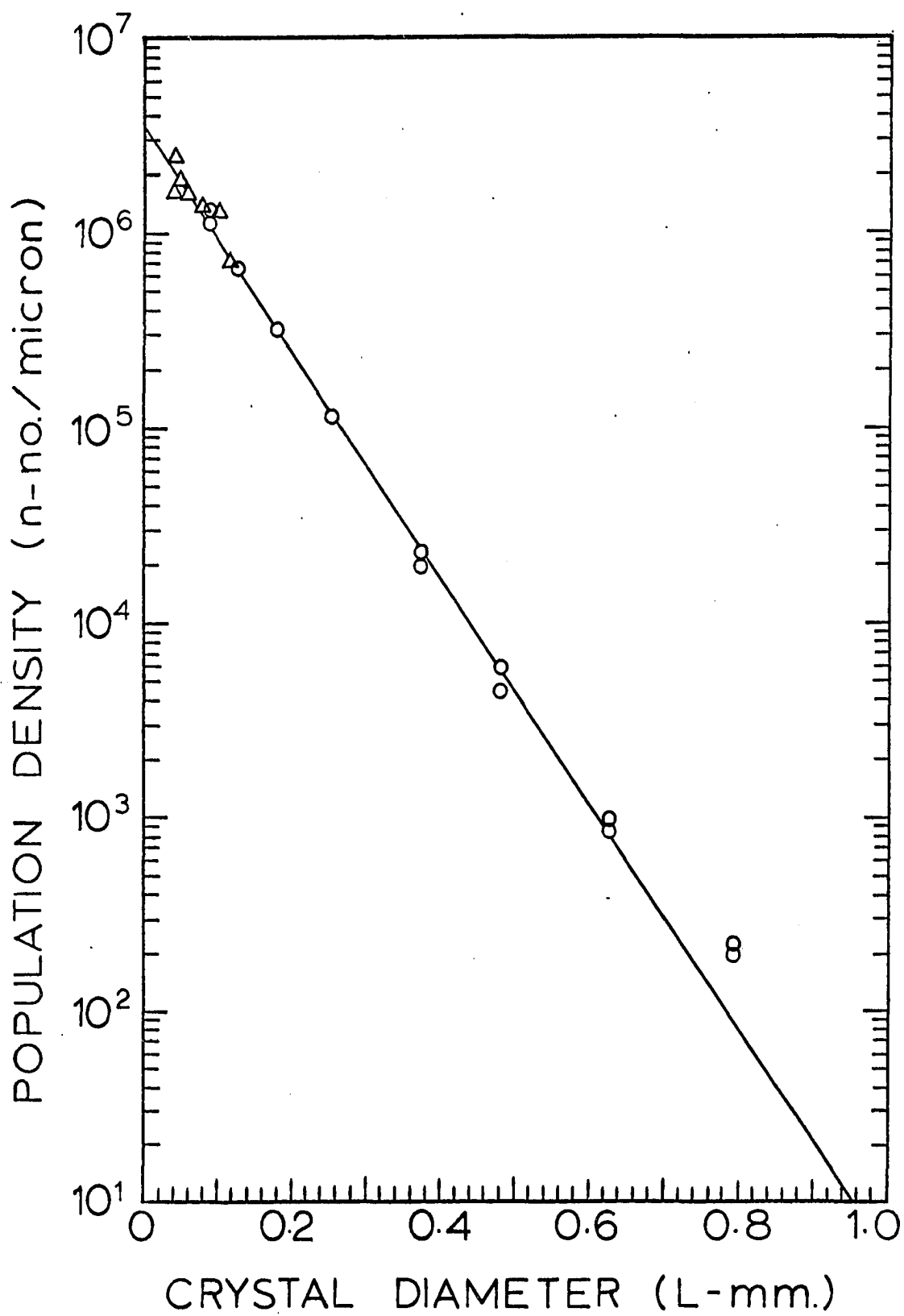
            Δ - Coulter Counter
            0 - Sieve

Figure 11.   Size distribution of ammonium alum in terms
             of population density

             Residence time = 15 minutes
             Suspension density = 21.9 grams crystals per
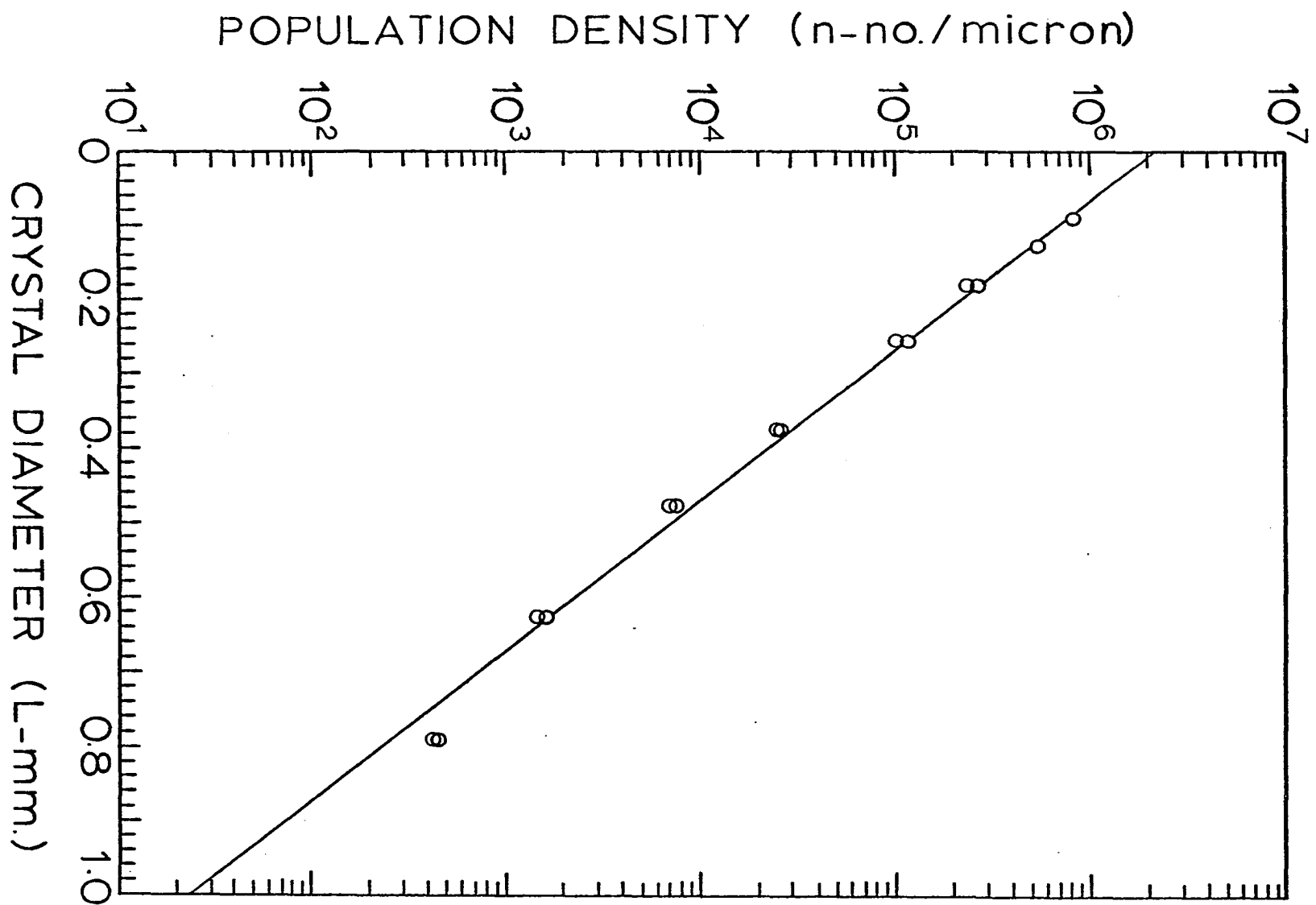   100 milliliters suspension

             Δ - Coulter Counter
             0 - Sieve

Figure 12.   Size distribution of ammonium alum in terms
             of population density

             Residence time = 30 minutes
             Suspension density = 22.0 grams crystals per
             100 milliliters suspension
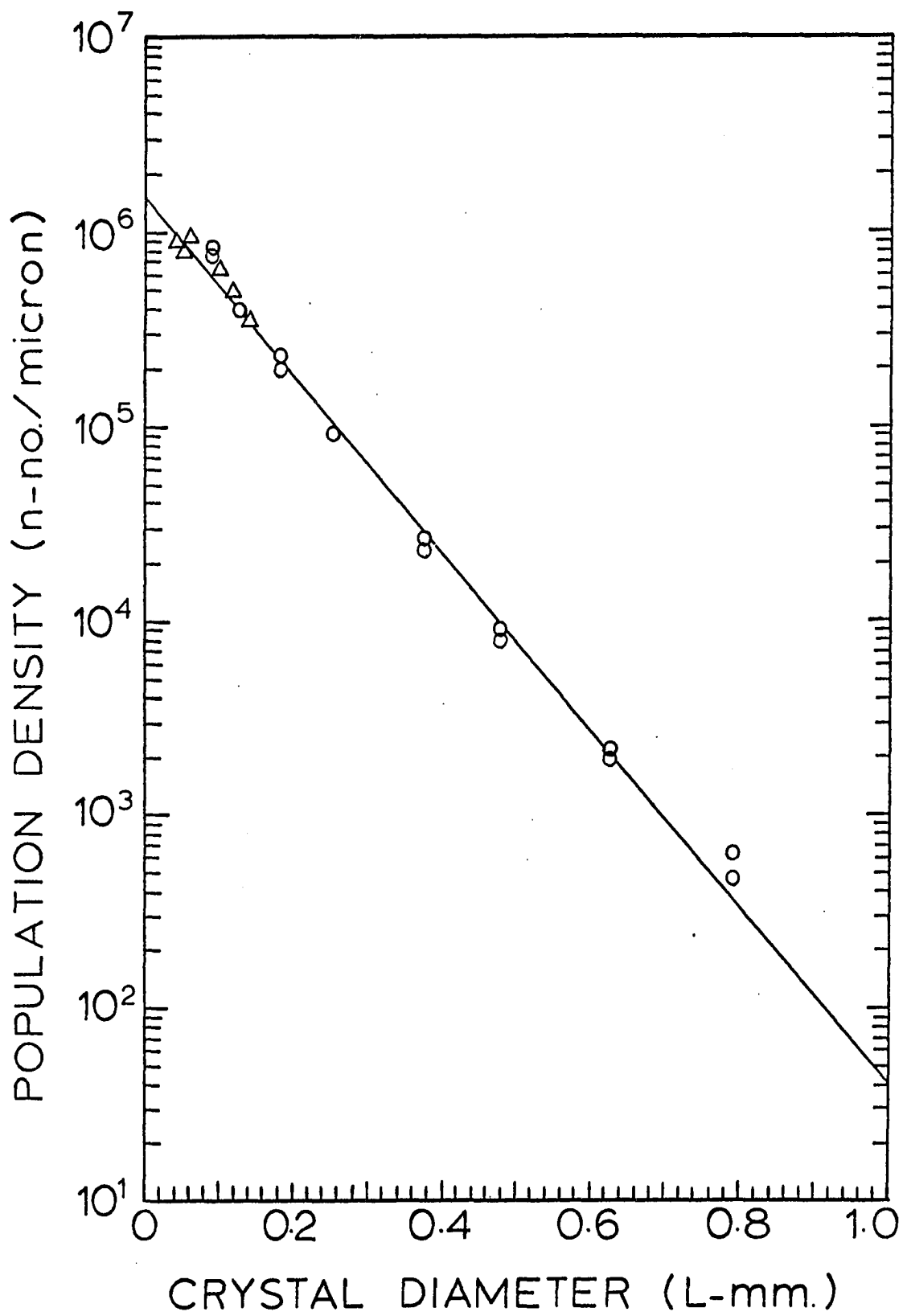
             Δ - Coulter Counter
             0 - Sieve

Figure 13. Size distribution of ammonium alum in terms
            of population density

            Residence time = 45 minutes
            Suspension density = 22.2 grams crystals per
            100 milliliters suspension

            Δ - Coulter Counter
            0 - Sieve .

Figure 14.   Size distribution of ammonium sulfate in
              terms of population density

              Residence time = 15 minutes
              Suspension dnesity = 2.55 grams crystals per
              100 milliliters suspension
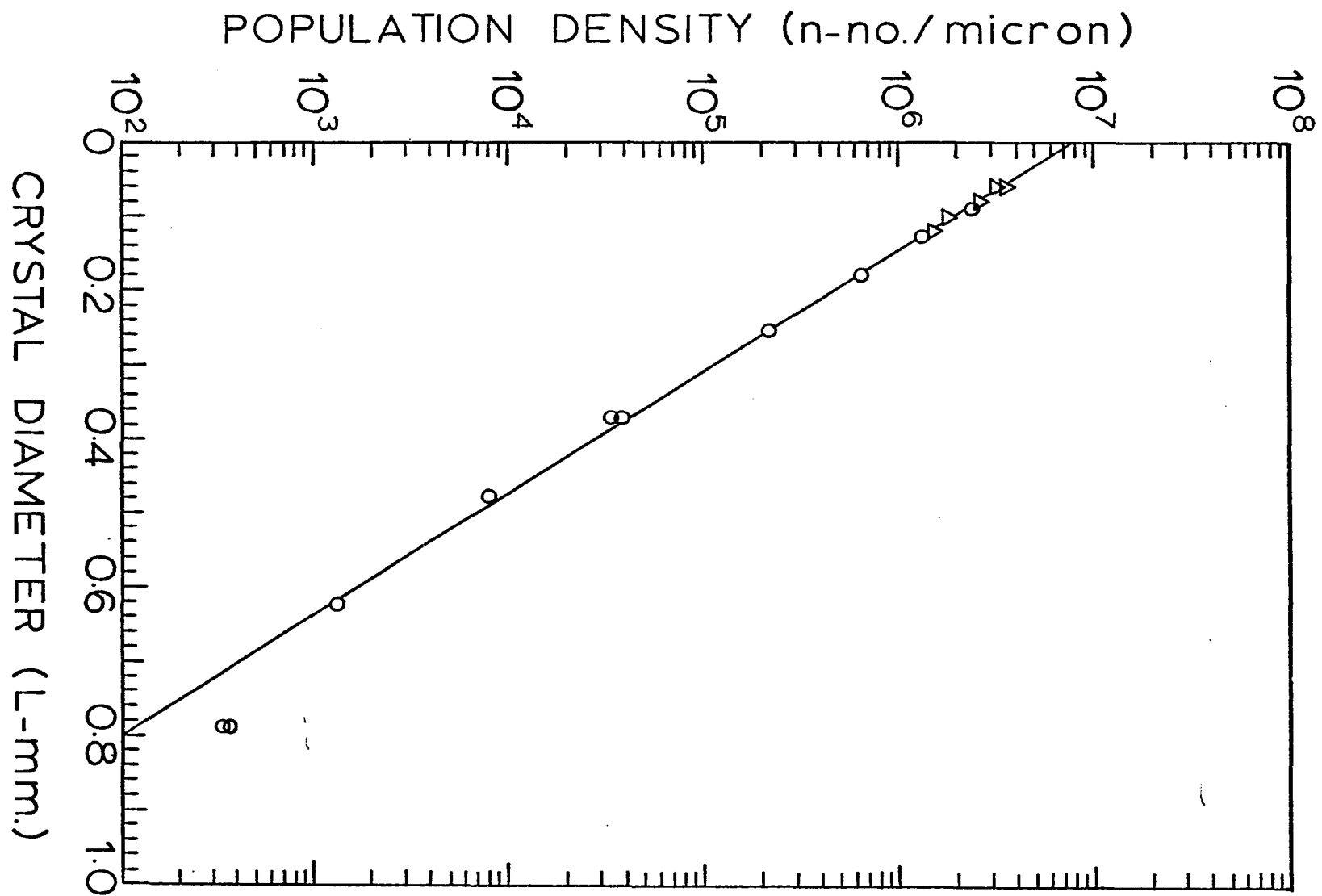
              Δ - Coulter Counter
              0 - Sieve

Figure 15. Size distribution of ammonium sulfate in terms
            of population density

            Residence time = 30 minutes
            Suspension density = 3.16 grams crystals per
            100 milliliters suspension
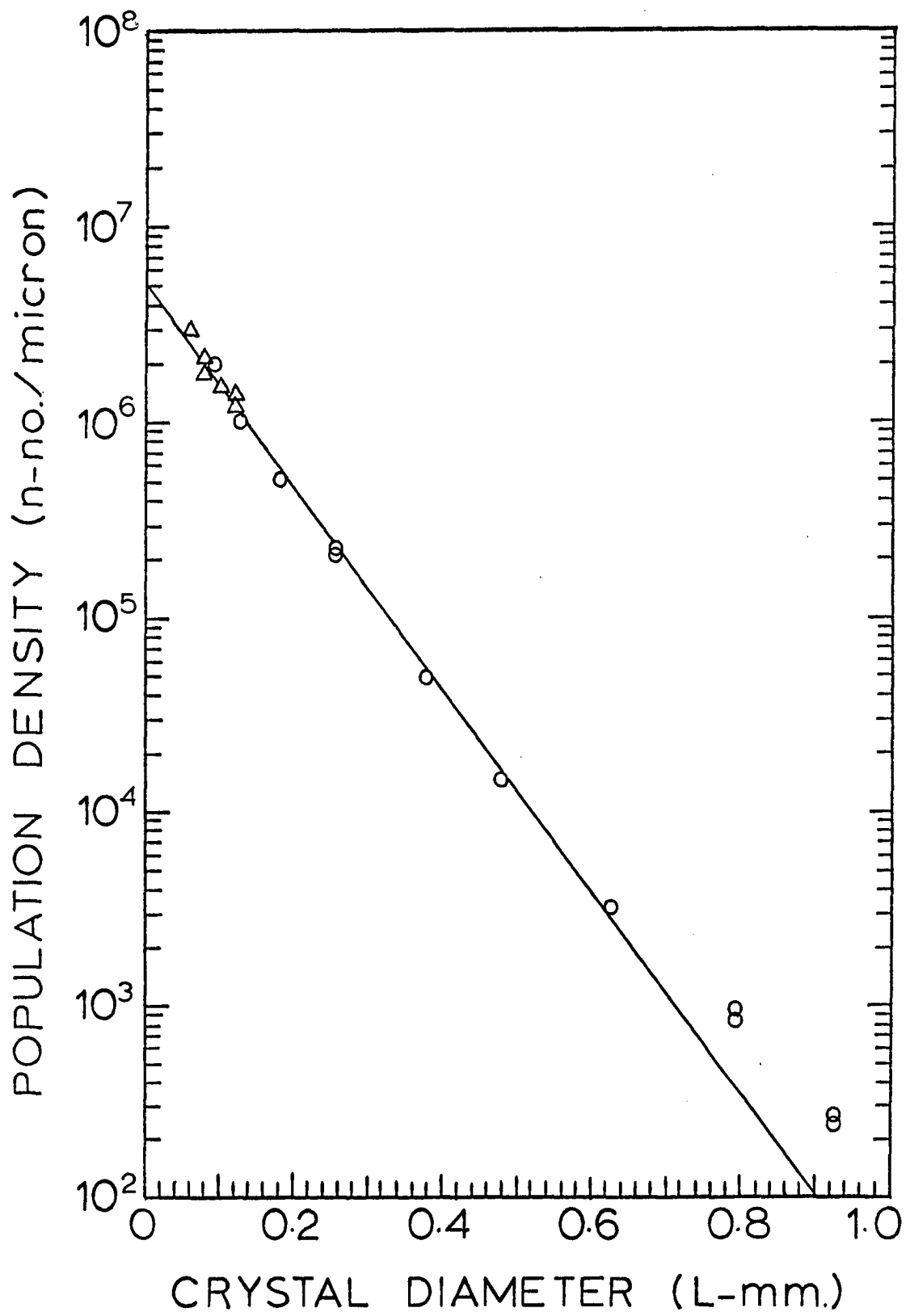
            Δ - Coulter Counter
            0 - Sieve

Figure 16. Size distribution of ammonium sulfate in terms
            of population density

            Residence time = 45 minutes
            Suspension density = 3.36 grams crystals per
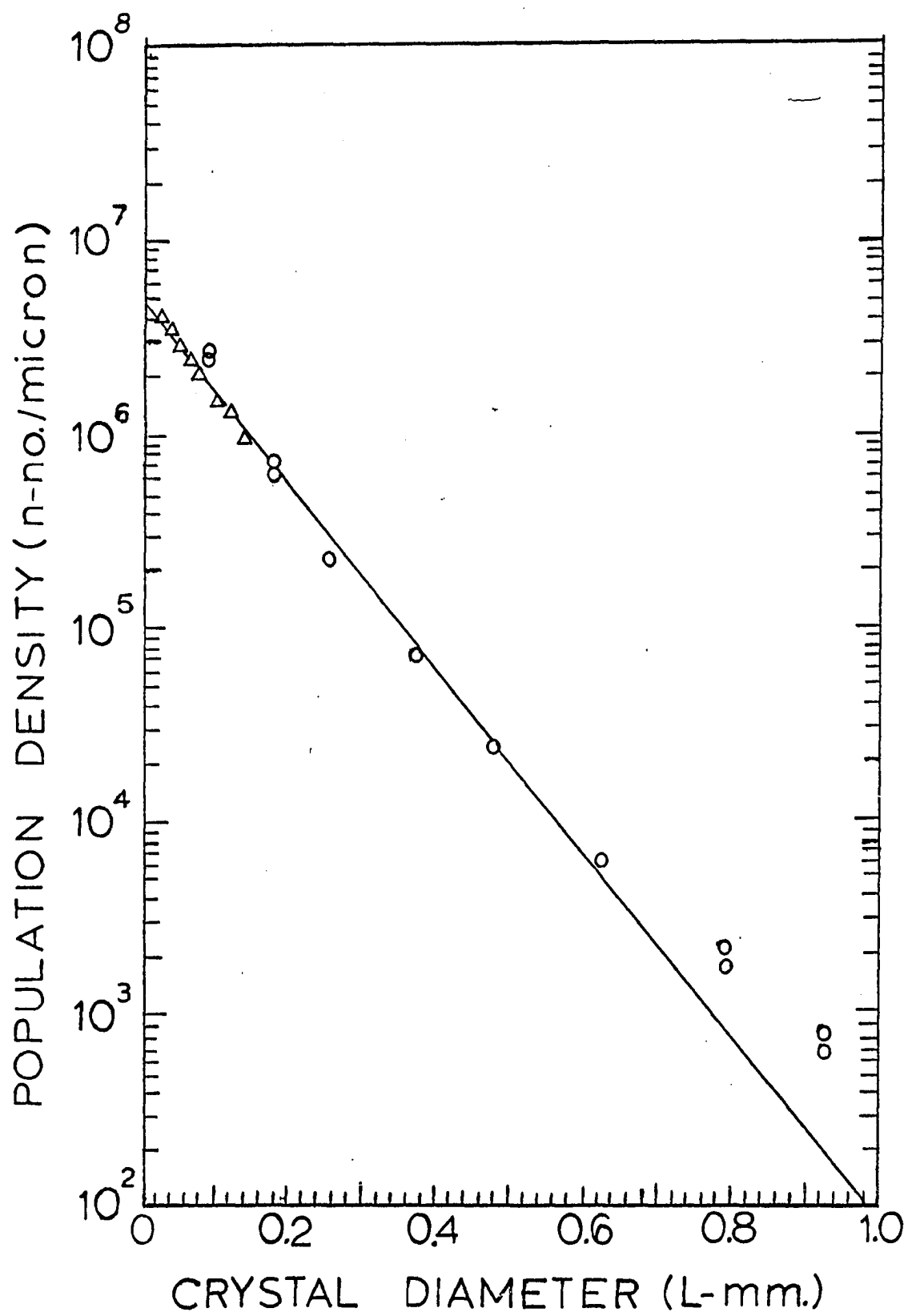   100 milliliters suspension

            Δ - Coulter Counter
            0 - Sieve

Figure 17. Size distribution of ammonium sulfate in terms
of population density

Residence time = 15 minutes
Suspension density = 3.92 grams crystals per
100 milliliters suspension

Δ - Coulter Counter
0 - Sieve

Figure 18. Size distribution of ammonium sulfate in terms
            of population density

            Residence time = 30 minutes
            Suspension density = 4.01 grams crystals per
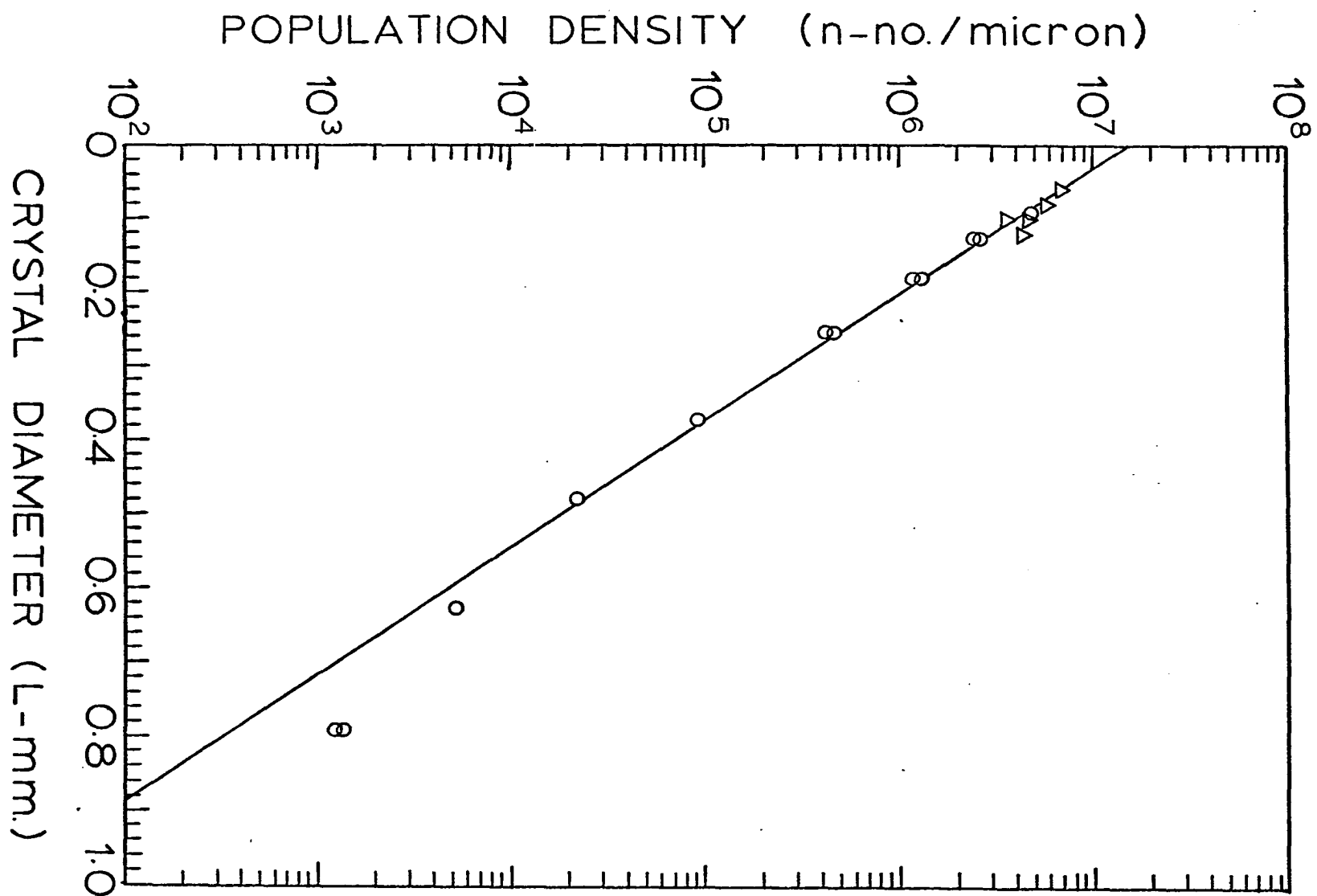   100 milliliters suspension

            Δ - Coulter Counter
            0 - Sieve
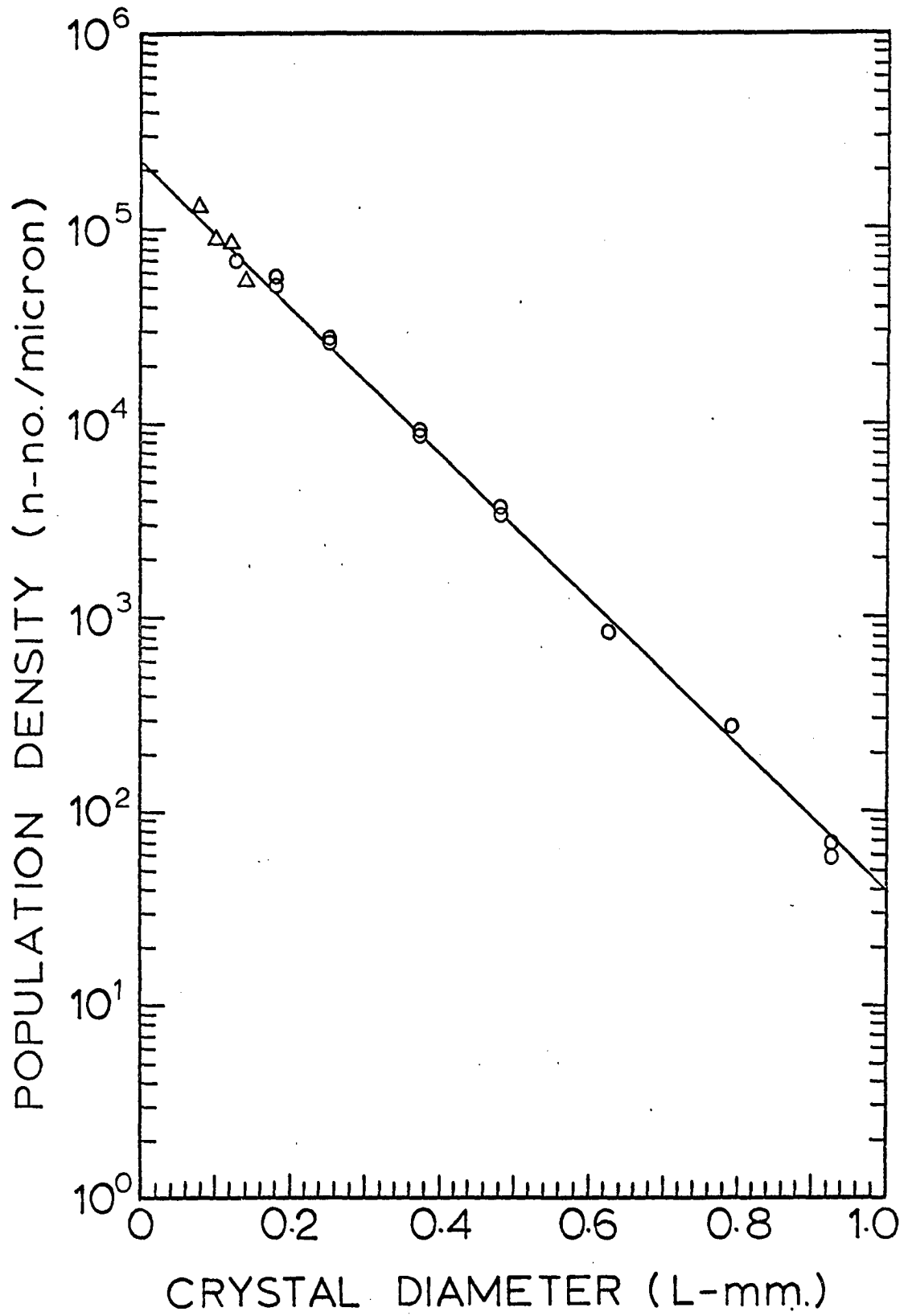
Figure 19. Size distribution of ammonium sulfate in terms
of population density

Residence time = 45 minutes
Suspension density = 4.33 grams crystals per
100 milliliters suspension
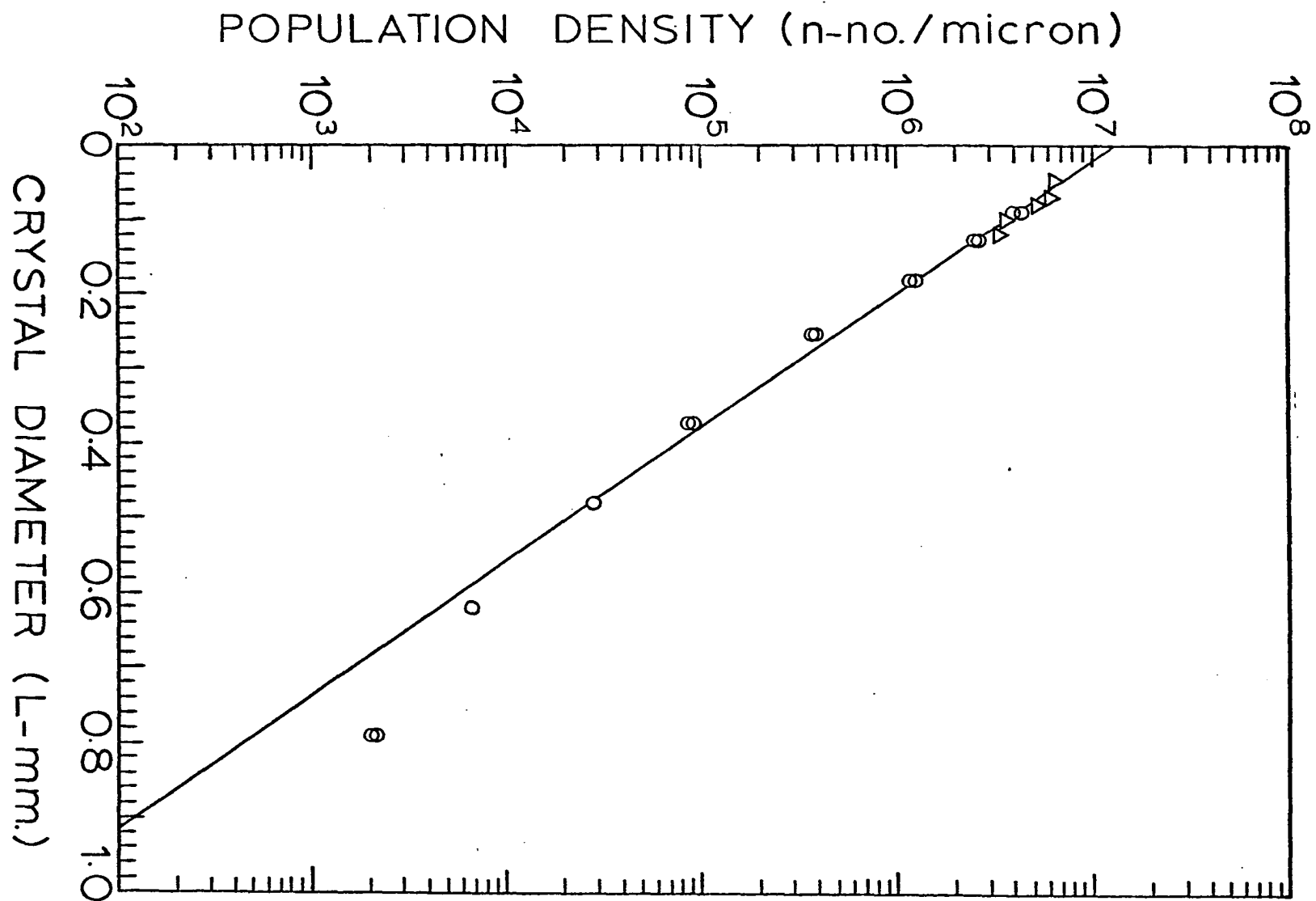
Δ - Coulter Counter
O - Sieve
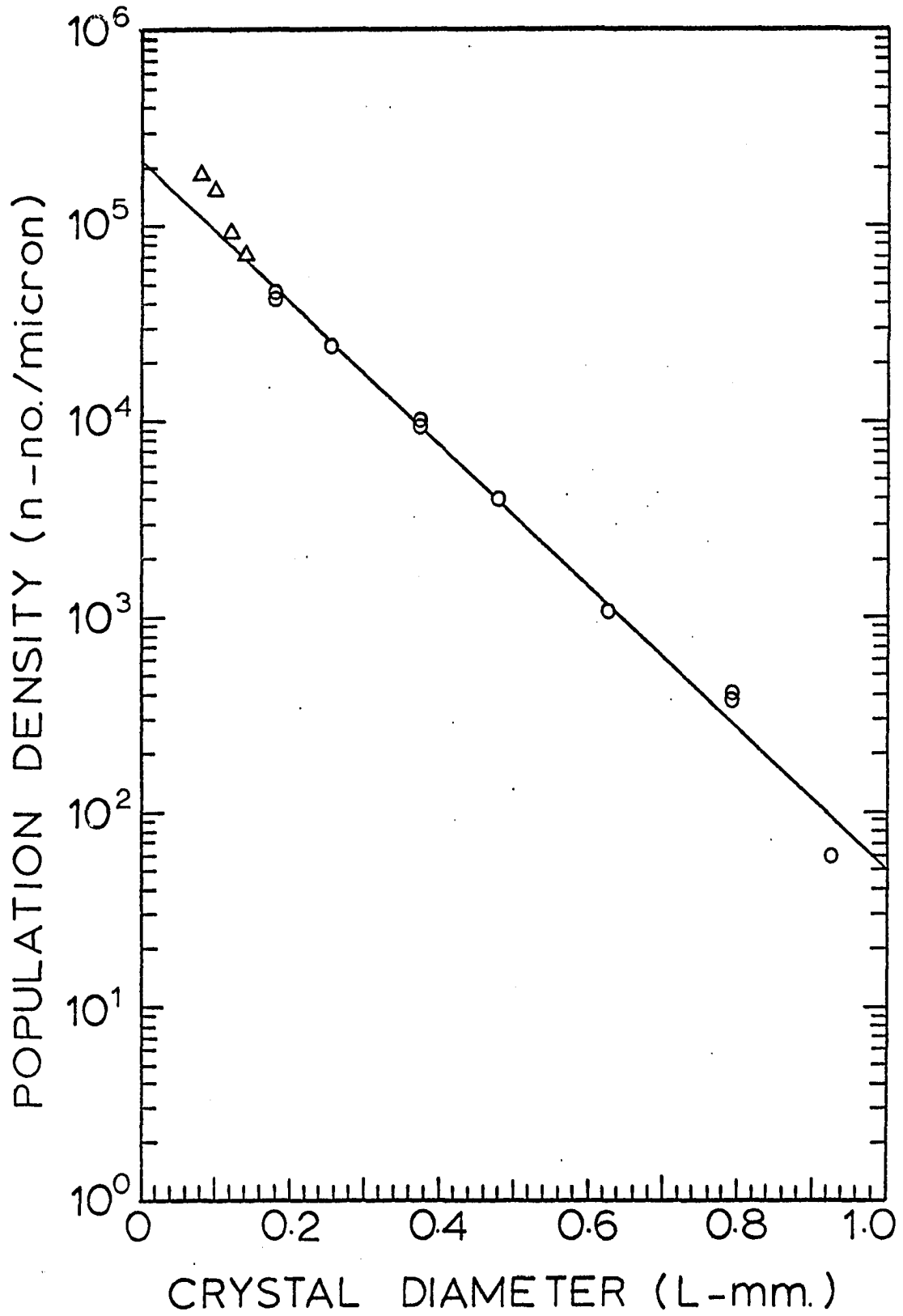
Figure 20. Size distribution of ammonium sulfate in terms
of population density

Residence time = 15 minutes
Suspension density = 5.78 grams crystals per
100 milliliters suspension

Δ - Coulter Counter
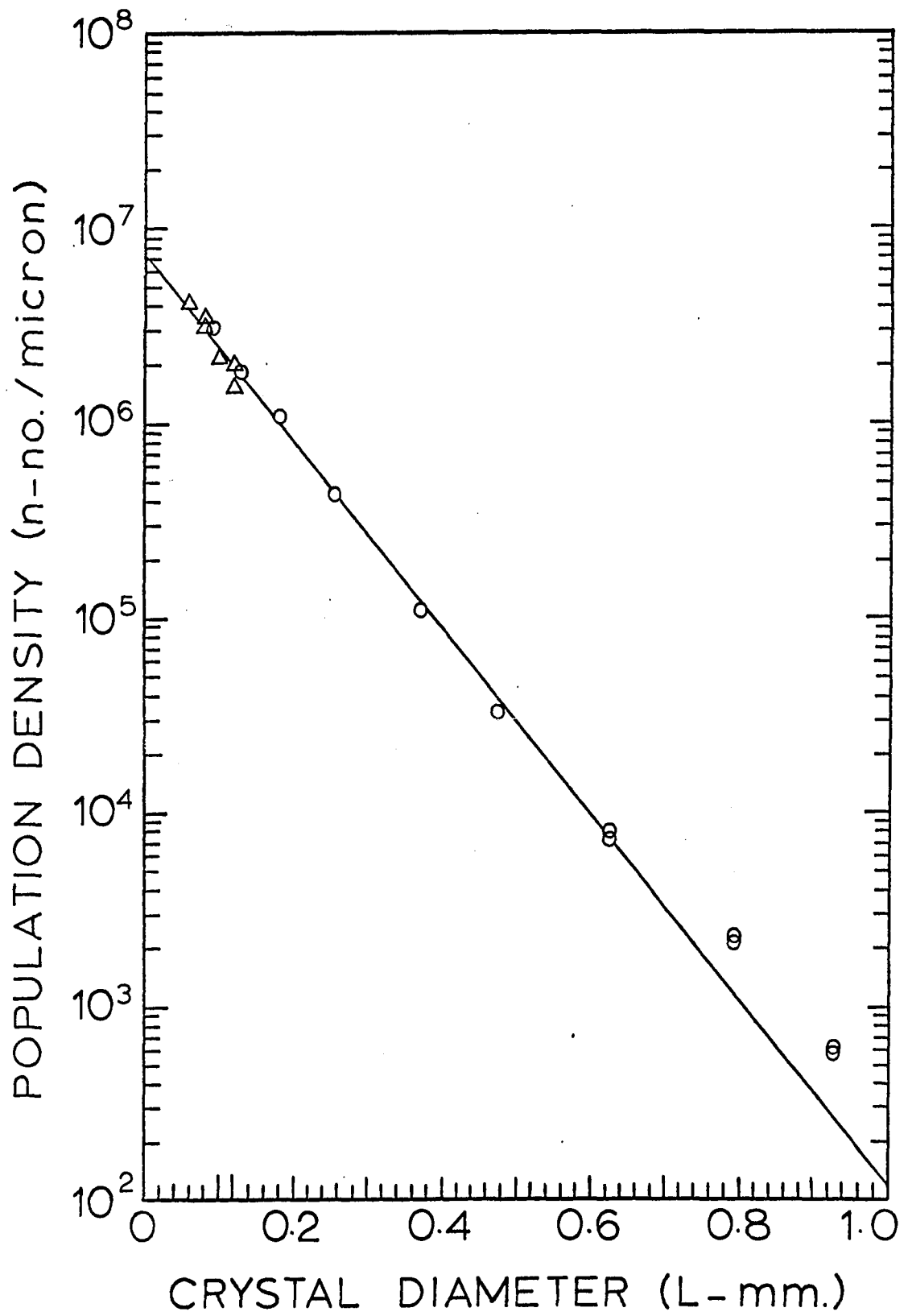0 - Sieve
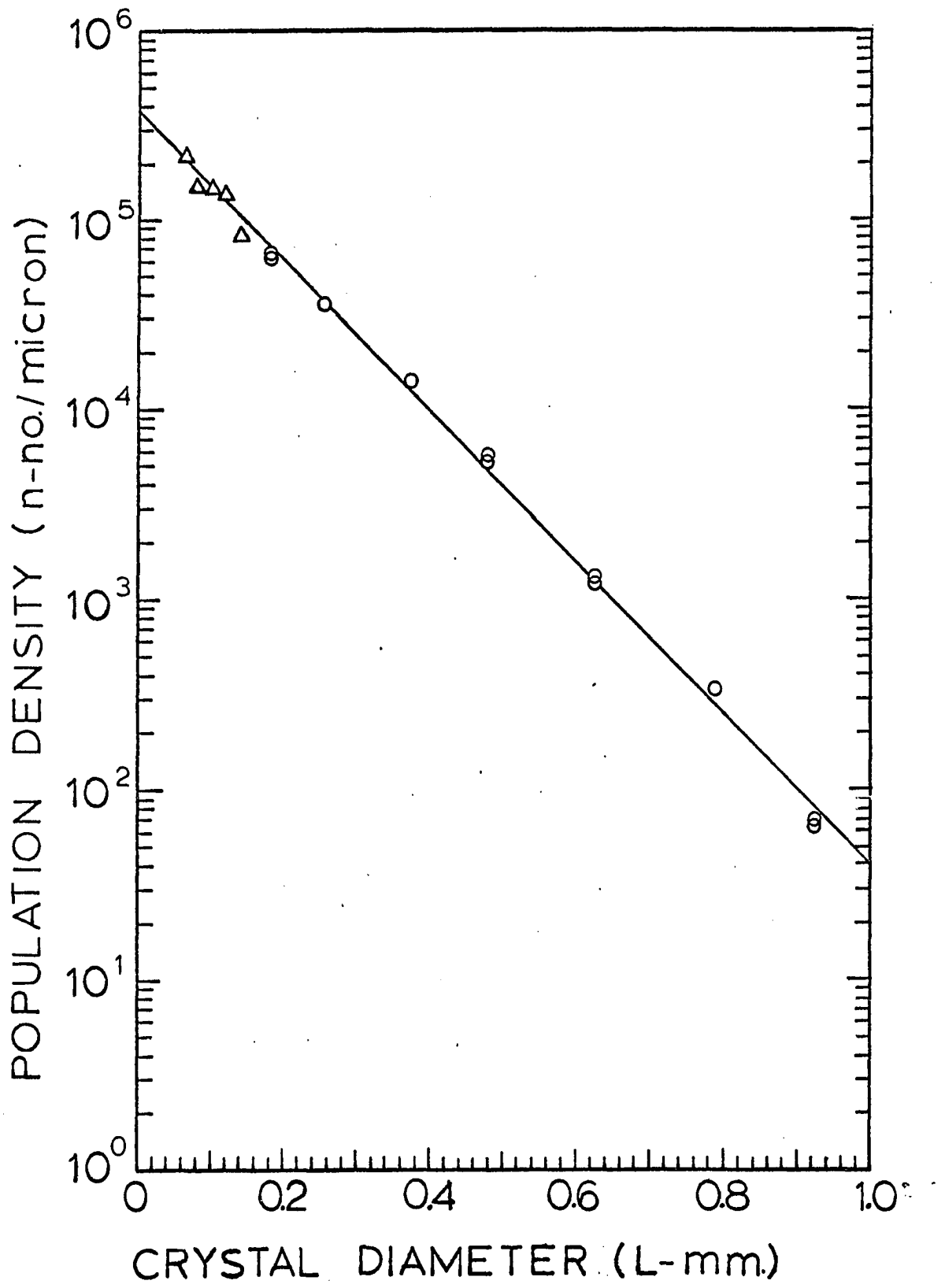
Figure 21. Size distribution of ammonium sulfate in terms
            of population density

            Residence time = 30 minutes
            Suspension density = 7.40 grams crystals per
            100 milliliters suspension   —

            Δ - Coulter Counter
            O - Sieve
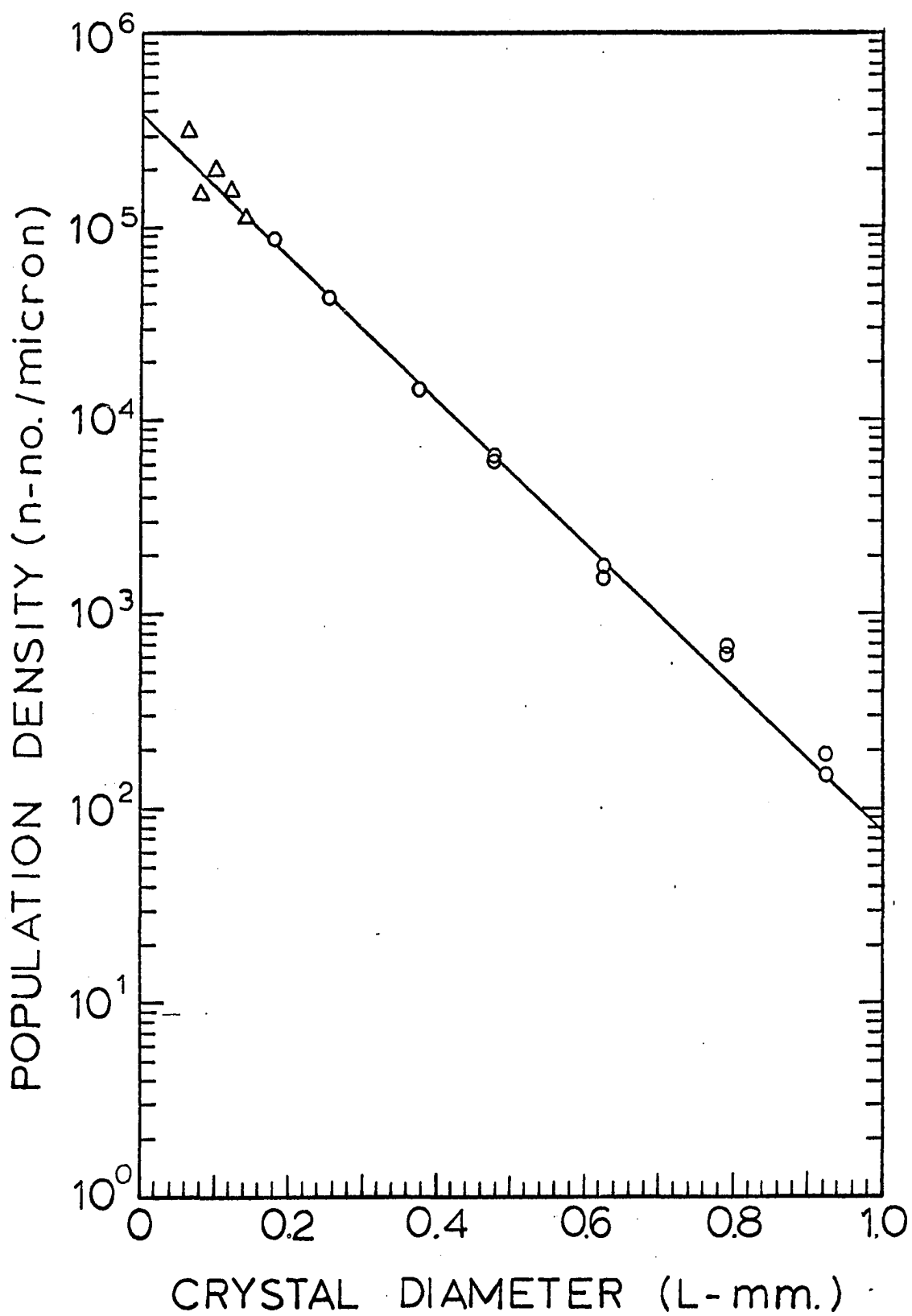
Figure 22. Size distribution of ammonium sulfate in terms
of population density

Residence time = 45 minutes
Suspension density = 7.46 grams crystals per
100 milliliters suspension
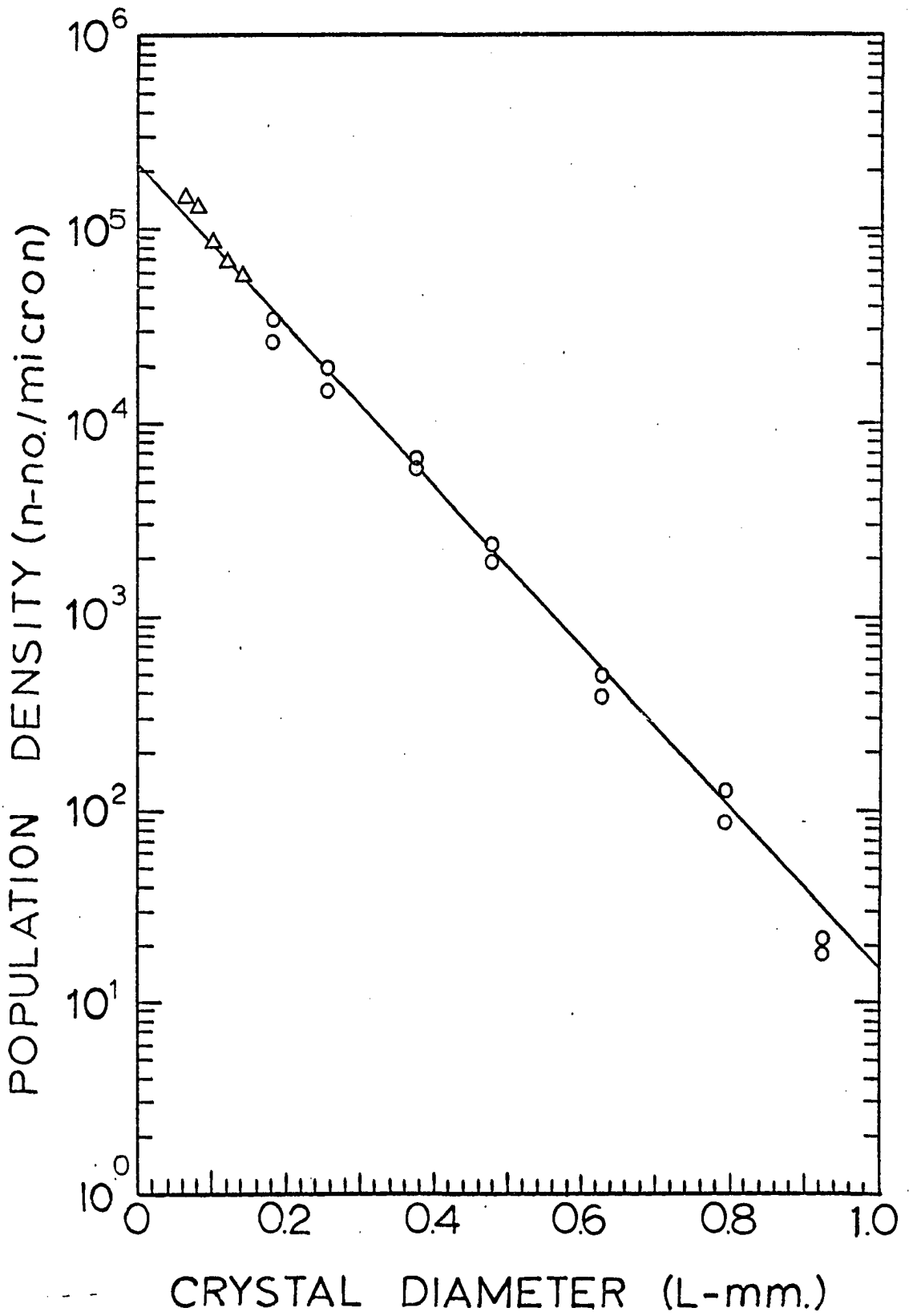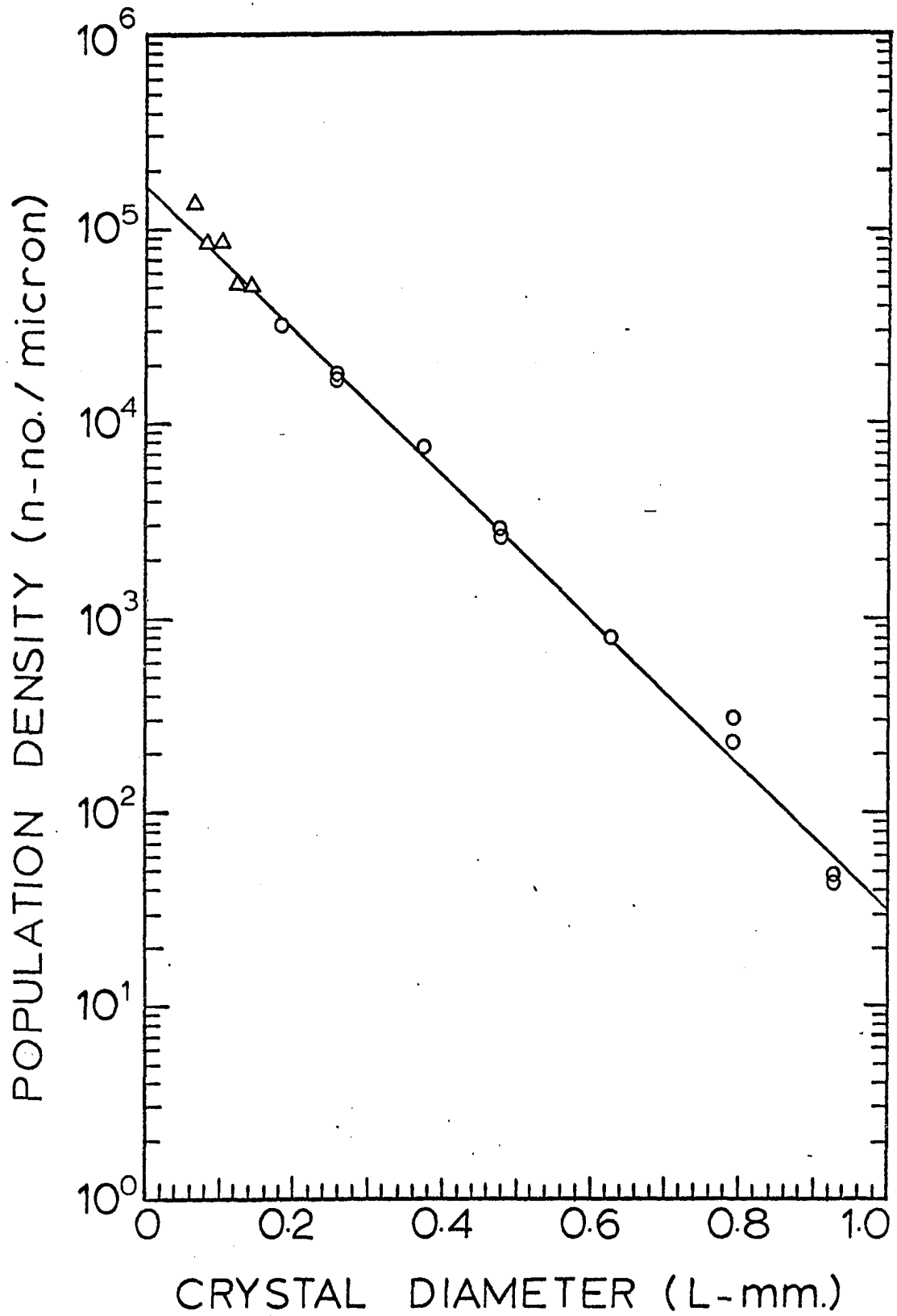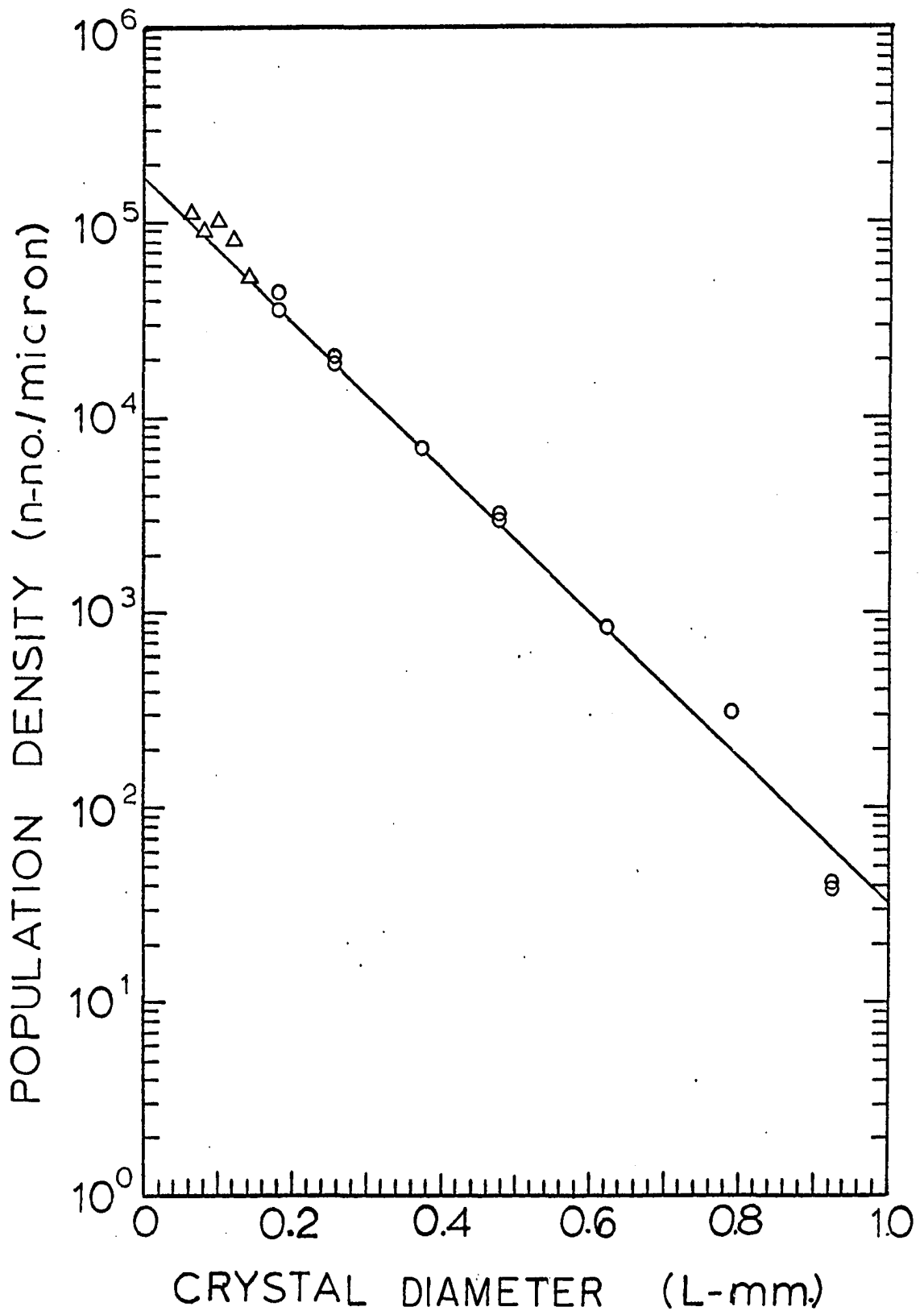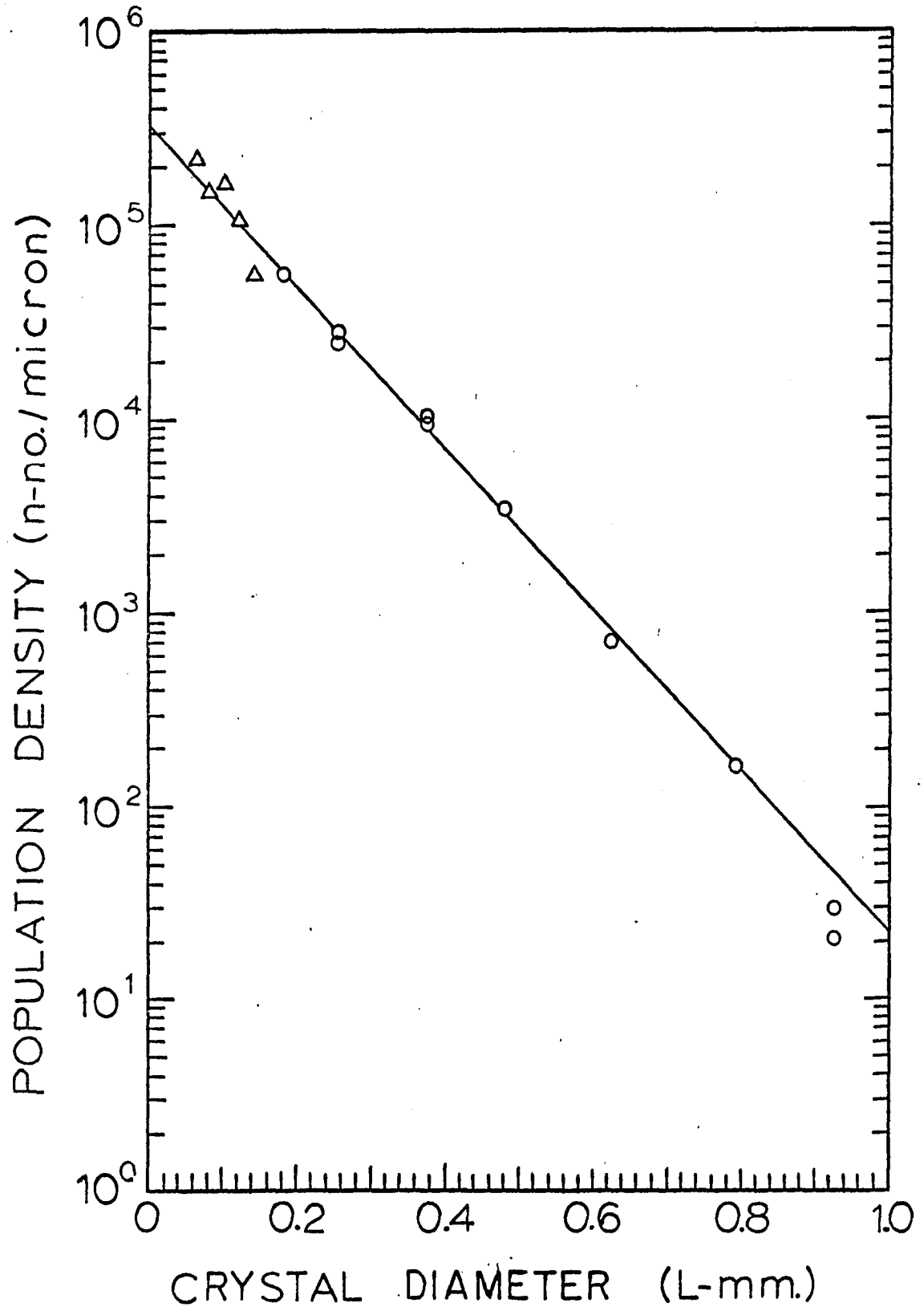
Δ - Coulter Counter
0 - Sieve
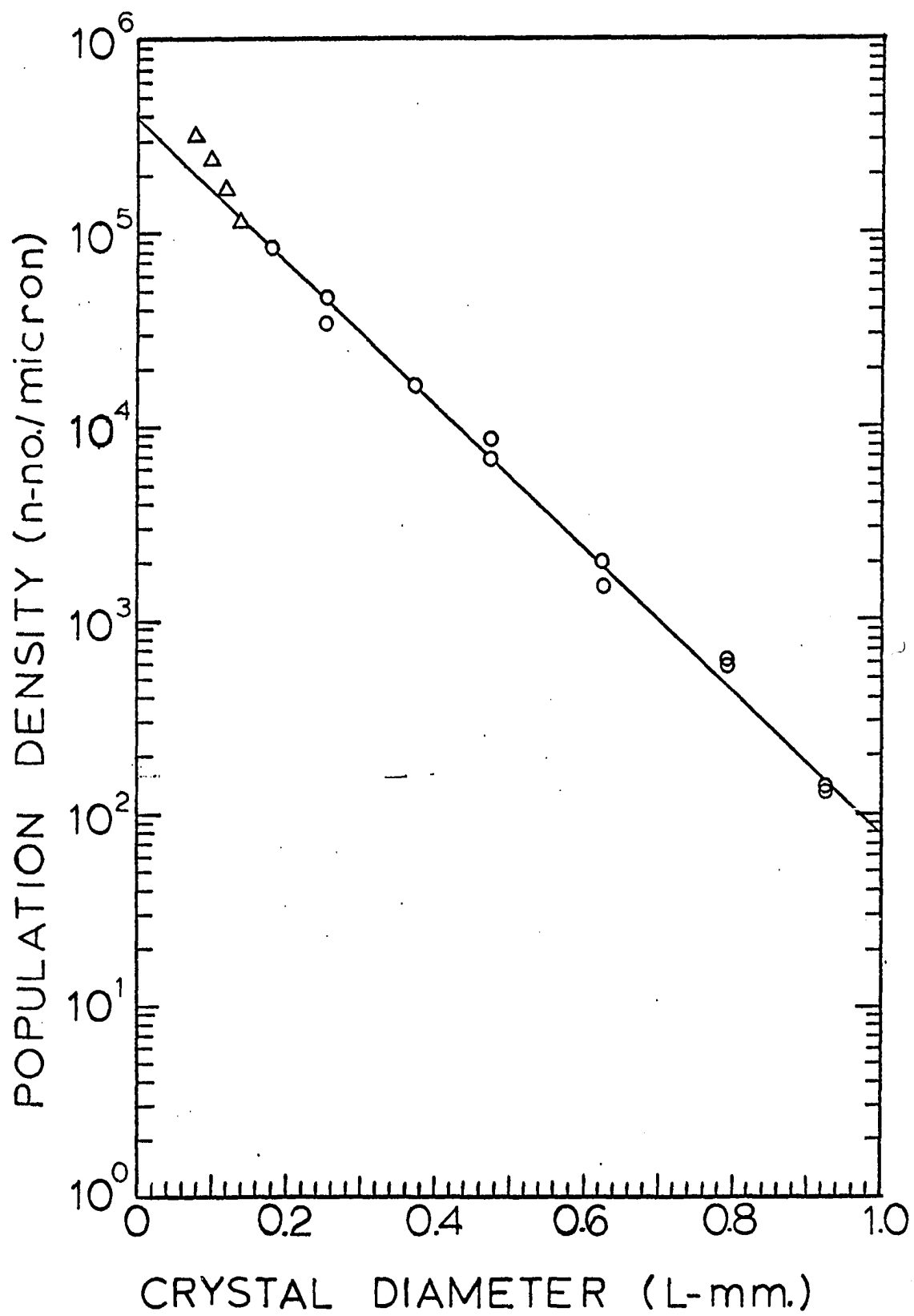
45 minute residence time were made for each system so that the effect of different levels of suspension density could be evaluated. Growth rates and nuclei population densities calculated from the steady state graphs are reported in Table 1 along with operating conditions and other pertinent parameters.

Different growth and nucleation rates were obtained by operating the crystallizer at different residence times. These different rates were obtained because of a variation in supersaturation with residence time. By varying residence time for three steady state runs, while holding suspension density and other variables constant, a correlation between growth rate and nuclei population density was obtained. This correlation in the form of a log-log plot of Equation 17 is shown in Figure 23 for alum and in Figure 24 for ammonium sulfate. These plots resulted in a linear relationship between log n_0^0 and log r_0 of slope $(i-1)$, where i is the kinetic order of nucleation. For alum, i was found to be 2.1, while i was 1.7 for ammonium sulfate.

The kinetic nucleation orders found from a steady state analysis of the cooling crystallization of alum and ammonium sulfate differ from those reported by Timm and Larson (23), who crystallized these materials from aqueous solution by the addition of alcohol. From a steady state

Table 1. Experimental Operating Conditions and Results for Alum and Ammonium Sulfate

T min.	$C_i$av.[1]	$C_o$av.	M gms. 100 ml.	r_o microns minute	n_o^o[2] no. micron	L_d micron
Alum						
15*	10.38	7.1	5.0	4.98	M = 5 3.58×10^6	224
30	9.88	7.0	5.5	2.92	1.90×10^6	263
45*	9.98	7.2	5.3	2.10	1.41×10^6	284
15	12.97	7.5	9.0	4.76	M = 10 8.65×10^6	214
30	13.25	7.0	10.5	2.77	4.75×10^6	249
45	12.87	6.0	14.7	2.02	3.32×10^6	273
15	19.38	6.9	21.9	4.96	M = 22 1.61×10^7	223
30	19.01	7.1	22.0	2.60	1.33×10^7	234
45	18.65	7.0	22.2	2.01	7.43×10^6	271
Ammonium Sulfate						
15	44.26	42.4	2.55	7.01	M = 3 2.42×10^5	316
30	44.53	43.0	3.16	3.89	1.54×10^5	350
45	44.47	42.9	3.36	2.63	1.52×10^5	355
15*	44.95	42.7	3.92	6.97	M = 4 3.32×10^5	314
30	44.74	--	4.01	3.86	2.20×10^5	348
45*	44.96	43.1	4.33	2.68	1.89×10^5	362
15	45.91	43.0	5.78	7.34	M = 7.5 5.05×10^5	330
15	46.14	43.0	6.58	6.93	6.38×10^5	312
30	45.89	42.8	7.40	3.94	3.86×10^5	354
45	46.09	42.5	7.46	2.61	3.92×10^5	352
45	46.03	42.8	7.42	2.56	4.25×10^5	346

*Transient runs.

[1] $C_i$av. and $C_o$av. indicate gms. anhydrous alum/100 gms. H_2O for alum and gms. ammonium sulfate/100 gms. solution for ammonium sulfate.

[2] n_o^o corrected to value of suspension density M shown in column above each set of three runs.

Figure 23. Correlation of nuclei population density
and growth rate for ammonium alum at three
levels of suspension density, M

O - M = 22 grams crystals per 100 milliliters
of suspension

Slope (i-1) = 0.8

△ - M = 10 grams crystals per 100 milliters
of suspension

Slope (i-1) = 1.1

□ - M = 5 grams crystals per 100 milliliters
of suspension
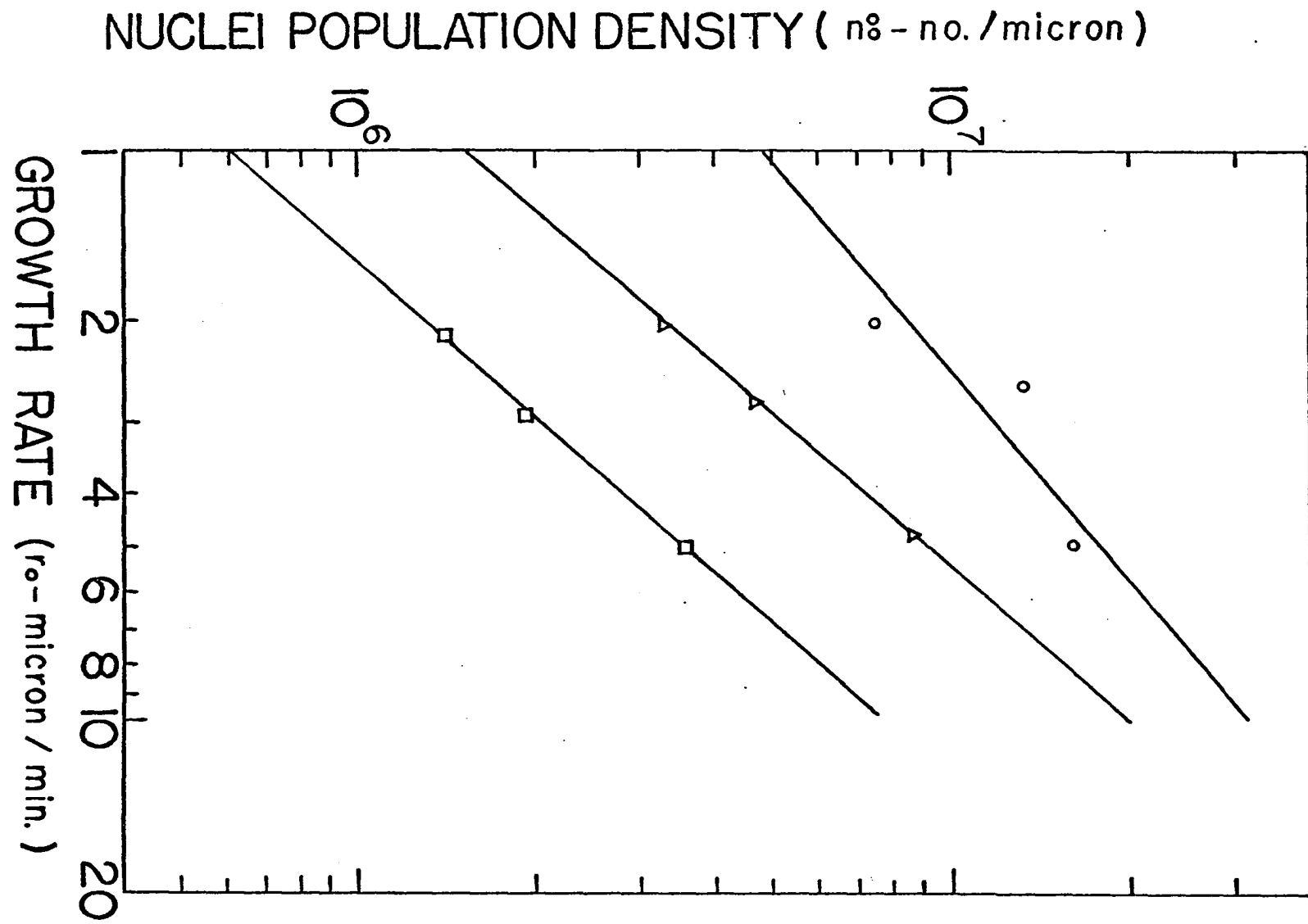
Slope (i-1) = 1.1

Figure 24. Correlation of nuclei population density and
growth rate for ammonium sulfate at three
levels of suspension density, M

O - M = 7.5 grams of crystals per 100 milliliters
of suspension

Slope (i-1) = 0.3

△ - M = 4.0 grams of crystals per 100 milliliters
of suspension

Slope (i-1) = 0.7

□ - M = 3.0 grams of crystals per 100 milliliters
of suspension

Slope (i-1) = 0.5

NUCLEI POPULATION DENSITY (n⁰ – no. / micron)
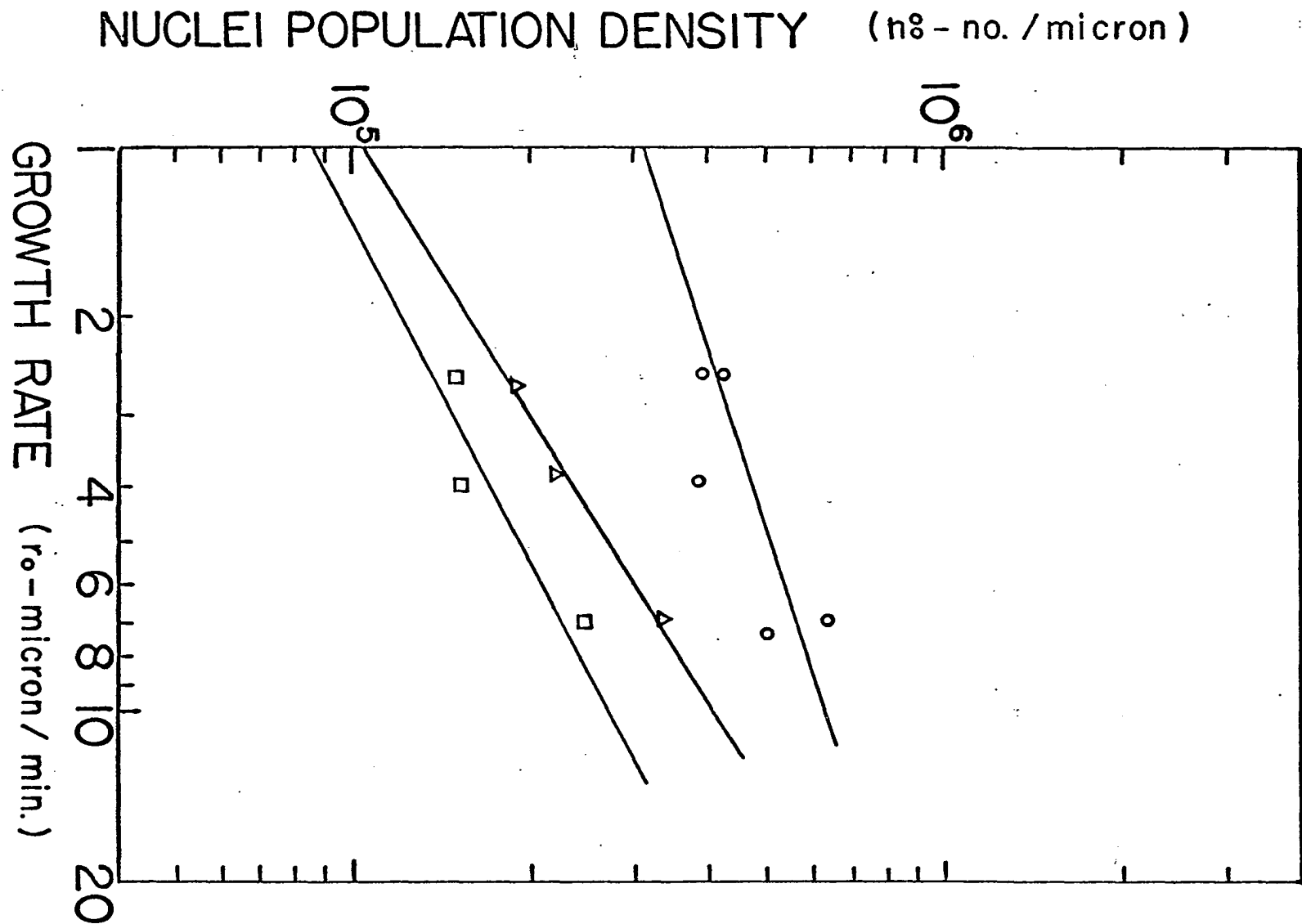
analysis, Timm reported that the kinetic order i was 1.0 for alum and 4.0 for ammonium sulfate. The habit of ammonium sulfate crystals produced by Timm was different from that obtained by cooling crystallization, perhaps because of the influence of the alcohol or some other habit modifier. Alum crystallized in the same form for each mode of crystallization.

Several factors could be responsible for the differing results. The interfacial tension between crystals and solution in an alcohol-water environment is probably different than in an aqueous solution. Likewise the viscosity and density of the two environments are dissimilar. In addition to these fundamental differences due to the mode of crystallization, the effect of different agitation, concentration levels, and temperatures must also be considered. These latter factors appear to be roughly the same, although the very small supersaturation level in each crystallizer could not be accurately determined in either case. A fundamental study might elucidate kinetic differences due to surface tension, but until a quantitative technique is devised, care should be exercised in the extrapolation of results from different modes of crystallization. These experiments along with those of Timm and Larson (23), however, do indicate that a simple power model of supersaturation may be used in either case for an analysis of

crystallizer behavior.

The importance of finding the best straight line through the data of Figures 5 through 22 cannot be overemphasized. The accuracy of the steady state determination of the nucleation order i depends on the proper location of this line. As mentioned earlier, the slope of the line determines the growth rate, while the intercept is the nuclei population density. A slight shift in the line changes the intercept n_0^0 considerably, because of the logarithmic vertical axis. Growth rate is affected to a lesser extent. Since these two variables are replotted to obtain i, a good correlation depends on their accurate determination.

The following procedure was used to insure that the best straight line through the data was obtained. Suspension density is related to population density at steady state by Equation 35. The experimental value of the suspension density was found by weighing the crystals found in a known volume of suspension sample from the crystallizer. Then by adjusting the slope $(-\frac{1}{r_0 T_0})$ and intercept (n_0^0) of the semilog plot of Equation 13, a suspension density was calculated from Equation 35 that agreed with the one found experimentally. This technique was used to find the best straight line for the data of Figures 5 through 22.

For several of the runs of different residence time

where suspension density was to be held constant, some variation in suspension density still occurred. This was because the exact feed composition could not be duplicated from run to run due to solvent evaporation at the high temperature required to keep the solution unsaturated.

Nuclei population density was corrected for suspension density variation before making the log-log plots of Figures 23 and 24 to determine nucleation order. This correction was made by multiplying n_0^o by the ratio of the desired suspension density to the actual one. As will be seen later this correction was in order because of the linear dependence of nucleation rate on suspension density.

Effect of Suspension Density or Area on Nucleation Rates

As pointed out in the Theoretical Development, the effect of suspension density can be determined by the relationship among lines on semilog plots of population density versus size for constant residence time and vary-ing suspension density. Figures 25 and 26 show that nearly parallel lines were obtained for both alum and ammonium sulfate at constant residence time. Since growth rate was not affected by the amount of solids in suspension, the slopes were the same. Case I for j and h = 1 in Equations 26 and 27 applies for parallel lines. Therefore nucleation rate was a linear function of suspension density or area for both systems. No enhancement in the crystal size

Figure 25. Effect of suspension density, M, on size
distribution for ammonium alum

Residence time = 45 minutes
1 - M = 5.3
2 - M = 14.7
3 - M = 22.2

Residence time = 30 minutes
4 - M = 5.5
5 - M = 10.5
6 - M = 22.0

Residence time = 15 minutes
7 - M = 5.0
8 - M = 9.0
9 - M = 21.9
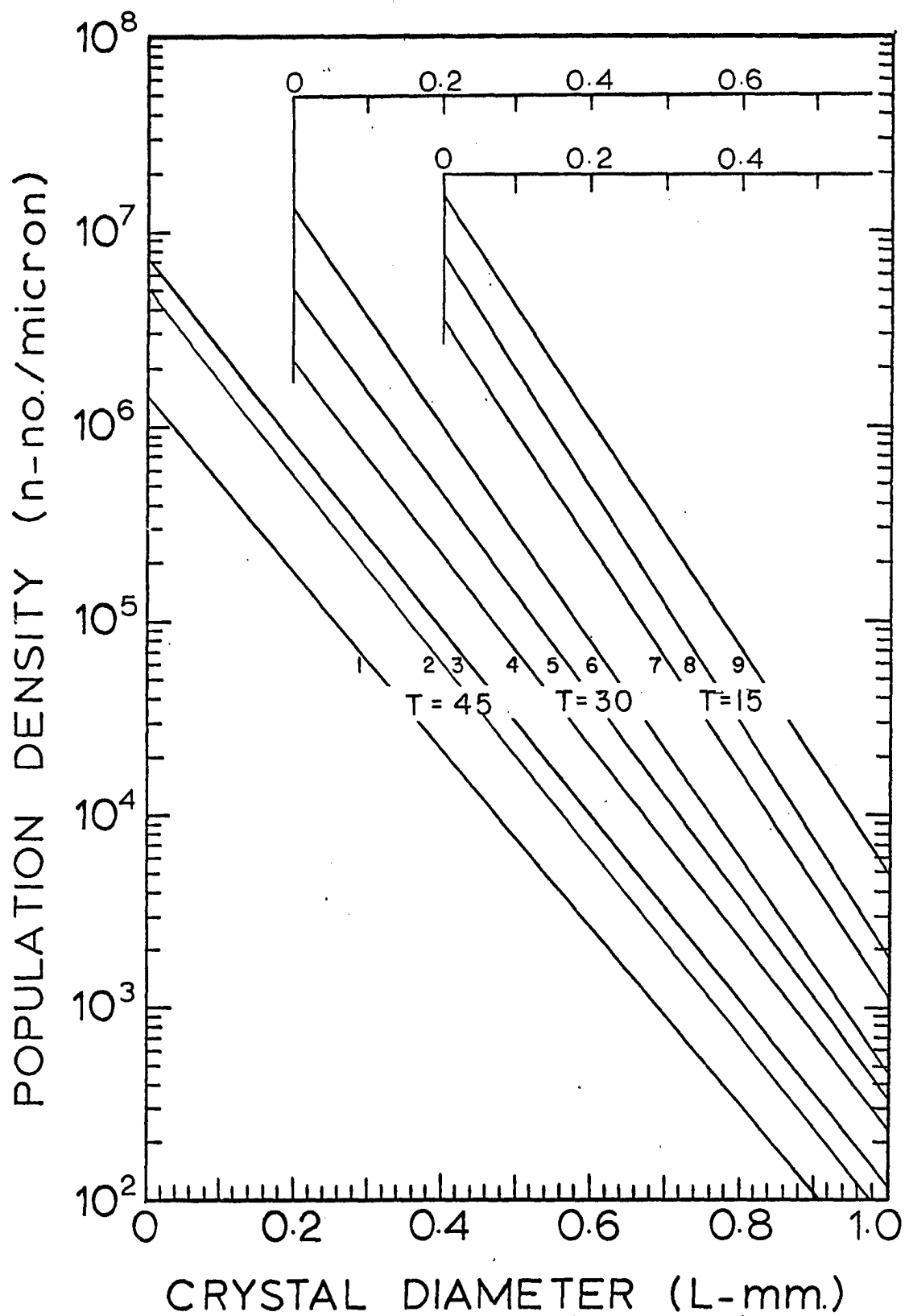
Figure 26. Effect of suspension density, M, on size
distribution for ammonium sulfate

Residence time = 45 minutes
1 - M = 3.36
2 - M = 4.33
3 - M = 7.46

Residence time = 30 minutes
4 - M = 3.16
5 - M = 4.01
6 - M = 7.40

Residence time = 15 minutes
7 - M = 2.55
8 - M = 3.92
9 - M = 5.78
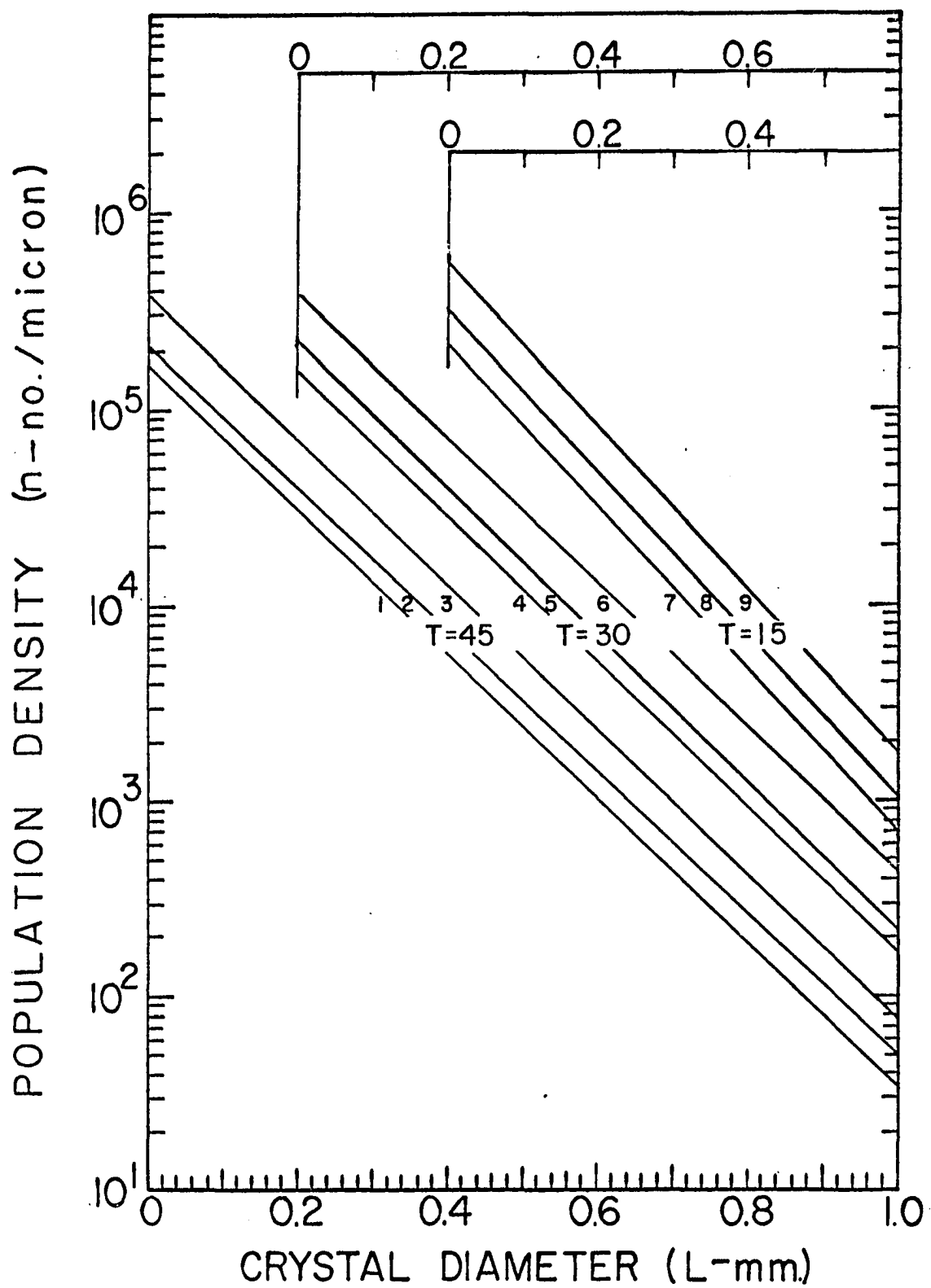
distribution for an increase in suspension density or area

was observed. This is evident from the values of L_d in

Table 1.

If nucleation rate had not been dependent on suspension

density or area, non-parallel lines and enhancement of the

size distribution would have occurred as in previously

described Case II. Thus from the steady state graphs and

L_d data, it is evident that a model which does not take

suspension density or area into account is inadequate. The

suspension density model is of special importance for

systems where yield is a variable because for these systems

suspension density cannot be held constant.

While this analysis was not designed to elucidate the

detailed mechanism of heterogeneous nucleation, it does

show that nucleation rate can be correlated with the solids

in suspension over a range of suspension densities in a

mixed suspension crystallizer. Thus these experiments and

others of this type can be used for more fundamental studies

of the causes of heterogeneous nucleation.

There are several methods of obtaining j and h in

Equations 26 and 27 if the steady state plots do not result

in parallel lines. First if the kinetic order i is known,

j and h can be obtained from Equations 34 and 37 for two

levels of suspension density and constant residence time.

Using the i's obtained from Figures 23 and 24 in these

equations, values of j and h approximately equal to one were found for both systems.

Another method utilizes a log-log plot of $\frac{dN^\alpha}{dt}$ versus M or A at constant growth rate to obtain j and h in accordance with Equations 46 and 47. From Figures 27 through 30 j and h were found to be equal to one for both alum and ammonium sulfate.

Effect of Residence Time on Size Distribution

The dominant particle size L_d defined by Equation 40 may be used to evaluate changes in overall size distribution. In Table 1, L_d is seen to increase with increasing residence time for constant suspension density, thereby indicating an enhancement in size distribution for both systems. For a threefold increase in residence time, the dominant particle size increased by about 60 microns for alum and by about 40 microns for ammonium sulfate.

The effect of residence time on the parameters r_α, n_α^0, and L_d is shown in Figure 31. Log-log plots of Equations 48, 49, and 50 afford still another means of calculating the kinetic nucleation order i. As can be seen from these equations, when i = 1 both n_α^0 and L_d are independent of residence time. However for both systems i was found to be near two. For i = 2, both growth rate and nuclei population density are proportional to residence time raised

Figure 27. Correlation of nucleation rate and suspension
            density for ammonium alum at three levels of
            growth rate, r

            0 - r = 5.00 microns per minute
                slope (j) = 1.0

            Δ - r = 2.75 microns per minute
                slope (j) = 1.3

            □ - r = 2.00 microns per minute
                slope (j) = 1.1
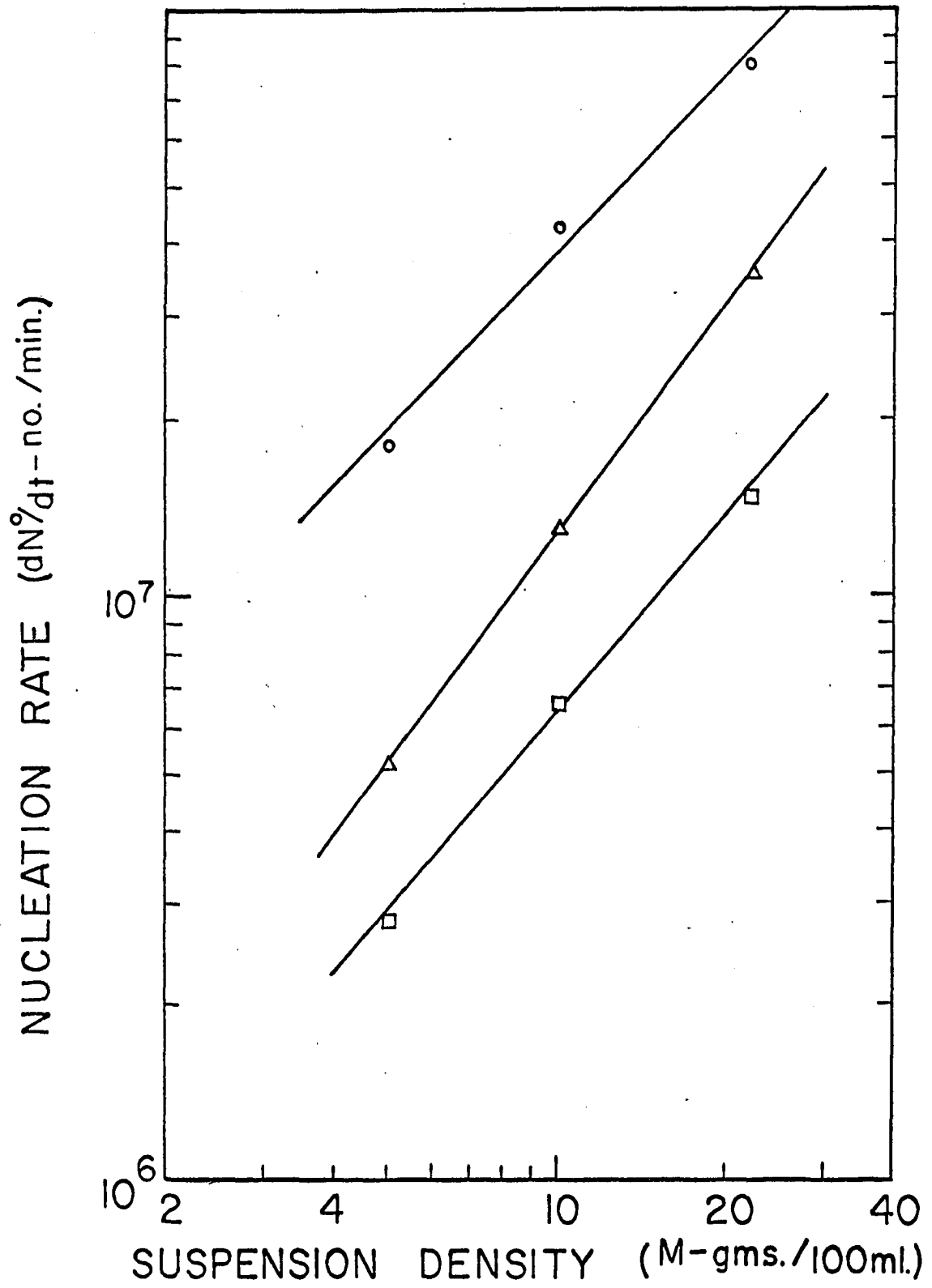
Figure 28.   Correlation of nucleation rate and suspension
             area for ammonium alum at three levels of growth
             rate, r

        O - r = 5.00 microns per minute
            slope (h) = 1.0

        Δ - r = 2.75 microns per minute
            slope (h) = 1.2

        □ - r = 2.00 microns per minute
            slope (h) = 1.1
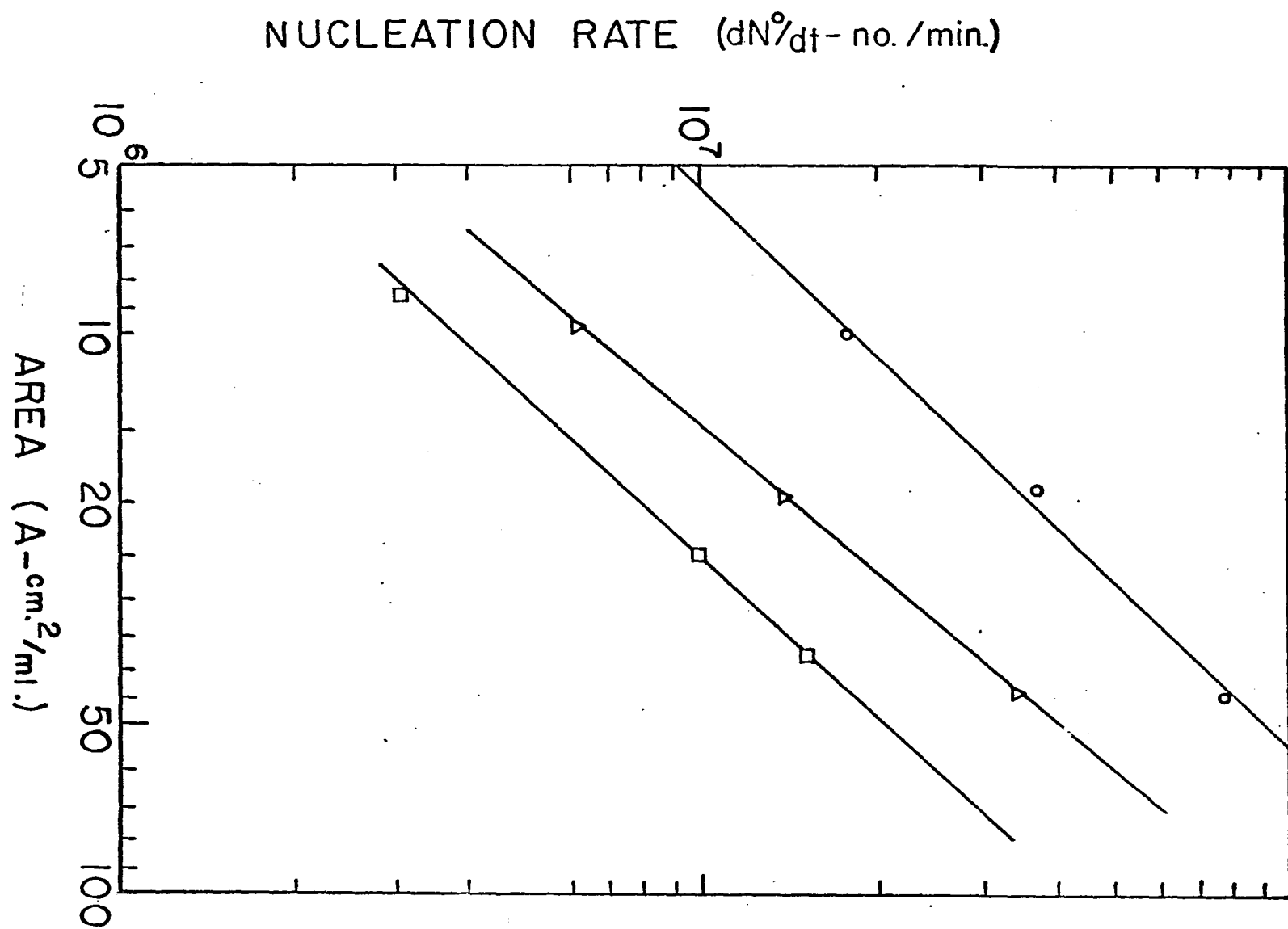
Figure 29.   Correlation of nucleation rate and suspension
             density for ammonium sulfate at three levels
             of growth rate, r

             O - r = 7.0 microns per minute
                 slope (j) = 1.1

             Δ - r = 4.0 microns per minute
                 slope (j) = 1.0

             □ - r = 2.6 microns per minute
                 slope (j) = 0.9

110
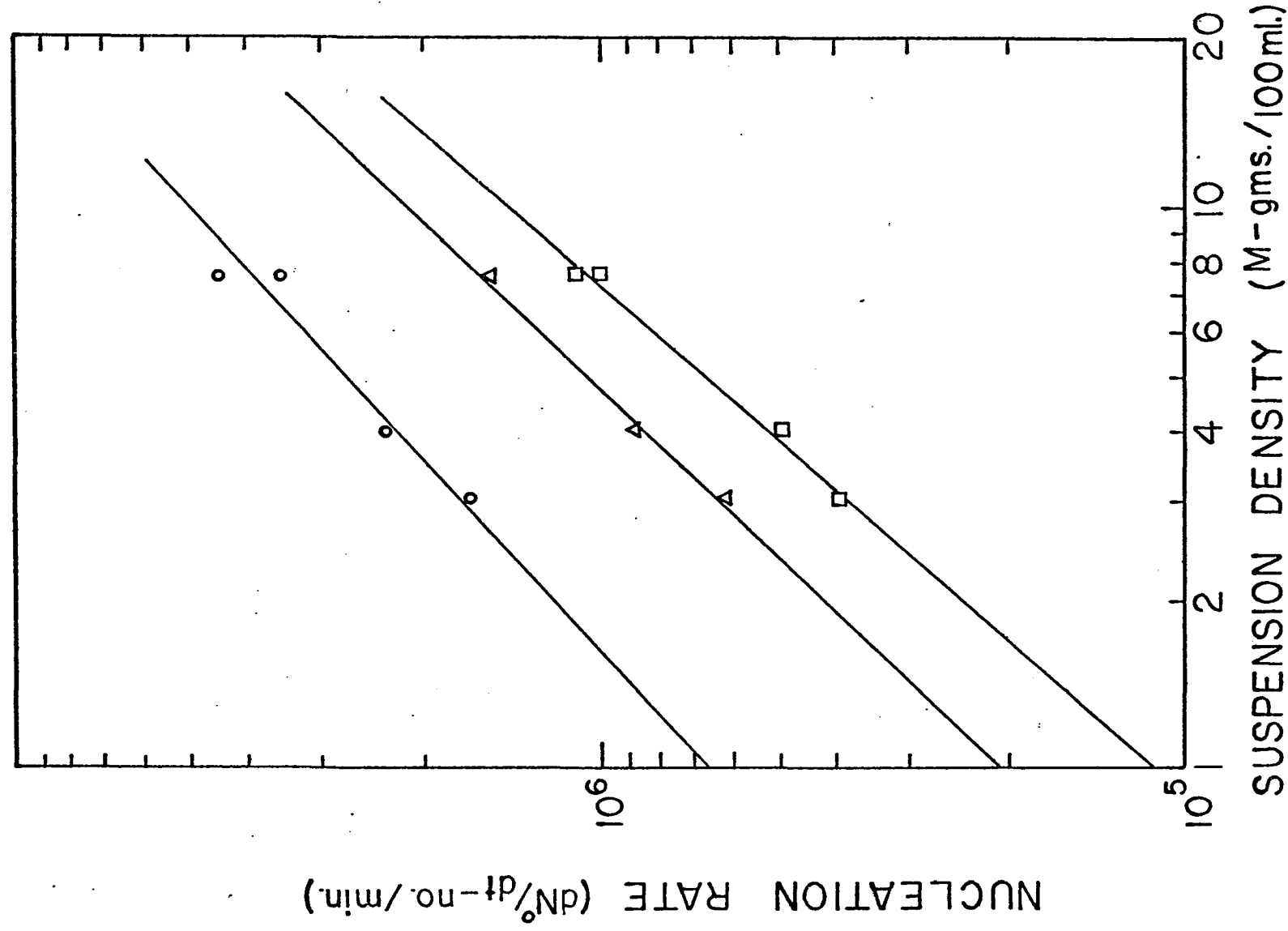
Figure 30. Correlation of nucleation rate and suspension
area for ammonium sulfate at three levels of
growth rate, r

   O - r = 7.0 microns per minute
       slope (h) = 1.0

   △ - r = 4.0 microns per minute
       slope (h) = 1.1

   □ - r = 2.6 microns per minute
       slope (h) = 1.1
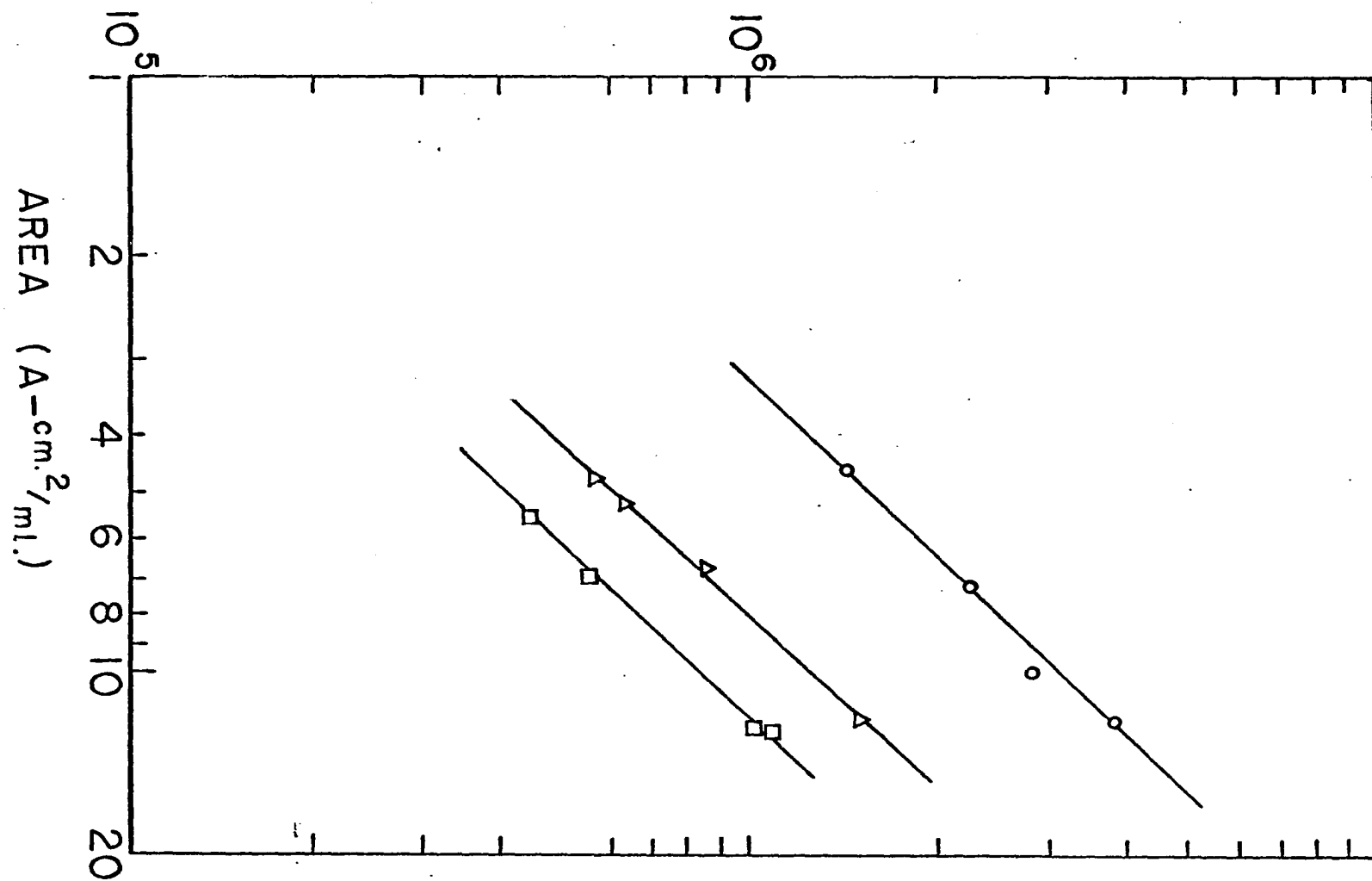
Figure 31. Correlation of growth rate r_G, nuclei population density n_0^0, and dominant particle size L_d with residence time T for ammonium alum - O and ammonium sulfate -Δ
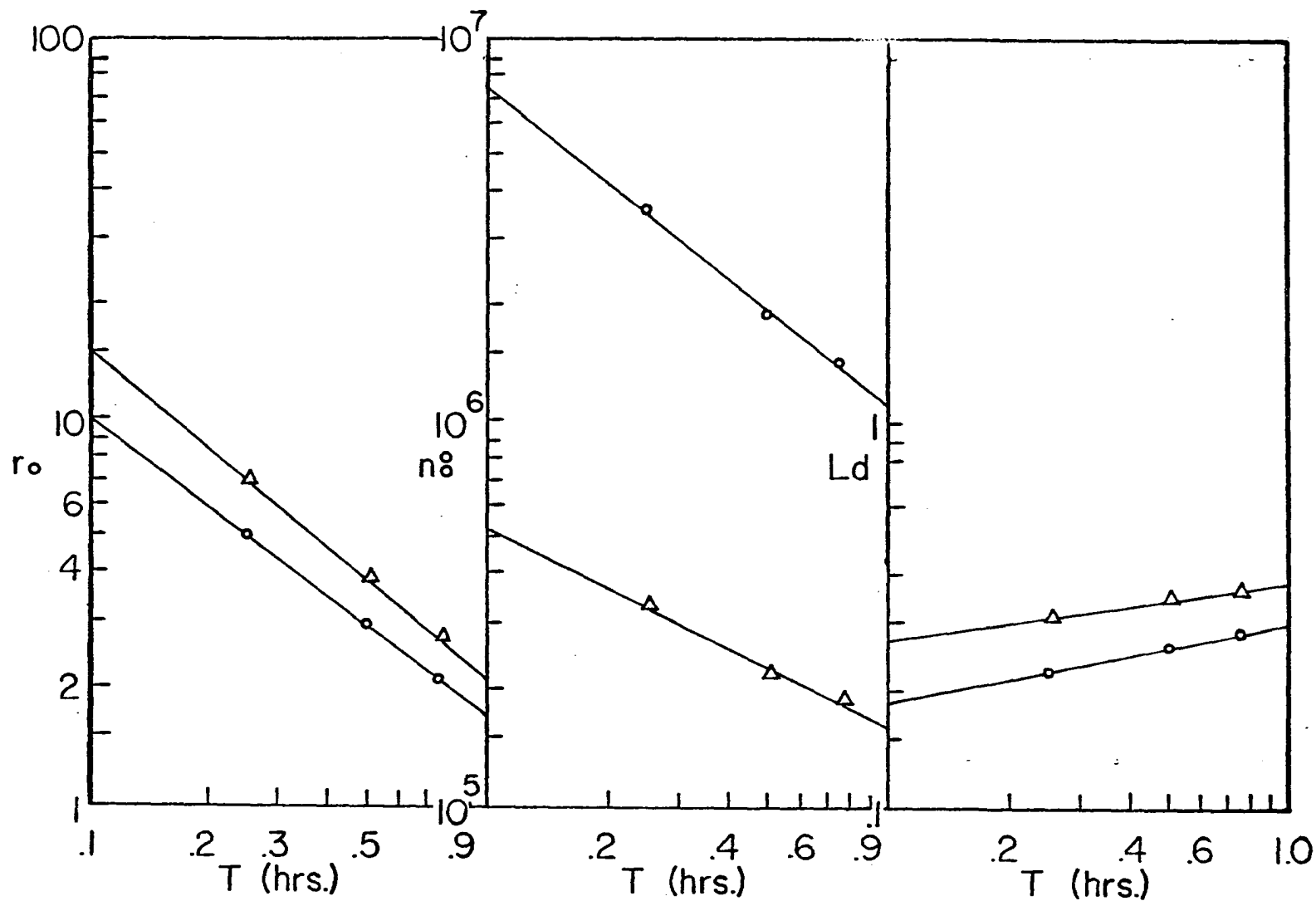
to the -0.8 power by Equations 48 and 49. Thus a 100 percent increase in production rate (reciprocal of residence time) causes a 75 percent increase in growth rate and in nuclei population density. However in the log-log plot of L_d versus T_0 (Figure 31) the size distribution decreases for increasing production rate $(\frac{1}{T_0})$. This can be explained with the aid of Equation 16. When the increase in nuclei population density is multiplied by the increase in growth rate, a nucleation rate increase in excess of 300 percent is obtained. This far overshadows the increase in growth rate. Hence the size distribution must be degraded for an increase in production rate for second order kinetics. From this example one can see the importance of knowing the kinetic nucleation order i, so that the proper production rate can be selected to give the desired size distribution.

Applicability of McCabe's ΔL Law

McCabe's ΔL law states that the growth rate of a crystal is not a function of the size of the crystal. While there are systems which do not follow this law in practice, one must consider the manner in which the suspension is being agitated in order to decide on its applicability. Even though a suspension is well mixed as in a baffled draft tube type crystallizer, deviations from

McCabe's ΔL law can occur after crystals reach a certain size. This critical size is dependent in part on the degree of the agitation. The relative velocity between the crystal and the liquid phase determines the mass transfer rate. The larger the crystal the more pronounced is the velocity difference and the greater the transfer rate up to a certain velocity where further increases in velocity are no longer important in reducing the resistance to diffusion. So while McCabe's ΔL law may hold quite well for small crystals in bench scale crystallizers, deviations from it may occur in commercial crystallizers producing larger crystals.

In terms of the experimental results obtained in this study, McCabe's ΔL law seems to be applicable for the size range (less than 1 mm.) of crystals produced. However, for alum the population density of larger crystals tended to be above the straight line relationship. This is sometimes attributed to agglomeration, but careful examination of the larger size fractions showed them to be made up almost entirely of single crystals. Thus the overabundance of larger crystals is better attributed to an increased growth rate with size. This observation was made only for the largest two or three size fractions analyzed, so it does not affect the significance of the major portion of the data as far as the assumption of McCabe's ΔL law is concerned.

Also, the weight of the crystals held on these three screens accounts for only about 6 percent of the total weight of crystals in the sample.

Transient Response to a Step Change in Residence Time

Experimental transient data were collected for a three-fold decrease in residence time so that it could be compared with the numerical solution of Equation 19 obtained by Timm (22). Transient runs for both alum and ammonium sulfate were made. In order to obtain data with the proper boundary conditions, the crystallizer was operated at a 45 minute residence time until steady state conditions were attained. Then the feed rate was step increased to give a 15 minute residence time. With this increase in production rate, a corresponding increase in heat removal was made to keep the temperature in the crystallizer constant. Finally, suspension samples were collected every 15 minutes until steady state was again attained after 20 residence times.

Dimensionless population density is plotted as a function of dimensionless residence time in Figures 32 and 33 with average crystal size as a parameter for alum and ammonium sulfate respectively. The initial point for each size curve was an average of the steady state population densities attained during the 45 minute residence time portion of the run. To obtain dimensionless population density

Figure 32.   Transient response to step decrease in residence time for
ammonium alum

O——O   Experimental data
X_e experimental size parameter

— —   Theoretical solution for 1.25 order kinetic
nucleation rate
X_t theoretical size parameter

DIMENSIONLESS POPULATION DENSITY (n/n_0)

DIMENSIONLESS TIME (t/T_0)
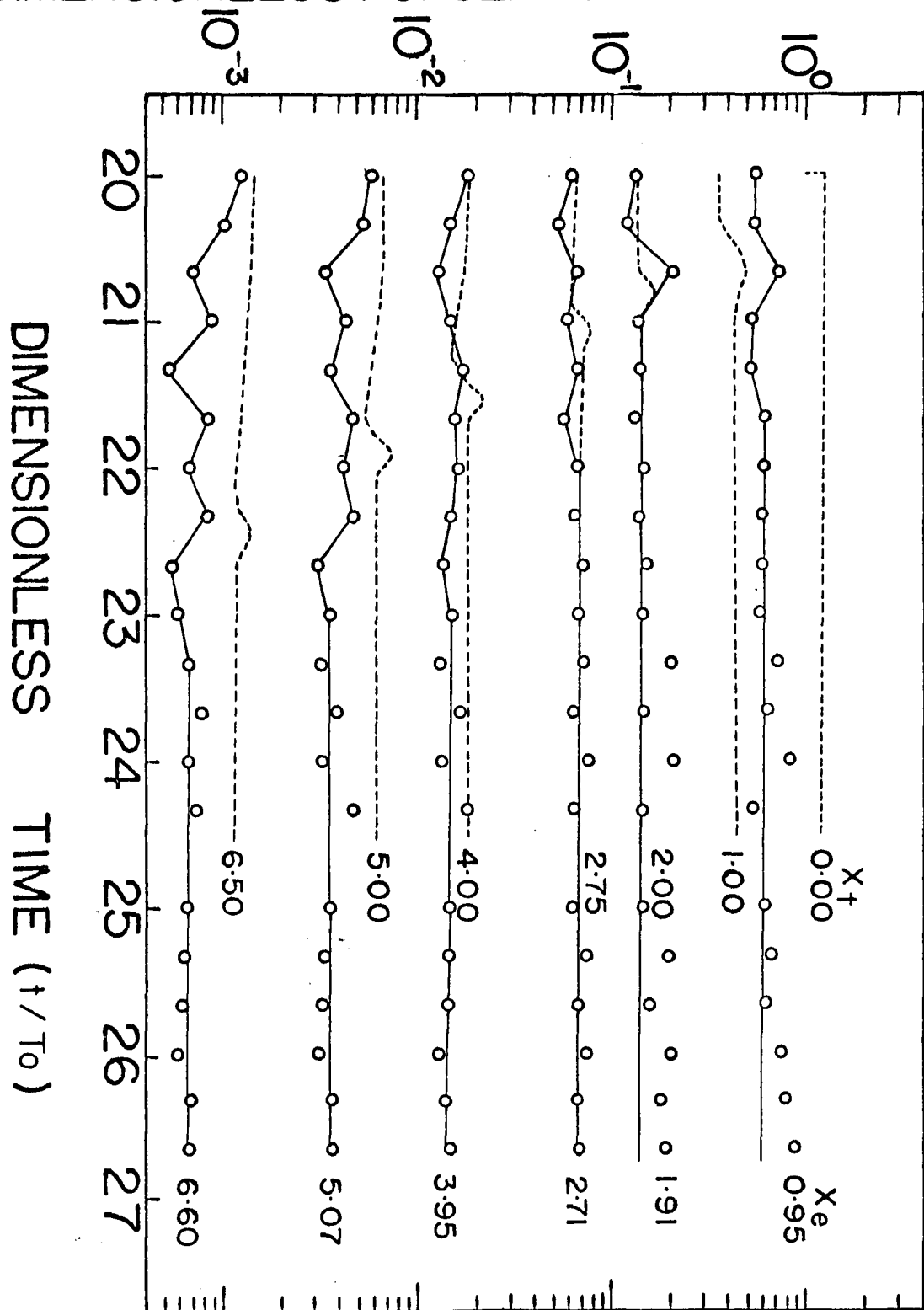
Figure 33.   Transient response to step decrease in residence time for ammonium sulfate

O——O   Experimental data
        X_e experimental size parameter

— —   Theoretical solution for second order kinetic nucleation rate
        X_t theoretical size parameter
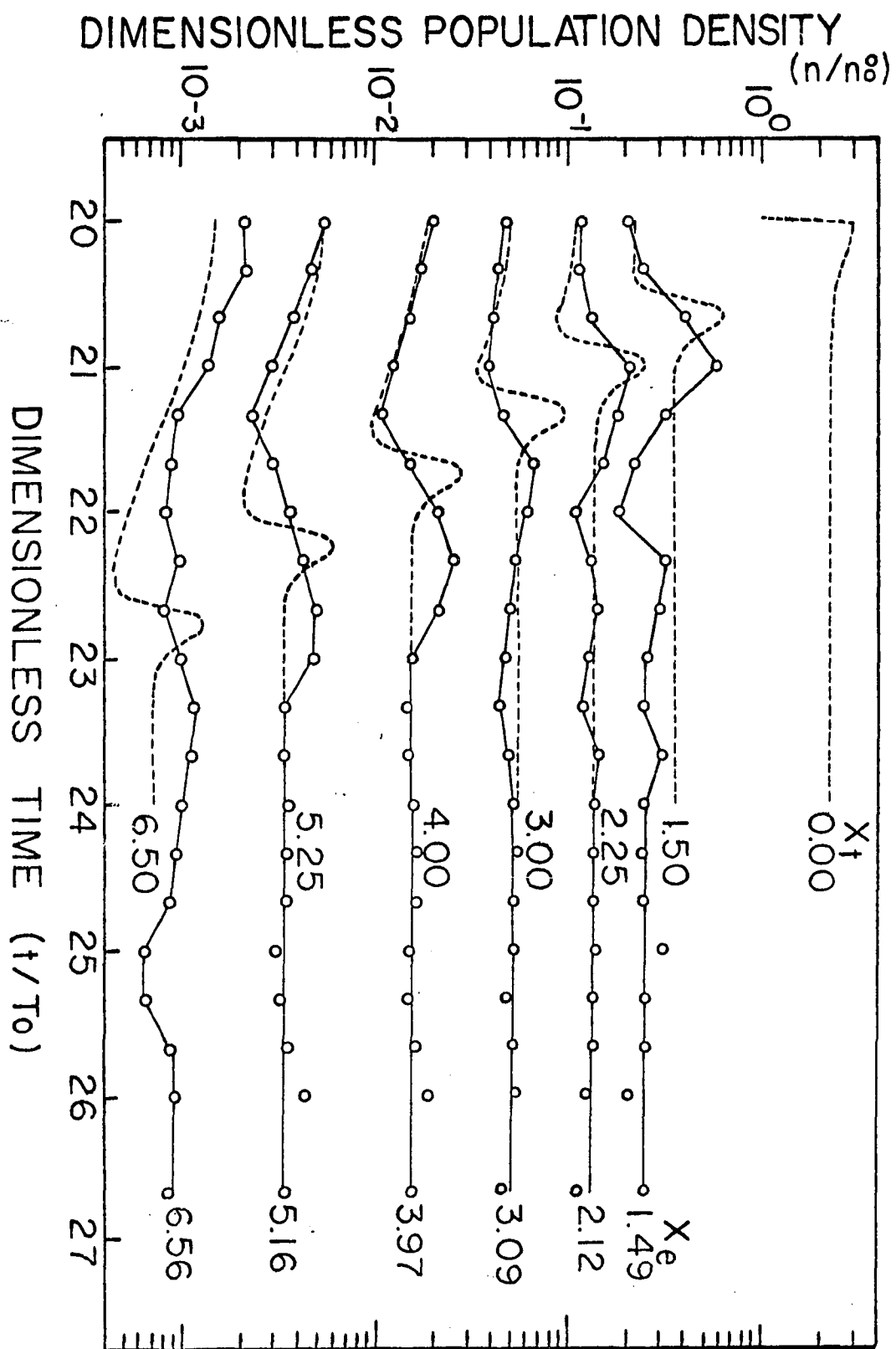
and dimensionless residence time, these variables were
divided by the steady state nuclei population density and
the residence time for the 45 minute portion of the run.
Crystal size was rendered dimensionless by dividing by the
steady state growth rate and residence time.

When the step change was made, an immediate increase
in the supersaturation occurred. This was reflected by a
shower of nuclei, since nucleation is a higher order
function of supersaturation than growth. As time elapsed
this shower propagated as a wave disturbance by "growing"
through larger and larger size fractions until steady state
was again attained. From Figures 32 and 33 all size
fractions achieved steady state after sixteen residence
times.

The overall effect of the step decrease in residence
time was to degrade the size distribution. This is evident
from a consideration of the changes in the population den-
sity of the various size fractions. The population density
of the larger crystals decreased, while that of the smaller
crystals increased. The dominant particle size on a weight
basis decreased by roughly 50 microns for both alum and
ammonium sulfate.

Timm (22) solved Equation 19 for kinetic nucleation
orders of i = 1, 1.25, 2 and 3. The numerical solution was
compared to the experimental curves in Figures 32 and 33.
For alum the 1.25 order model gave the best representation

of the experimental results, while the second order model

most nearly corresponded to the ammonium sulfate data.

The alum system was quite unresponsive to the step

decrease in residence time. Significant peaks appeared in

only the first two size fractions. However, there was a

definite degradation in the size distribution in going from

the 45 to 15 minute residence time. This indicates more

than first order kinetics, which would have been represented

by horizontal lines for each size fraction. From the tran-

sient data one can only conclude that the kinetic nucleation

order was between one and two for the alum system.

A significant disturbance was created by the step

decrease in residence time for the ammonium sulfate system.

Initial and final values of the population densities for

the various size fractions fit the experimental curves very

well for the second order theoretical model. However, the

peaks of the experimental curves, with the exception of the

second size fraction, lagged and were more rounded than the

theoretical peaks. The peak heights coincided. After the

first two size fractions, the experimental data went through

a minimum just as the theoretical model suggested. A third

order model would more nearly coincide with the experimental

peaks because as the order increases the peaks shift to the

right on the time axis. However, the end points for the

third order model are far out of line and the peak heights

are too great. Also the minimums are shifted still further

to the right. Except for the time displacement and shape

of the peaks the second order model represents the experi-

mental data quite well. The pronounced peaks in the

theoretical curves arise from an assumption of a step change

in supersaturation and consequently growth rate. In prac-

tice this is probably not the case and a modification in the

model is needed to better represent the experimental behavior.

Analysis Evaluation

As a result of this work, the analysis proposed by

Randolph and Larson (17) appears to be a reliable way of

obtaining growth and nucleation rates. The experimental

technique and the analysis of the data in terms of popu-

lation density were not dependent on the kinetic models

proposed. Therefore other more fundamentally based theories

can be verified experimentally with the approach used in

this work.

The simple theoretical models used in this work are

based on the use of supersaturation as the driving force

for phase change. Fundamental theories also recognize

supersaturation as the primary driving force for phase

change, but these theories include other factors which are

involved in the energetics of nucleation such as the inter-

facial tension. For condensed systems these quantities are

not presently known, therefore application of the classic theories is difficult, if not impossible. A further difficulty lies in the fact that the classic theories generally assume homogeneous nucleation and thus do not apply to crystallization in mixed suspensions. The simple power models used here including the suspension density dependent model proposed by Larson et al. (7) permit the detection and correlation of heterogeneous nucleation arising from the crystals already in suspension. These models also provide a useful correlation of nucleation and growth rates for crystallizer deisgn.

Experiments conducted in a continuous mixed suspension crystallizer and analyses based on a population balance have certain advantages over previous experiments and analyses for the determination of nucleation and growth rates. These advantages are:

1) A constant, low supersaturation level can be achieved as opposed to the supersaturation in batch-type experiments which changes with time. Supersaturation transients are difficult to measure and this concentration variation makes the determination of reproducible growth and nucleation rates difficult. Nucleation and growth rates obtained at constant levels of supersaturation are easily reproduced. As a result of this investigation it was found that nucleation and growth rates can be predicted

with reasonable certainty for given system conditions and constraints.

2) Macro-size particles are counted and sized instead of microscopic particles. This can be done accurately and reproducibly. A simple sieve analysis of the crystal product appears to give sufficient information for systems of industrial importance. The counting of macro-sized particles is preferable at present because of the unavailability of a particle counter which can operate directly in the crystal suspension.

3) A crystal population analysis is more easily related to nucleation rate than weight distribution analyses. Also it is easier to analyze a sample of crystals on the basis of their number and size than to measure supersaturation at the levels found in continuous crystallizers.

4) This experimental and analytical approach is more realistic than attempting to measure nucleation rates from clear solution where the effects of small amounts of solution impurities, vessel wall conditions, and other nucleation inducers may become the predominant source of heterogeneously formed nuclei. At least reproducible nucleation rates can be achieved using this approach.

5) This approach can also be used to evaluate the effect on nucleation and growth rates of various habit modifiers used in industry to improve the form and handling

characteristics of product crystals.

The complete analysis, including the proposed power models, provides a realistic way of "getting at" the quantity which is most important in determining crystal size distribution, namely the relationship between nucleation and growth rates. While the absolute rates are of interest, the relationship of the rates relative to each other is the factor which determines size distribution and is the variable of interest to industry from an operation and control standpoint.

CONCLUSIONS

1. A continuous, mixed suspension, mixed product removal, cooling crystallizer can be operated on a laboratory scale to obtain reliable, reproducible nucleation and growth rate data. The constraints necessary for the required analysis can be achieved and the applicability of McCabe's ΔL law may be assumed. With the baffled, draft tube arrangement vigorous agitation is possible without significant attrition of the crystals.

2. The kinetic nucleation rate for the steady state crystallization of ammonium alum from aqueous solution by cooling is related to the growth rate by:

$$\frac{dN^o}{dt} = k_2 \, r^{2.1}$$

or in terms of supersaturation by:

$$\frac{dN^o}{dt} = k_1 \, s^{2.1}$$

3. The kinetic nucleation rate for the steady state crystallization of ammonium sulfate from aqueous solution by cooling is related to the growth rate by:

$$\frac{dN^o}{dt} = k_2' \, r^{1.7}$$

or in terms of the supersaturation by:

$$\frac{dN^o}{dt} = k_1' \, s^{1.7}$$

4. The proportionality constants in the nucleation rate equations are linearly related to the amount of solids in suspension. This indicates that the crystals in suspension are a heterogeneous source of nuclei and that this mode of nucleation is predominant in the cooling crystallization of ammonium alum and ammonium sulfate.

5. Experimental transient data for a threefold step change in residence time can be obtained for comparison with computer solutions of the transient equation. The experimental data for ammonium sulfate is reasonably represented by a solution based on second order kinetics, while the data for ammonium alum only qualitatively agrees with a solution using a 1.25 order kinetic model. Modifications of the computer program so that the solutions more nearly coincide with actual conditions in the crystallizer after the step change may provide better theoretical representation of transient data.

6. The experimental models can be used to effectively predict the size distribution for different levels of suspension density and for different residence times. For the systems studied, changes in the suspension density had no effect on the size distribution because of the linear dependence of nucleation rate on suspension density. However, the size distribution of both systems can be enhanced by an increase in residence time.

RECOMMENDATIONS

1. The same experimental technique as used in this work should be used to generate data for a detailed study of the applicability of the classic theories.

2. Further data should be obtained with a cooling crystallizer for other systems. An organic compound of suitable habit which could be crystallized from aqueous solution and analyzed with the Coulter Counter should be found. Also an inorganic compound of high kinetic nucleation order such as NaCl, but with a steeper solubility curve than NaCl should be crystallized by cooling.

3. A cooling crystallizer should be designed for lower temperature operation than can be achieved with cooling water. A unit of this type would be more versatile in its applicability to systems with moderately steep solubility curves, unheated feed solutions could be used, and a constant suspension temperature could be more easily maintained. Major disadvantages of such a unit would be the crystal buildup likely to occur on its walls and the difficulty of handling suspension samples at room temperature without affecting their size distribution.

NOMENCLATURE

A	surface area of crystal suspension, cm^2/ml
C	concentration, gms/ml
c_i	inlet concentration, gms/ml
$c_{i_{av}}$	average feed concentration, gms/100 gms H_2O
$c_{o_{av}}$	average filtrate concentration, gms/100 gms H_2O
c	frequency factor
D	characteristic dimension of ammonium sulfate crystal, microns
i	kinetic order of nucleation
K_A	proportionality constant
K_C	proportionality constant
K_M	proportionality constant
K_1	proportionality constant
K_2	proportionality constant
k_A	proportionality constant
k_a	area shape factor
k_d	proportionality constant
k_G	mass growth rate proportionality constant
k_g	linear growth rate proportionality constant
k_M	proportionality constant
k_n	proportionality constant
k_T	proportionality constant
k_V	volumetric shape factor
k_1	proportionality constant

k_2 proportionality constant

k_1' proportionality constant

k_2' proportionality constant

L crystal diameter, microns, measured along a characteristic dimension

ΔL width of size fraction, microns

L_d dominant particle size on a weight basis, microns

M suspension density, gms of crystals/100 ml suspension

ΔN number of crystals in a size fraction

N^o number of nuclei

n population density of crystal suspension, numbers/micron

$\bar{n}$ point population density, numbers/micron/ml

$\bar{n}_i$ inlet point population density, numbers/micron/ml

$\bar{n}_o$ outlet point population density, numbers/micron/ml

$\bar{n}_s$ point population density at suspension surface, numbers/micron/ml

n^o nuclei population density, numbers/micron

n_s^o steady state nuclei population density, numbers/micron

Q_i inlet volumetric flow rate, ml/minute

Q_o outlet volumetric flow rate, ml/minute

r linear crystal growth rate, microns/minute

r_o steady state crystal growth rate, microns/minute

S ratio of supersaturated concentration to equilibrium concentration

s supersaturated concentration minus equilibrium concentration, gms/ml

T	residence time, minutes
T_o	steady state residence time, minutes
t	time, minutes
V	volume of suspension in crystallizer, ml
v	suspension sample volume, ml
v_c	volume of crystal slurry traversing aperture during a count, ml
v_e	total volume of electrolyte solution in which crystals are dispersed for counting, ml
W	weight of crystals on sieve, gms
w_e	weight of crystals dispersed in solution for counting, gms
w_t	total weight of crystals from which count sample is taken, gms
x	dimensionless crystal size, $L/r_o T_o$
y	dimensionless population density, n/n_o^o
ρ	crystal density, gm/ml
θ	dimensionless time, t/T_o
$\emptyset$	dimensionless crystal growth rate, r/r_o

LITERATURE CITED

1. Behnken, D. W., Horowitz, Jacob, and Katz, Stanley. Particle growth processes. Industrial and Engineering Chemistry Fundamentals 2: 212-216. 1963.

2. Bransom, S. H., Dunning, W. J., and Millard, B. Kinetics of crystallization in solution. Faraday Society Discussions 5: 83-103. 1949.

3. Buckley, H. E. Crystal growth. New York, N.Y., John Wiley and Sons. 1951.

4. Frank, F. D. Influence of dislocations on crystal growth. Faraday Society Discussions 5: 48-54. 1949.

5. Jenkins, J. D. The effect of various factors upon the velocity of crystallization on substances from solution. American Chemical Society Journal 47: 903-907. 1925.

6. LaMer, V. Nucleation in phase transitions. Industrial and Engineering Chemistry 44: 1270-1273. 1952.

7. Larson, M. A., Timm, D. C., and Wolff, P. R. Effect of suspension density on crystal size distribution. Unpublished mimeographed paper. Ames, Iowa, Chemical Engineering Department, Iowa State University of Science and Technology, 1965.

8. McCabe, W. L. Crystal growth in aqueous solutions. Industrial and Engineering Chemistry 21: 112-117. 1929.

9. McCabe, W. L. and Stevens, R. P. Rate of growth of crystals in aqueous solutions. Chemical Engineering Progress 47, No. 4: 168-174. 1951.

10. Miers, H. A. and Issac, F. J. Refractive indices of crystallizing solutions. Chemical Society Journal 89: 413-415. 1906.

11. Mullin, J. W. Crystallization. London, England, Butterworths. 1961.

12. Murray, D. C. Size distribution dynamics in continuous crystallization. Unpublished Ph.D. thesis. Ames, Iowa, Library, Iowa State University of Science and Technology, 1964.

13. Nielsen, A. E. Kinetics of precipitation. New York, N.Y., Macmillan Co. 1964.

14. Powers, H. E. C. Nucleation and early crystal growth. Industrial Chemist 39: 351-355. 1963.

15. Randolph, A. D. Mixed suspension, mixed product removal crystallizer as a concept in crystallizer design. American Institute of Chemical Engineers Journal 11: 424-430. 1965.

16. Randolph, A. D. Size distribution dynamics in a mixed crystal suspension. Unpublished Ph.D. thesis. Ames, Iowa, Library, Iowa State University of Science and Technology. 1962.

17. Randolph, A. D. and Larson, M. A. Transient and steady state size distributions in continuous mixed suspension crystallizers. American Institute of Chemical Engineers Journal 8: 639-645. 1962.

18. Robinson, J. N. and Roberts, J. E. A mathematical study of crystal growth in a cascade of agitators. Canadian Journal of Chemical Engineering 35: 105-112. 1957.

19. Saeman, W. C. Crystal size distributions in mixed suspensions. American Institute of Chemical Engineers Journal 2: 107-112. 1956.

20. Schoen, H. M. Crystallization equipment theory. Industrial and Engineering Chemistry 53: 607-611. 1961.

21. Strickland-Constable, R. F. and Mason, R. E. A. Breeding of nuclei. Nature 197: 897-898. 1963.

22. Timm, D. C. Crystal size distribution dynamics. Unpublished M.S. thesis. Ames, Iowa, Library, Iowa State University of Science and Technology. 1965.

23. Timm, D. C. and Larson, M. A. Effect of nucleation kinetics on the dynamic behavior of a continuous crystallizer. Unpublished paper presented at American Institute of Chemical Engineers 59th National Meeting, Columbus, Ohio, May, 1966. Ames, Iowa, Department of Chemical Engineering, Iowa State University of Science and Technology. 1966.

24. Ting, H. H. and McCabe, W. C. Supersaturation and crystal formation in seeded solutions. Industrial and Engineering Chemistry 26: 1201-1204. 1934.

25. Turnbull, D. and Fisher, J. C. Rate of nucleation in condensed systems. Journal of Chemical Physics 17: 71-73. 1949.

26. Uhlmann, D. R. and Chalmers, B. The energetics of nucleation. Industrial and Engineering Chemistry 57: 19-31. 1965.

27. Van Hook, A. Crystallization. New York, N.Y., Reinhold Publishing Corporation. 1961.

28. Wolff, P. R. Suspension density transients in a mixed suspension crystallizer. Unpublished M.S. thesis. Ames, Iowa, Library, Iowa State University of Science and Technology. 1965.

ACKNOWLEDGMENTS

APPENDIX A

Tartaric Acid

Tartaric acid was the initial compound crystallized in the cooling crystallizer. For this system a substantially different suspension density was obtained for runs of different residence time despite constant feed composition. The suspension density doubled for a threefold increase in residence time. This indicates a sizeable supersaturation level at the shorter residence time. With other systems only a small supersaturation level was achieved. In these other systems supersaturation varied with residence time, but since such a small amount of supersaturation was present, the variation did not affect the suspension density significantly. However, for tartaric acid the substantial increase in suspension density with residence time was due to the high level of supersaturation at the shorter residence time which decayed and increased the suspension density for the longer residence time. Yield is variable for a system of this type. A steady state analysis is still applicable according to Randolph (15), if only crystal size distribution and not yield is of interest.

A number of steady state runs were made with tartaric acid, but a straight line relationship between log (n) and L was not obtained. Since the size distribution was small, a Coulter Counter analysis would have clarified and extended the data in the small size range. An extensive search for

a suitable electrolyte-solvent combination in which to disperse tartaric acid crystals for counting proved fruitless. Solvents in which tartaric acid was even slightly soluble were unsuitable because of the small amount of sample required for counting (0.1 gram) and the small size of the crystals in the sample. During the counting of crystals of a certain size, the number of counts would drop due to dissolution of the crystals in that size range. Solvents in which tartaric acid was insoluble were very non-polar and would not dissolve any of the electrolytes tried. Thus it was not possible to use the Coulter Counter for tartaric acid. Filtration and handling of the pentagonal, platelike crystals was also a problem. Because of these difficulties, the resulting tartaric acid data were inconclusive and work on the system was concluded.

APPENDIX B

Volumetric Shape Factor for Ammonium Sulfate

The approximate volumetric shape factor for ammonium
sulfate was calculated by two different methods:

1) From the photomicrograph shown in Figure 4;

2) By physically counting the number of crystals in a
size fraction.

According to Mullen (11) the second largest dimension of a
non-spherical particle should be chosen as an equivalent
diameter. Then the other dimensions of the crystal are
expressed in terms of the equivalent diameter. Next the
volume of the crystal is calculated with the equivalent
diameter as the only unknown. The coefficient of the cube
of the equivalent diameter is the volumetric shape factor
k_v.

1) The smaller crystal in Figure 4 was measured and
its width was chosen as the equivalent diameter, d. Several
other crystals of different sizes were examined on a
calibrated microscope slide to be sure that the measured
length to width ratio was constant. To calculate the volume
of the crystal in the photograph, the middle portion of
length b (Figure 34) was assumed to be hexagonal, while the
ends were assumed to be hexagonal pyramids of altitude c.
In the photograph the edges of the top face of the middle

Figure 34. Ammonium sulfate crystal showing dimensions used in calculation
            of shape factor

TOP VIEW
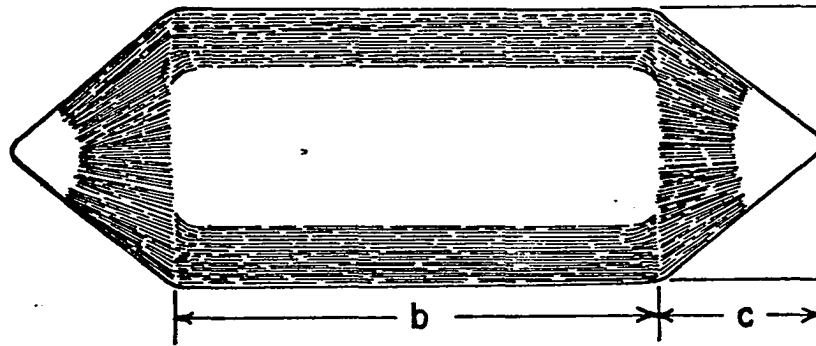
END VIEW
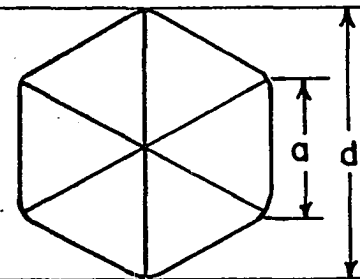
portion are not sharply defined, therefore, the length of a side, a, of the hexagon was calculated by geometry from the width, d. Figure 34 shows that a hexagon may be divided into six equilateral triangles. Hence the length of a side, a, is one-half the width or equivalent diameter, d. By measuring the crystal, a, b, and c can be expressed in terms of d: a = 0.50d, b = 1.68d, c = 0.58d. The volume of the hexagonal part V_H may be calculated by multiplying the area of a hexagon, $1.5a^2$ cot 30°, by the length, b. The volume of the two ends $2V_E$ may be calculated from the formula for the volume of a pyramid, $\frac{1}{3}$ (area of base) (altitude) or $\frac{1}{3}$ $(1.5a^2 \cot 30°)(c)$.

$$V_{crystal} = V_H + 2V_E = 1.5a^2b \cot(30°) + a^2c \cot 30° \qquad (60)$$

Substituting for a, b, and c in terms of d:

$$V_{crystal} = 1.35 \ d^3 \qquad (61)$$

and the volumetric shape factor, $k_v = 1.35$.

By method 2), the volumetric shape factor was calculated from the following equation:

$$k_v = \frac{W}{\rho N L_{av.}^3} \qquad (62)$$

where W is the weight of crystals held on a given sieve, $L_{av.}$ is the average of the aperture diameters of the sieve above and the sieve on which the crystals were held, ρ is the crystal density, and N is the total number of crystals held on the sieve determined by counting. Volumetric shape

factors ranging from 0.95 to 1.25 were calculated by this method.

APPENDIX C

Steady State Data

Sieve and Coulter Counter data for all eighteen steady state alum and ammonium sulfate runs are included in Tables 2 and 3. Population density and average crystal size are tabulated for one sample from each run. Individual runs are identified by residence time, $T(min)$, and suspension density, M (gms crystals/100 ml slurry).

Table 2. Population Density, $n(\frac{no.}{micron})$ and Average Crystal

L	n T = 15 M = 5.0	n T = 30 M = 5.5	n T = 45 M = 5.3	n T = 15 M = 9.0	n T = 30 M = 10.5
1093	7.63	3.56×10^{1}	3.02×10^{1}	1.50×10^{1}	5.13×10^{1}
923	4.85×10^{1}	1.22×10^{2}	1.46×10^{2}	8.91×10^{1}	2.66×10^{2}
792	1.98×10^{2}	4.47×10^{2}	4.85×10^{2}	3.12×10^{2}	9.82×10^{2}
623	9.95×10^{2}	1.55×10^{3}	1.95×10^{3}	1.49×10^{3}	3.24×10^{3}
479	5.63×10^{3}	7.01×10^{3}	8.83×10^{3}	7.98×10^{3}	1.41×10^{4}
373	2.33×10^{4}	2.47×10^{4}	2.76×10^{4}	3.74×10^{4}	4.98×10^{4}
256	1.04×10^{5}	1.08×10^{5}	9.17×10^{4}	2.17×10^{5}	2.05×10^{5}
180	2.92×10^{5}	2.59×10^{5}	1.96×10^{5}	6.56×10^{5}	5.10×10^{5}
127	6.64×10^{5}	5.31×10^{5}	4.02×10^{5}	1.24×10^{6}	9.93×10^{5}
90	1.34×10^{6}	8.25×10^{5}	8.23×10^{5}	2.39×10^{6}	1.95×10^{6}
140[a]	4.75×10^{5}		3.62×10^{5}	1.07×10^{6}	6.50×10^{5}
120	7.31×10^{5}		4.95×10^{5}	1.57×10^{6}	1.29×10^{6}
100	1.34×10^{6}		6.49×10^{5}	1.79×10^{6}	1.57×10^{6}
80	1.44×10^{6}		8.24×10^{5}	2.25×10^{6}	1.83×10^{6}
80	1.49×10^{6}			2.59×10^{6}	2.28×10^{6}
7C	2.27×10^{6}		8.85×10^{5}	2.99×10^{6}	2.59×10^{6}
60	1.94×10^{6}		1.19×10^{6}	3.09×10^{6}	3.60×10^{6}
50	1.91×10^{6}		8.12×10^{5}	3.49×10^{6}	2.72×10^{6}
40	2.53×10^{6}		9.18×10^{5}	3.14×10^{6}	3.29×10^{6}

[a]Coulter Counter data

and Average Crystal Size, L(microns) for Alum

n $T = 15$ $M = 9.0$	n $T = 30$ $M = 10.5$	n $T = 45$ $M = 14.7$	n $T = 15$ $M = 21.9$	n $T = 30$ $M = 22.0$	n $T = 45$ $M = 22.2$
1.50×10^1	5.13×10^1	1.78×10^2	1.33×10^2	1.62×10^2	1.31×10^2
8.91×10^1	2.66×10^2	5.94×10^2	5.06×10^2	6.33×10^2	6.29×10^2
3.12×10^2	9.82×10^2	1.76×10^3	1.48×10^3	2.08×10^3	2.19×10^3
1.49×10^3	3.24×10^3	5.80×10^3	5.02×10^3	6.70×10^3	8.01×10^3
7.98×10^3	1.41×10^4	2.07×10^4	2.29×10^4	2.76×10^4	3.14×10^4
3.74×10^4	4.98×10^4	6.64×10^4	9.27×10^4	9.02×10^4	1.03×10^5
2.17×10^5	2.05×10^5	2.35×10^5	4.51×10^5	3.81×10^5	4.18×10^5
6.56×10^5	5.10×10^5	6.79×10^5	1.26×10^6	1.29×10^6	1.10×10^6
1.24×10^6	9.93×10^5	1.21×10^6	2.38×10^6	2.73×10^6	1.88×10^6
2.39×10^6	1.95×10^6	2.32×10^6	4.84×10^6	5.21×10^6	3.22×10^6
1.07×10^6	6.50×10^5	8.70×10^5	1.72×10^6	2.10×10^6	1.28×10^6
1.57×10^6	1.29×10^6	1.28×10^6	4.32×10^6	3.12×10^6	2.06×10^6
1.79×10^6	1.57×10^6	1.31×10^6	4.77×10^6	3.82×10^6	2.14×10^6
2.25×10^6	1.83×10^6	1.86×10^6	5.74×10^6	4.27×10^6	3.06×10^6
2.59×10^6	2.28×10^6	2.11×10^6	4.94×10^6	5.44×10^6	3.14×10^6
2.99×10^6	2.59×10^6	2.33×10^6	5.70×10^6	6.10×10^6	3.56×10^6
3.09×10^6	3.60×10^6	4.34×10^6	6.62×10^6	7.62×10^6	4.16×10^6
3.49×10^6	2.72×10^6	2.92×10^6	6.40×10^6	9.27×10^6	3.74×10^6
3.14×10^6	3.29×10^6	3.31×10^6	5.61×10^6	6.20×10^6	3.52×10^6

Table 3. Population Density, $n(\frac{no.}{micron})$ and Average Crystal S

L	n T = 15 M = 2.55	n T = 30 M = 3.16	n T = 45 M = 3.36	$\dot{n}$ T = 15 M = 3.92	n T = 30 M = 4.01
1093	5.94	7.35	4.71	6.25	1.66×10^1
923	2.12×10^1	4.52×10^1	4.10×10^1	2.98×10^1	6.80×10^1
792	1.28×10^2	2.31×10^2	3.09×10^2	1.70×10^2	2.89×10^2
623	4.98×10^2	7.70×10^2	8.43×10^2	6.94×10^2	8.31×10^2
479	2.35×10^3	2.93×10^3	3.08×10^3	3.29×10^3	3.61×10^3
373	6.60×10^3	7.69×10^3	7.04×10^3	9.13×10^3	8.96×10^3
256	1.94×10^4	1.76×10^4	1.94×10^4	2.46×10^4	2.62×10^4
180	3.42×10^4	3.26×10^4	3.71×10^4	5.31×10^4	4.94×10^4
140	5.77×10^4	5.15×10^4	5.06×10^4	5.44×10^4	5.33×10^4
120	6.74×10^4	5.15×10^4	8.17×10^4	1.03×10^5	8.20×10^4
100	8.65×10^4	8.84×10^4	1.03×10^5	1.73×10^5	8.71×10^4
80[a]	1.33×10^5	8.53×10^4	9.09×10^4	1.59×10^5	1.40×10^5

[a]Smaller sizes were not determined because of a scarcit
procedure.

) and Average Crystal Size, L(microns) for Ammonium Sulfate

$\dot{n}$ T = 15 M = 3.92	n T = 30 M = 4.01	n T = 45 M = 4.33	n T = 15 M = 5.78	n T = 30 M = 7.40	n T = 45 M = 7.46
6.25	1.66×10^1	8.79	1.11×10^1	3.78×10^1	3.13×10^1
2.98×10^1	6.80×10^1	5.84×10^1	6.89×10^1	1.63×10^2	1.42×10^2
1.70×10^2	2.89×10^2	3.89×10^2	3.33×10^2	6.84×10^2	5.73×10^2
6.94×10^2	8.31×10^2	1.09×10^3	1.27×10^3	1.78×10^3	1.59×10^3
3.29×10^3	3.61×10^3	4.02×10^3	5.35×10^3	6.50×10^3	6.64×10^3
9.13×10^3	8.96×10^3	1.01×10^4	1.51×10^4	1.58×10^4	1.77×10^4
2.46×10^4	2.62×10^4	2.49×10^4	3.75×10^4	4.14×10^4	4.80×10^4
5.31×10^4	4.94×10^4	4.51×10^4	6.07×10^4	8.75×10^4	8.56×10^4
5.44×10^4	5.33×10^4	7.10×10^4	8.17×10^4	1.08×10^5	1.08×10^5
1.03×10^5	8.20×10^4	9.18×10^4	1.40×10^5	1.75×10^5	1.82×10^5
1.73×10^5	8.71×10^4	1.56×10^5	1.53×10^5	2.06×10^5	2.37×10^5
1.59×10^5	1.40×10^5	1.95×10^5	1.48×10^5	1.48×10^5	3.26×10^5

ed because of a scarcity of small crystals as explained in the